QATAR UNIVERSITY

COLLEGE OF ENGINEERING

GRID-CONNECTED SINGLE-STAR BRIDGE-CELLS MODULAR MULTILEVEL CASCADED CONVERTER WITH SELECTIVE HARMONIC ELIMINATION TECHNIQUES

BY

MENA GUIRGUIS FAKHRY

A Thesis Submitted to

the Faculty of the College of

Engineering

in Partial Fulfillment

of the Requirements

for the Degree of

Master of Science in Electrical Engineering

January 2018

COMMITTEE PAGE

The members of the Committee approve the Thesis of Mena Guirguis Fakhry defended on 11/12/2017.

Ahmed Mohammed Massoud
Thesis/Dissertation Supervisor

Lazhar Ben Brahim
Committee Member

Marco Liserre
Committee Member

Abbes Amira
Committee Member

Approved:

Khalifa Al-Khalifa, Dean, College of Engineering

ABSTRACT

FAKHRY, MENA, GUIRGUIS., Masters : January : 2018,

Master of Science in Electrical Engineering

Title: Grid-Connected Single-Star Bridge-Cells Modular Multilevel Cascaded Converter with Selective Harmonic Elimination Techniques

Supervisor of Thesis: Dr. Ahmed, Mohamed, Massoud.

Nowadays, Renewable Energy Sources (RESs) are receiving enormous attention due to the noticeable exhaustion of fossil fuel and its emission of greenhouse gases. DC-AC converters have attracted the attention of the researchers, as they are entailed to integrate RESs to the grid to comply with the grid frequency and voltage requirements. Due to the high penetration of RESs, especially with elevated power levels, high-power converters are needed, which necessitates higher voltage and current ratings of the semiconductor devices. The unavailability of high voltage semiconductor devices has directed the attention to the use of either series connection of semiconductor devices or Multilevel Inverters (MLIs). MLIs allow using several low rated semiconductors to hold the high output power of the inverter. The MLI output waveform is close to sinusoidal in nature, therefore it may require a small filter to enhance the output power quality. There are many types of MLIs, where the most common MLIs are Flying Capacitor, Diode Clamped, and Modular Multilevel Cascaded Converter (MMCC). The MMCC can be classified into three main formations, the Single-Star Bridge-Cells MMCC (SSBC-MMCC), the Double-Star Bridge-Cells MMCC (DSBC-MMCC), and the Double-Star Chopper-Cells MMCC (DSCC-MMCC). The main advantage of the MMCC is the modularity and scalability.

In addition, the MMCC does not require any clamping diodes or flying capacitors for clamping the voltage across the switches.

In this thesis, the MMCC will be used to integrate high-power RESs to Grid. Nevertheless, the high-power applications necessitate low switching frequency operations. One of the most common controlling techniques of MLI with low frequency operation is the Selective Harmonic Elimination (SHE). SHE insures also the output current Total Harmonic Distortion (THD) to be minimized. One disadvantage of the SHE method is that the complexity of the algorithm along with the equations used is increased by the increase of the MMCC number of levels. Therefore, other alternatives of SHE techniques will be studied in this work to overcome this complexity.

This thesis focuses typically on MMCC, particularly the SSBC-MMCC. In this work, a high-power grid-connected SSBC-MMCC is controlled with three different SHE techniques, complying with low switching frequency operation limitation in high-power applications. In addition to the Conventional SHE (C-SHE) technique, Quasi-SHE (Q-SHE) and Asymmetrical-SHE (A-SHE) approaches are proposed and assessed. Q-SHE and A-SHE approaches are based on eliminating selected low order harmonics (for instance, eliminating the fifth and seventh order harmonics), irrelevant to the number of employed levels provided that the number of levels allows for the required harmonic elimination. Compared with the C-SHE approach, the Q-SHE and A-SHE require less computational burden in solving the required equation groups, especially when a high number of levels and/or multiple switching angles for each voltage level are needed, while maintaining the same *dv/dt* of the output voltage. A 5MW, 17-level, grid-connected SSBC-MMCC, controlled in the synchronous rotating reference frame,

is employed for assessing the addressed SHE techniques. The assessment is validated through simulation results using Matlab/Simulink platform.

DEDICATION

It is my genuine gratefulness and warmest regard that I dedicate this work to my family, to express my gratitude for their support.

ACKNOWLEDGMENTS

Firstly, I would like to express my sincere appreciation to my supervisor Dr. Ahmed Massoud for his guidance, continuous support throughout my thesis study, patience, motivation, and immense knowledge. His supervision helped me in all the time of study and writing of this thesis.

In addition, I would like to thank the rest of my thesis committee and the Department of Electrical Engineering for their comments and encouragement, and for providing me with the required technical background.

Finally, my gratitude goes to my family, friends and colleagues for their support through my study.

TABLE OF CONTENTS

LIST OF TABLES

LIST OF FIGURES

CHAPTER 1: INTRODUCTION

1.1 Background

Hitherto, countries are relying heavily on fossil fuels for their energy generation. These types of energy sources are considered non-renewable, since they depend on finite resources that will eventually deplete. With the high increase in the energy demand, many researches now are focusing on Renewable Energy Sources (RESs) and their grid integration.

1.1.1 Why RESs?

RESs are constantly replenished and will never run out, such as wind energy, solar energy, and geothermal energy. Based on the Renewable Energy Policy Network for the 21st Century (REN21), approximately 1.2 billion people (17% of the global population), located in the Asia Pacific region and sub-Saharan Africa are disconnected from electricity [1]. RESs provide security of supply, unlike the oil & gas resources, which are concentrated in certain regions, and getting more technically challenging and more expensive to reach.

As per the United States Department of Energy, the land-based wind power, utility and distributed Photo-Voltaic (PV) solar power, Light Emitting Diodes (LEDs), and Electric Vehicles (EVs) cost has decreased by 41% since 2008 [2]. Where, as per the REN21, Figs 1.1 and 1.2 show clearly the cost of PV and wind turbines has steadily declined year after year, falling over 64% since 2008, where the cumulative energy capacity produced by wind and PV is increasing year by year.

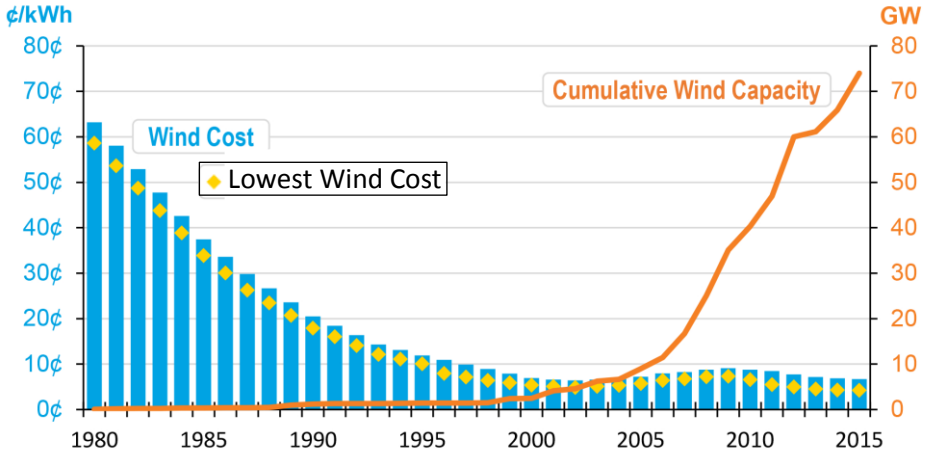

Fig 1.1 The cumulative capacity and cost (in US cents) for wind turbines since 1980 as per the U.S Department of Energy [2]

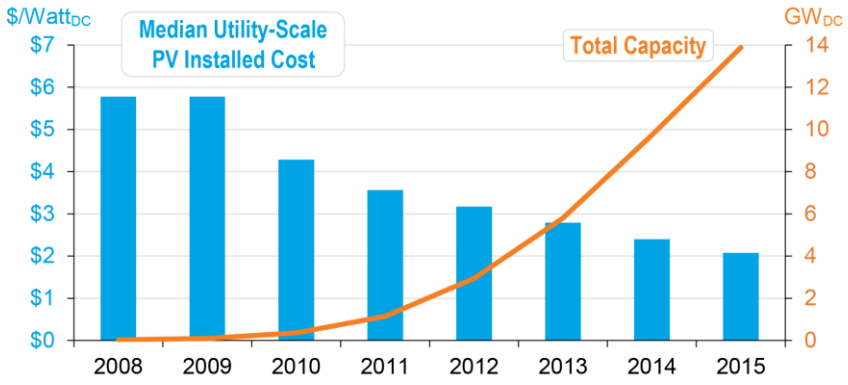

Fig 1.2 Cumulative capacity and the cost (in US $) for PV since 1980 as per the U.S Department of Energy [2]

It can be seen in Figs. 1.1 and 1.2 that the price of the wind turbines and solar PV was dropped down. This drop in cost has enabled the utilities and the power sector now to install more utility-scale PV and wind turbines, with an exponentially-increased power capacity.

1.1.2 The Present Status Of RESs

Nowadays, RESs span a wide range of power, ranging from low power generators used in rural and remote areas up to high power RESs generation for utility scale applications. Different countries are supporting RESs projects, where by 2005, 15 countries adjusted their policies to support renewable energy. On the other hand, after 10 years (until 2015), 164 countries adjusted their policies to support renewable energy; 95 of them were developing countries [3].

Until now, the power sector is experiencing a large increase in the annual capacity in all regions. In the last 10 years, wind and solar PV have observed a massive average annual growth in installed capacity of 23% and 51%, respectively [3]. Nowadays, the world is increasing the renewable power capacity compared to the power capacity added from fossil fuels. By the end of 2015, the installed renewable energy capacity was sufficient to supply 23.7% of worldwide electricity, while the hydropower supplies about 16.6%. Table 1.1 shows the status of renewable power capacity for 2014 and 2015.

Table 1.1: The current status of renewable power capacity for 2014 and 2015 as per REN21 [1]

Renewable Power Type	**Unit**	**2014**	**2015**
Total Renewable Power Capacity (not including hydro)	GW	665	785
Total Renewable Power Capacity (including hydro)	GW	1,701	1,849
Wind Power Capacity	GW	370	433
Solar Power Capacity	GW	177	227
Geothermal power Capacity	GW	12.9	13.2
Hydropower Capacity	GW	1,036	1,064
Bio-Power Capacity	GW	101	106
Concentrated Solar thermal Power Capacity	GW	4.3	4.8

REN21 recorded an increase of 50 GW in the renewable energy capacity in 2015. Fig. 1.3 shows this increase and the share of the top countries for the last 10 years for PV.

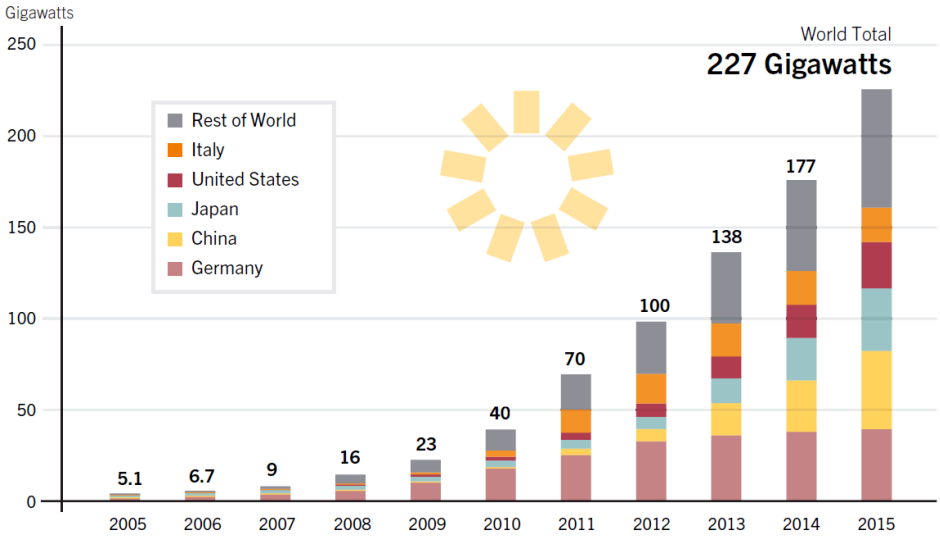

Fig 1.3 Solar PV Global Capacity, by Country/Region 2005-2015 as per REN21 [1]

Fig 1.4 compares between the total renewable energy capacity added until 2014 and the added capacity in 2015 for each country from the top 10 countries.

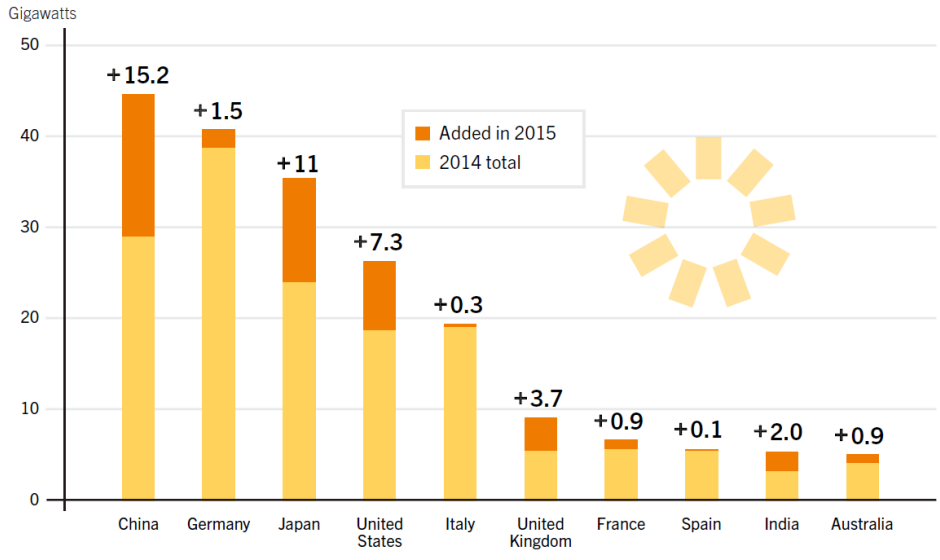

Fig 1. 4 Solar PV Capacity in 2014 and the added capacity in 2015 as per REN21 [1]

It can be seen from this chapter that the renewable energy sources are receiving more attention as a source of generating electricity, where the cost of generating electricity from renewable energy sources are getting lower, and the energy capacity produced by renewable energy sources is increasing.

1.1.3 Integration Of RESs To Grid

The challenge now is to integrate the RESs to the power grid, to enable utilizing these RESs as a grid-connected distributed generation. One of the challenges is the DC-AC converters especially at elevated power levels. There are two main types of DC-AC converters based on the input source (voltage source converters or current source converters). The voltage source converter is the converter to be addressed throughout this work due its higher reliability, better efficiency, and faster dynamic response when compared with current source converter [4].

A DC-AC converter, or inverter, is a power electronic device that converts DC waveforms to AC waveforms in order to match the grid voltage and frequency. This, in turn, enables interfacing the power converters to the grid. Grid-connected inverters should be controlled with a dedicated controller in order to maintain the required voltage and frequency. With the penetration of high-power RESs, high power converters are required. This has directed the attention of researchers to multilevel inverters, instead of the typical two-level converter, in order to meet the high power requirements with semiconductor devices of low voltage ratings. A practical example of the high power RESs can be seen in the following two stations:

1. In 2016, China built the largest solar plant with 1547MW at the Tengger Desert Solar Park in Zhongwei, Ningxia. This is considered the largest solar power plant until now [5].

2. In April 2017, India built solar plant with 1,000 MW at the Kurnool Ultra Mega Solar Park in the state of Andhra Pradesh. This is considered one of the largest solar power plant [6].

1.2 Thesis Objective

The objective of this thesis is to investigate, design and test different techniques to control the high power grid connected DC-AC converter (Multilevel Inverter). The assessment is done by designing a cascaded 17-level H-Bridge Multilevel Inverter controlled by three different techniques. The three Selective Harmonic Elimination techniques assures acceptable Total Harmonic distortion (THD) output, where the output of the inverter will be controlled to achieve the required real and reactive power flow between the grid and the converter.

1.3 Thesis Scope

In this thesis, a high-power grid-connected SSBC-MMCC is controlled with three different SHE techniques. In addition to the Conventional SHE (C-SHE) technique, Quasi-SHE (Q-SHE) and Asymmetrical-SHE (A-SHE) approaches are proposed and assessed. Q-SHE and A-SHE approaches are based on eliminating selected low order harmonics (5^{th} and 7^{th} order harmonics). The output power of the high-power grid-connected SSBC-MMCC is also designed to control the real and reactive power transfer between the MMCC and the grid.

1.4 Thesis Outline

The thesis report is structured firstly with an introduction to overview the importance of utilizing and integrating the renewable energy sources to the grid, and the current status of utilizing the renewable energy sources. Then the second chapter

focuses typically on Multilevel Inverter types, particularly the SSBC-MMCC. Next chapter introduces different modulation controlling techniques of the SSBC-MMCC, and states advantages and disadvantage of each technique. Chapter 4 explains the three different SHE techniques, namely, Conventional SHE (C-SHE), Quasi-SHE (Q-SHE) and Asymmetrical-SHE (A-SHE), where the three proposed approaches are assessed. Chapter 5 focuses on connecting the MMCC to the grid and controlling the real and reactive power transfer between the MMCC and the grid. A 5MW, 17-level, grid-connected SSBC-MMCC, controlled in the synchronous rotating reference frame, is employed for assessing the addressed SHE techniques. The assessment is validated through simulation results using Matlab/Simulink platform.

CHAPTER 2: MULTILEVEL INVERTERS

High-power grid-connected inverters can be divided into two main categories, two-level inverters and Multilevel Inverters (MLIs). High-power two-level converters depend on series connection of semiconductors. One of the main disadvantages of the high-power two-level inverter is the high THD and dv/dt of the output voltage. In the series-connected devices, the static and dynamic voltage sharing should be maintained. During the switching action, the parasitic effects can cause a dynamic imbalance of the voltage sharing, with over voltage acting on one or more of the switches [7]. Therefore, active gate control can be used, but at the expense of adding more complexity to the system and increasing the switching losses.

In high-power applications, MLIs can overcome the challenges faced in two-level converters. One of the main advantages of the MLIs is to yield a high output power using semiconductor devices with lower voltage ratings. Yet, the MLI controlling techniques are more complicated than the two-level converter controlling techniques, since it should control each level in the MLI to maintain the desired output voltage and frequency. The literature shows different types of MLIs, such as flying capacitor [8-13], diode clamped [14-21], Modular Multilevel Cascaded Converter (MMCC). MMCC can be classified into Single-Star Bridge-Cells MMCC (SSBC-MMCC) [22-24], Single-Delta Bridge-Cells MMCC (SDBC-MMC), Double-Star Bridge-Cells MMC (DSBC-MMC), and Double-Star Chopper-Cells (DSBC-MMC) [25-28], which will be elaborated in the following subsections. A tree diagram of the different types and families of the DC-AC converters (voltage source converters) is illustrated in Fig 2.1.

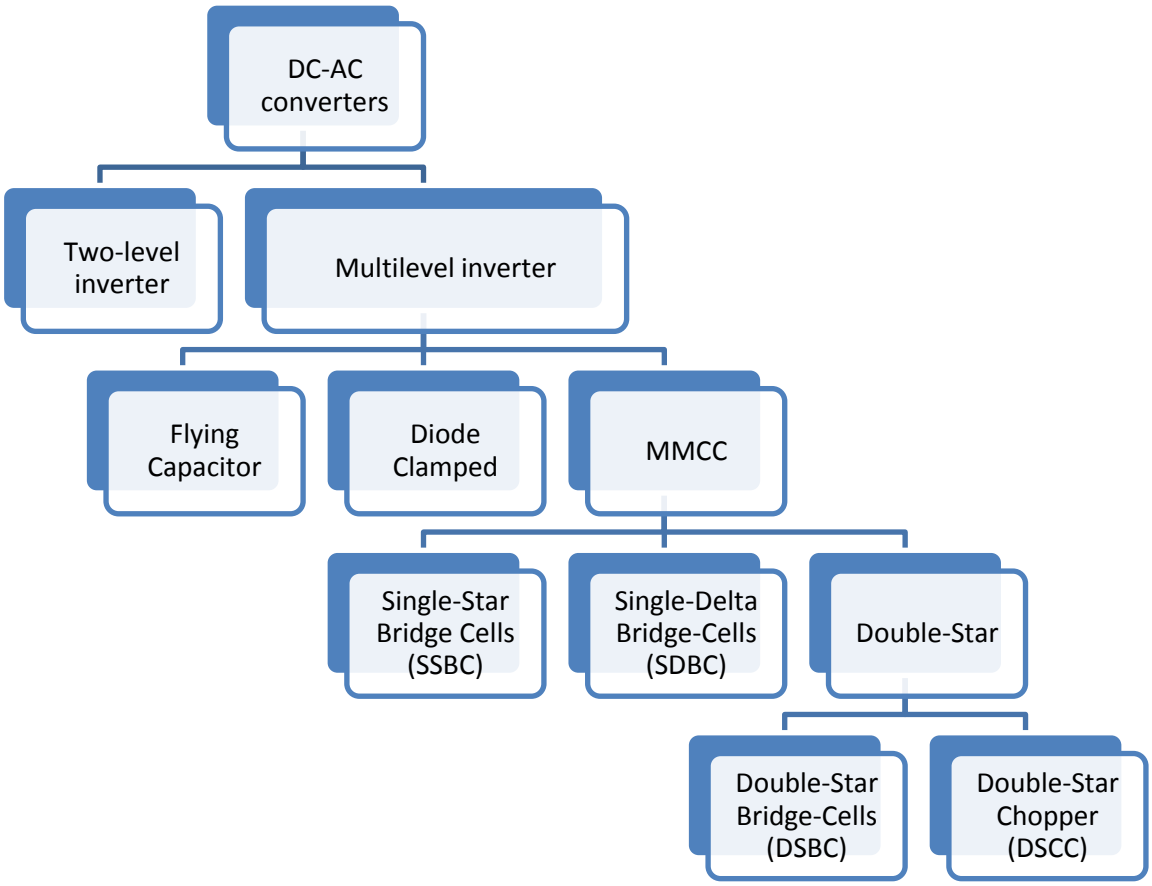

Fig. 2.1 DC-AC Converters Tree Diagram

2.1 Flying Capacitor

Flying Capacitors MLIs are a common type of MLIs. Flying capacitors MLIs employ capacitors for clamping the voltage across the switches [12]. The flying capacitor-based MLI requires a large number of capacitors compared to MMCC. Moreover, the flying capacitor requires voltage-balancing method to balance the capacitor voltages, in order to produce the required output voltage level of the MLI [9, 12]. As the number of voltage levels increases, the output voltage is closer to sine wave [13]. The other disadvantage is that the capacitors should be pre-charged before

operation, which is why its named flying capacitor, since the capacitor float with respect to earth's potential. The 5-level flying capacitor MLI is shown in Fig. 2.2.

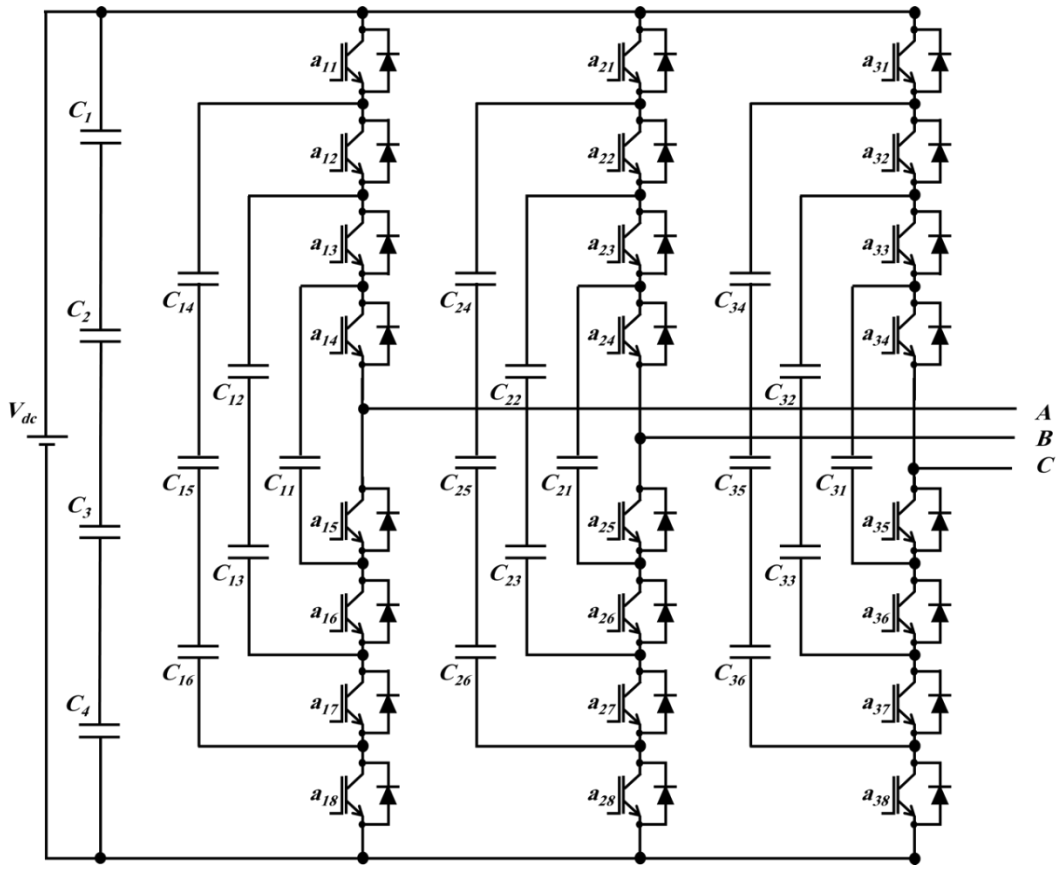

Fig. 2.2 3-Phase 5-level Flying capacitor MLI

2.2 Diode Clamped

The diode clamped MLI uses clamping diodes in order to limit the voltage stress of power devices [18]. One of the disadvantages of the diode clamped MLI is the significant increase in the number of diodes with the number of levels. Another disadvantage of the diode clamped MLI is the charge-up, discharge and balancing of

the DC-link capacitors [15]. Also Diode Clamped MLI uses single high power DC source as an input [19], which is not suitable for some applications, some papers as [20] discussed dividing the single DC power source into isolated DC sources. The 5-level Diode Clamped MLI is shown in Fig. 2.3 [21].

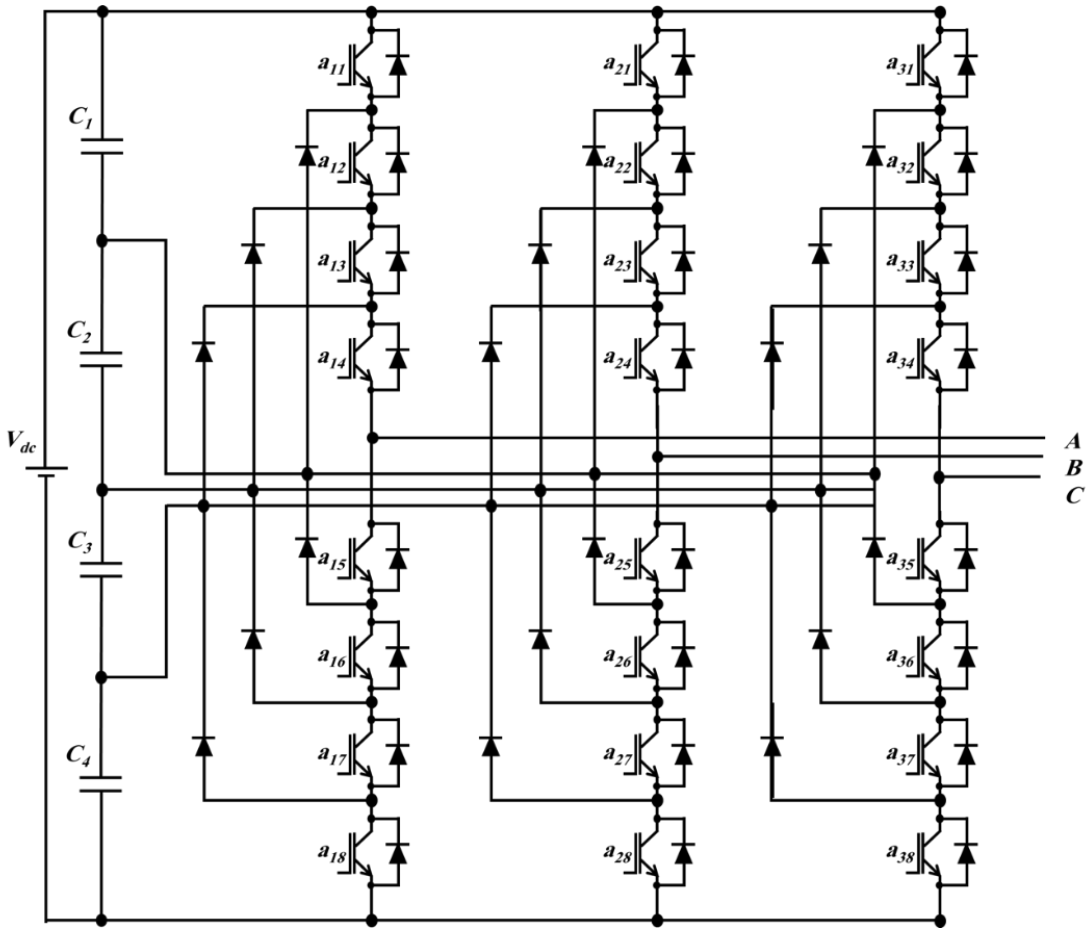

Fig. 2.3 3-Phase 5-Level Diode-clamped MLI

2.3 Modular Multilevel Cascaded Converter (MMCC)

The main advantages of the MMCC are the modularity and scalability. MMCC is built using cells as the main building block. Hence, MMCC is one of the simplest MLI inverter in terms of designing. The MMCC can be classified into four main formations:

1. Double-Star Chopper-Cells MMCC (DSCC-MMCC) [25-31]
2. Double-Star Bridge-Cells MMCC (DSBC-MMCC) [31-33]
3. Single-Star Bridge-Cells MMCC (SSBC-MMCC) [34-36]
4. Single-Delta Bridge-Cells MMCC (SDBC-MMC) [37-39]

2.3.1 Double-Star Chopper-Cells MMCC (DSCC-MMCC) And Bridge-Cells MMCC (DSBC-MMCC)

Both the DSCC and DSBC use the same concept of the MMCC. The difference between them is that the DSCC uses half-bridge (chopper) cell as a modular building block, and the DSBC uses full-bridge (H-Bridge) cell as a modular building block. The DSCC topology uses less number of switching components compared to DSBC and other conventional topologies [40]

For a three phase DSCC or DSBC MMCC, it consists of three legs to produce three-phase output voltage. Each leg contains two arms, upper and lower arms. Fig. 2.4 illustrates the upper and lower arms of a three-phase DSCC/DSBC-MMCC.

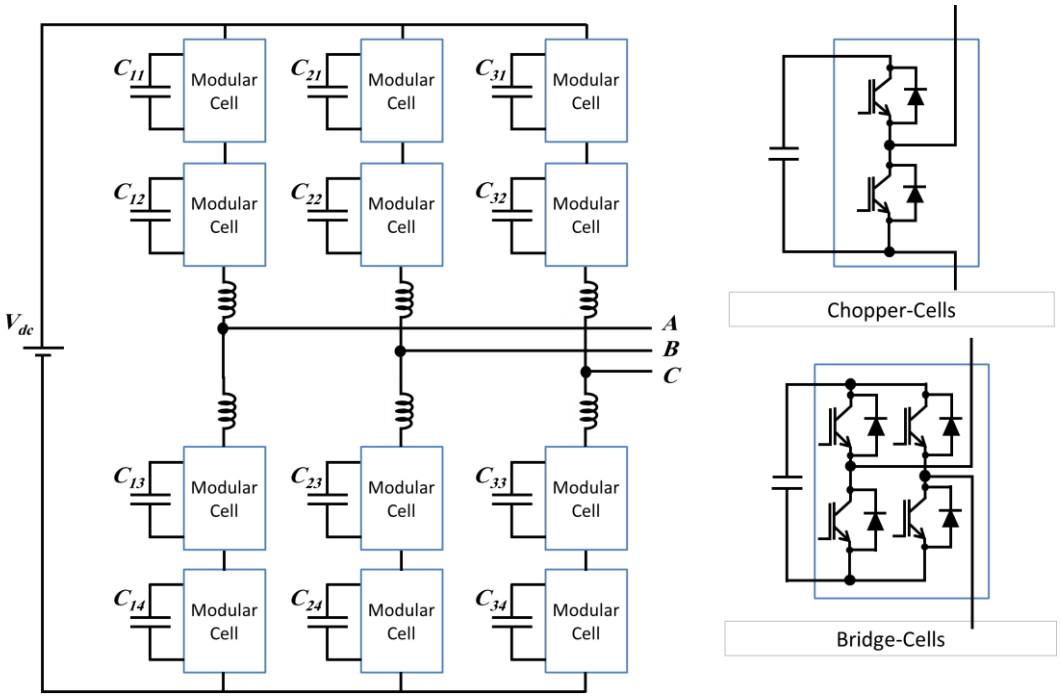

Fig. 2.4 Double-Star Chopper-Cells (DSCC) and Bridge-Cells (DSBC) MMCC

For m-level MMCC, the upper and lower arms should contain m-1 cells connected in series, where the sum of the voltages of all the capacitors in both arms of one leg must be equal to the total DC link voltage minus the AC voltage drop in the arm inductances [25].

One disadvantage of this type of MMCC is that it uses many capacitors in its design; capacitor voltage balancing represents a bottleneck in MMCC operation. To control the charging and discharging of the capacitor, the flow of current should be controlled, where the capacitor is charged if the current flows towards the cell from the positive terminal, and is discharged if the current flows in the opposite direction [27].

2.3.2 Single-Star Bridge-Cells (SSBC-MMCC) And Single-Delta Bridge-Cells (SDBC-MMCC)

Both the SSBC and SDBC use the same concept of the MMCC. The difference between them is that the SSBC is star-connected to the grid, and SDBC is delta-connected to the grid. However, isolated DC supplies are required in this configuration.

The SSBC-MMCC and SDBC-MMCC typically can be built using more than one H-bridge (bridge-cell) as a building block, where these building blocks are connected together in series. Each H-Bridge block produces three output states (V_{dc}, 0, and $-V_{dc}$). Fig. 2.5 shows a three-phase 5-level SSBC-MMCC, where each phase consists of two H-Bridges cascaded together.

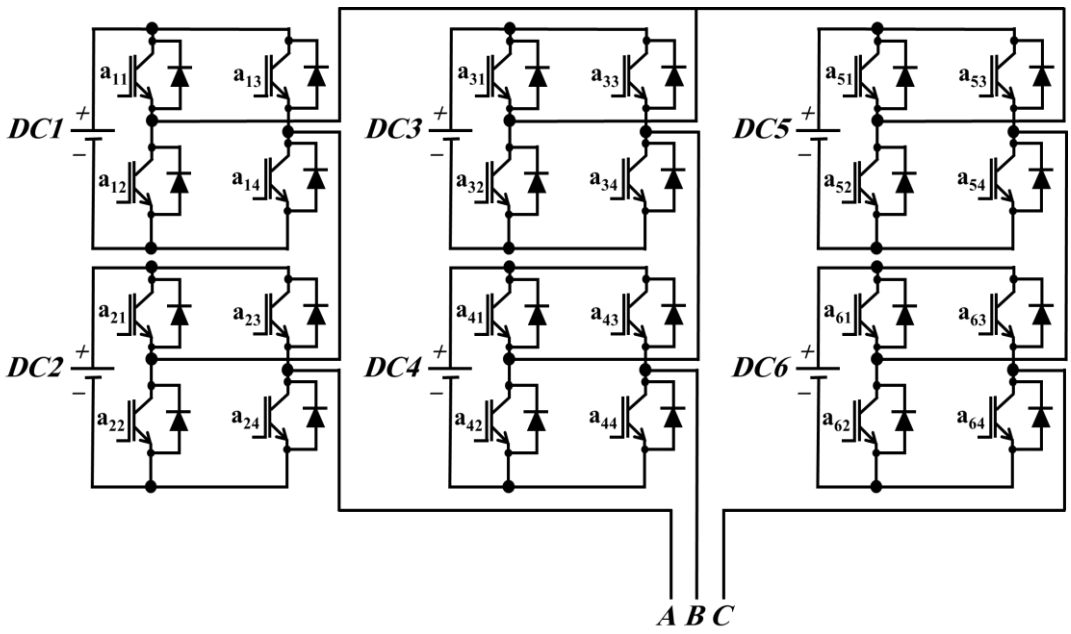

Fig. 2.5 Single-Star Bridge-Cells (SSBC) MMCC.

An m-level SSBC-MMCC contains n H-bridges per phase, and produces m-levels as output voltage per phase. In the following subsections, a brief introduction to the controlling techniques is introduced for the SSBC-MMCC. Table 2.1 shows a brief comparison between all the aforementioned MLI types.

Table 2. 1: Required components for different m-level inverter types

Converter Type	**Switches**	**Flying Capacitors**	**Clamping Diodes**	**Level Capacitor**	**DC supply**
Flying Capacitor	6(m-1)	3(m+1)(m+3)/8	-----	m-1	1
Diode Clamped	6(m-1)	-----	3(m+1)(m+3)/8	m-1	1
DSCC-MMCC	3(m-1)	-----	-----	6(m-1)	1
DSBC-MMCC	6(m-1)	-----	-----	6(m-1)	1
SDBC-MMCC	6(m-1)	-----	-----	3(m-1)/2	3(m-1)/2 isolated
SSBC-MMCC	6(m-1)	-----	-----	3(m-1)/2	3(m-1)/2 isolated

As seen from the previous table that SDBC-MMCC and SSBC-MMCC have the least components MLI types, since there is no any flying capacitors, clamping diodes, and level capacitors in their structure. This work focusses typically on SSBC-MMCC type.

CHAPTER 3: CONTROLLING TECHNIQUES OF MULTI LEVEL INVERTERS

There are several control techniques to control the Multilevel Inverters (MLIs). In the surveyed literature, the most common controlling techniques are presented, namely sinusoidal Pulse Width Modulation (PWM) with level shifts and/or phase disposition [41-44], Space Vector Modulation (SVM) [45-49], and Selective Harmonic Elimination (SHE) [50-83].

3.1 Sinusoidal Pulse Width Modulation (SPWM)

Sinusoidal PWM (SPWM) technique is one of the simplest modulation techniques. As illustrated in Fig. 3.1, simply to generate SPWM, a sinusoidal reference is compared to high frequency triangular carriers, where the number of carriers depends on the number of levels. The result represents the gating signals to the switches. The carrier frequency should be high enough in order to be able to filter its effect later using a small and simple filter. Otherwise, if the carrier frequency is low and close to the fundamental frequency, it will be difficult to filter out the harmonics, and a bulky filter will be needed. Power Electronics based Converters generate discrete output waveforms. Discrete output waveforms contain high harmonic, which require large inductances connected in series to reduce and filter the harmonic [41]. The increase in harmonics causes heating and de-rating of the electronic devices which affect the performance the devices [42]. As a result, the SPWM technique is used to reduce harmonics, especially with high frequency operation [43].

A main limitation in SPWM is the harmonic performance at low frequency operation. Yet a trade-off exists, where in high power applications, high rated power electronics switches, with low switching frequency capability, are needed. In addition, in low power applications, the switching losses will be high; hence, the efficiency will decrease [44].

An m-level inverter can be controlled using a sine wave reference and ‘m-1’ triangular carriers. The sine wave is compared to each triangular carrier and the result will control one level of the m-level inverter. Carriers used in multilevel inverter can be classified into vertically shifted (Fig 3.1) and horizontally shifted (Fig 3.2).

Advantage of horizontally shifted carriers scheme is that, each module is switched on and off with a constant number of times by period, i.e. all the switches of all levels will remain switching given any modulation index. On the other hand, in the vertically shifted carrier operated at low modulation index, some switches will stop switching depending on the modulation index required. Advantage of Vertically shifted carriers is that it can be easily implemented using any digital controller.

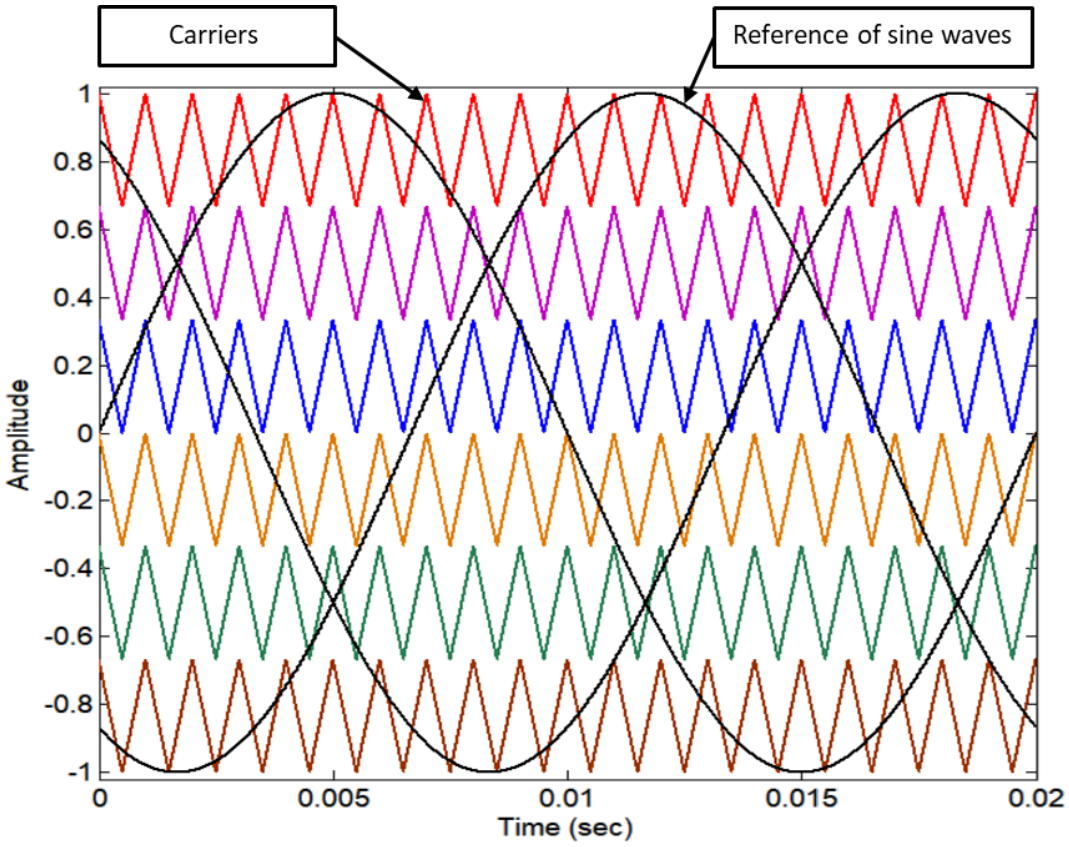

Fig. 3.1 SPWM modulation technique with vertically shifted carriers for 7-level inverter

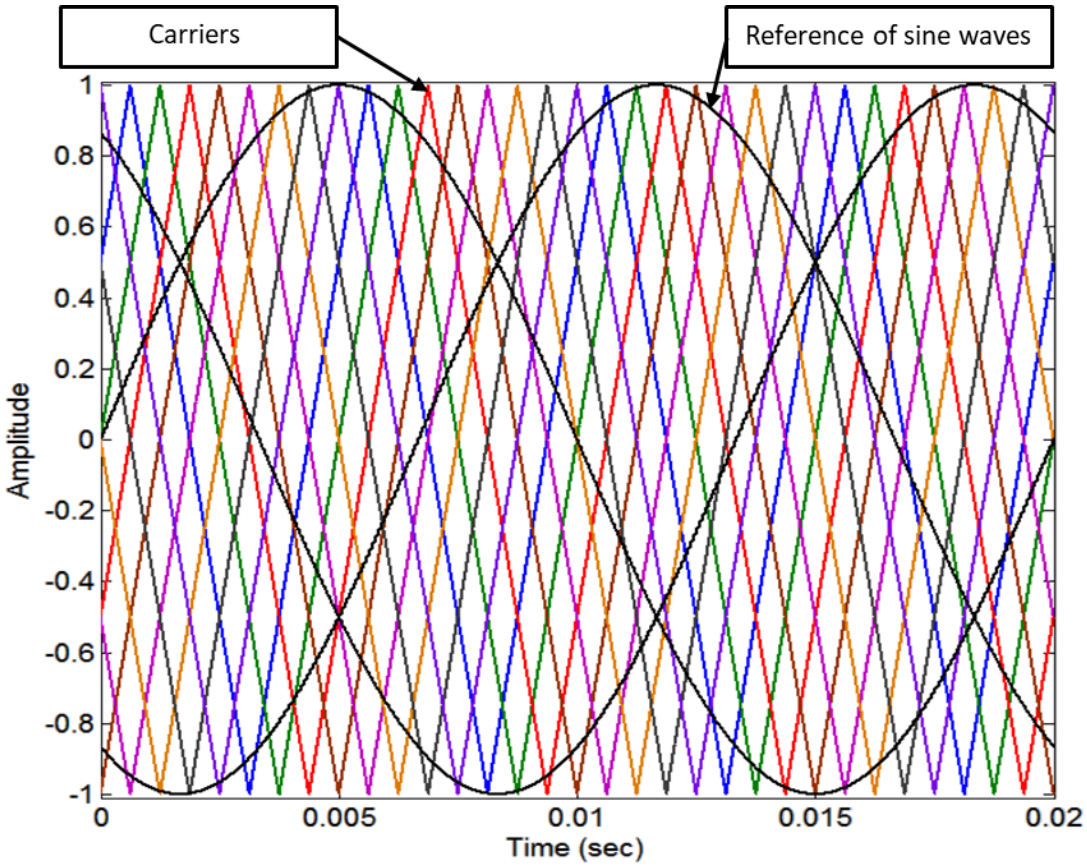

Fig. 3.2 SPWM modulation technique with horizontally shifted carriers for 9-level inverter

3.2 Space Vector Modulation (SVM)

SVM identifies the switching state of the cells in the inverter as a point in the complex α-β space [45]. Then a phasor reference which rotates in the α-β plane at the fundamental frequency is sampled within each switching period, and the nearest three switching states are selected with duty cycles calculated to reach the desired inverter output voltage [46-48]. One of the main advantages of SVM is the 15% increase in the linear range of the inverter gain when compared with sinusoidal PWM. Fig 3.2 shows

all possible switching vectors for a three-level inverter [49]. However, the complexity in SVM will exponentially increase with the increase in number of levels.

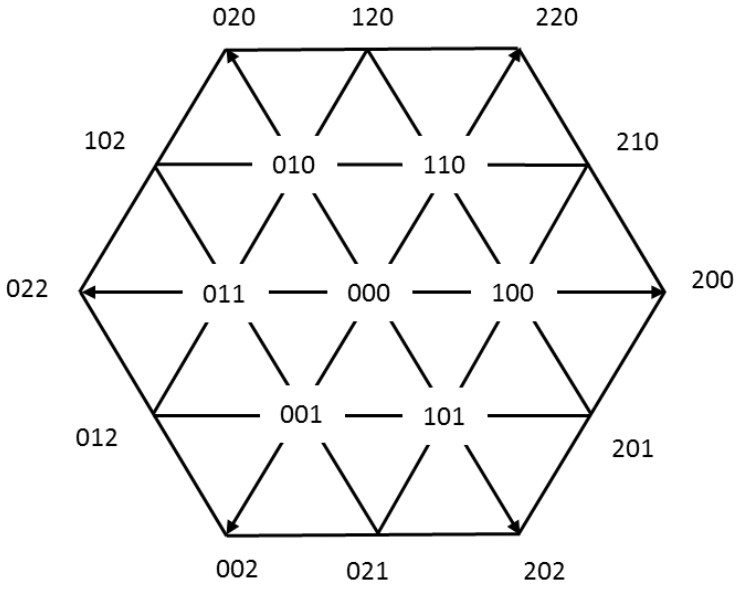

Fig. 3.3 Space Vector Modulation reference vectors for 3-level MLI.

3.3 Selective Harmonic Elimination (SHE) Technique

In high power applications, Selective Harmonic Elimination (SHE) approach is the preferred modulation technique due to the limited switching frequency capability at that level of power [50, 51], which causes less switching power losses, where the output voltage quality of the inverter is enhanced by eliminating the low order harmonics. The SHE technique provides the highest output power quality at a low switching frequency when compared with other PWM techniques [50].

SHE problem can be defined by several ways, as mentioned in the next figure. SHE technique is complicated and it takes time to solve the SHE equations [51], since a set of non-linear transcendental equations should be solved to find the desired switching angles for any value of the modulation index [52]. SHE technique involves solving number of nonlinear, transcendental equations that relates between the amplitude of fundamental wave and each harmonic, and the switching angles. [53]

Usually, the non-linear transcendental SHE equations were solved using Newton Raphson method. The disadvantage in using numerical iterative computation in such application that it will add more computational effort and the solution time can be difficult in real-time operation [54,55]. By increasing the number of levels, more harmonics could be eliminated, so the produced output voltage Total Harmonic Distortion (THD) will be reduced. On the other hand, increasing the number of levels increases the numbers and complexity of the non-linear equations.

SHE for MLIs has been surveyed extensively in literature. The study in [56] presents a dc-link voltage ripple compensation method using SHE-PWM. This method modifies the modulation index according to the dc-link voltage ripple. This modification changes the switching functions so that the low-order harmonics generated in the output due to the dc-link voltage ripple are eliminated. The method implemented in [57] was applied on three-phase, 5-level MLI only while compensating the voltage ripple of the dc-link for flying-capacitor (FC)-based active neutral- point-clamped MLIs. The method implemented in [58] was applied on a 7-level MLI only using the Bee optimization method for SHE. The method implemented in [59] was applied on 5-level MLI, using a method based on rules of equal area and superposition of Centre of Gravity (CG) of the PWM. The study presented in [60] showed that

switched-mode operation allows the miniaturization of excitation circuitry, but suffers from high harmonic distortion. Ref [61] provided a comprehensive review of the SHE-PWM modulation technique, aimed at its application to multilevel converters. Ref [62] demonstrates SHE technique that allows grid-connected PV inverters to be controlled using a switching frequency of less than 1 kHz , and the proposed system was able to meet utilities regulations, IEEE and IEC standards. Ref [63] used SHE-PWM to eliminate low-order harmonics, enabling a more efficient design of the LCL filter. Ref [64] developed harmonics injection and equal area criteria based on four equation method to realize optimal SHE-PWM where the proposed method does not involve complex group of equations and in the case of a large number of switching angles it is much easier to be utilized. Ref [65] proposed a method called selective harmonic mitigation PWM, which avoids the elimination of some specific harmonics, and studies all harmonics and the THD as a global problem. Ref [66] introduced a new three-phase harmonic decomposition technique to extract selected harmonics from grid connected converters. Ref [67] proposed a new technique named Selective Harmonic Compensation (SHC), which compensates the power system background harmonics, while operating at very low switching frequencies.

A generalized formulation for SHE-PWM control approach has been presented in [68] which is suitable for high-power cascaded multilevel. Ref [69] confirmed the complexity of SHE and presented a method of solution to find the switching angles based on the rapid expansion of $\cos(n\alpha)$. Ref [70] proposed a unified approach to simplify the complex SHE nonlinear equations and to compute the switching angles, where this method is confirmed and used in this thesis.

Depending on some factors like DC component, even harmonics and odd harmonics are all equal zero, the nonlinear equations can be reduced and simplified, hence, the Quarter wave Symmetry can be chosen. [71]

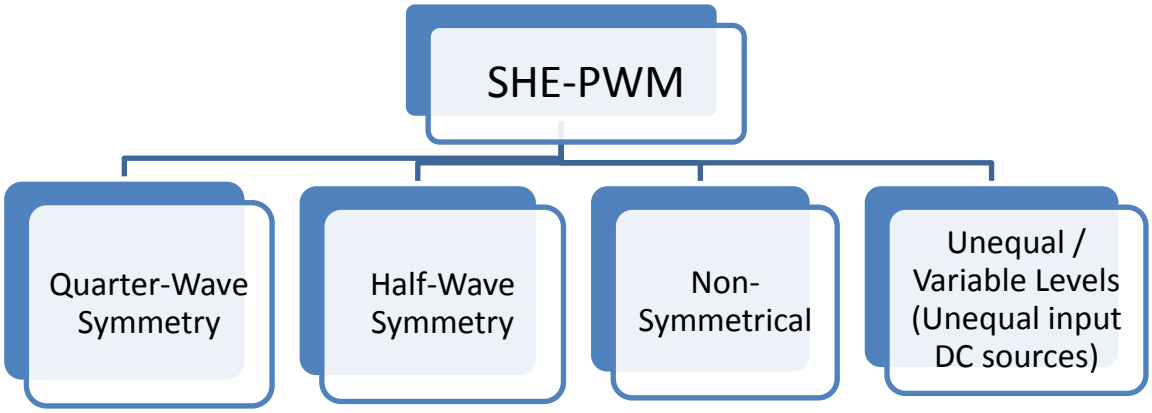

Fig. 3.4 SHE-PWM types

The Quarter Wave Symmetry is chosen to simplify the complex SHE non-linear equation in order to use it online. The simplified non-linear equations are solved first offline for the required range of modulation index. Then all the angles are stored in a lookup table or a trained Artificial Neural Network (ANN) as addressed in chapter 5. Finally using ANN, the online SHE technique can be applied. One of the important advantage of using online SHE is the full controllability of the converter to control the power flow between the converter and the grid with optimized harmonic performance. In addition, it is hard to solve the non-linear transcendental equations for the entire range of modulation region. In [72], Artificial Neural Network (ANN) has been used to

achieve quick results for the SHE non-linear transcendental equations. By using a proportional-integral (PI) control, the control can perform a real-time calculation for multilevel inverter's (MLI) switching angles over a wide range of modulation indexes. [73]

3.4 SHE Operation For SSBC-MMCC

In addition to controlling the fundamental component, every level can be used to eliminate one harmonic in which n cells in SSBC-MMCC can eliminate (n-1) harmonics. For example, in MMCC with 4 cells, 3 harmonics can be eliminated. In order to obtain an output phase voltage with a low THD, the H-bridges in the SSBC-MMCC are controlled to eliminate the low order harmonics and yield the required fundamental component. This means that for an m-level SSBC-MMCC, (m-3)/2 harmonics can be eliminated for a single pulse operation of each H-bridge with a controllable modulation index. The Fourier series of the SSBC-MMCC single-phase output phase voltage can be expressed as:

$$v_o(\omega t) = \sum_{h=1,3,5\ldots}^{\infty} V_h sin(h\omega t) \tag{3.1}$$

In order to obtain a low THD, the lower order harmonics should be eliminated first. For instance, in three-phase 9-level (4 cells per phase) SSBC-MMC, the 5^{th}, 7^{th}, and 11^{th} order harmonic should be eliminated. Therefore, four nonlinear voltage equations for the fundamental, 5^{th}, 7^{th}, and 11^{th} order harmonics will be produced based on (3.1) as shown in (3.2).

$$4V_{dc}[\qquad\qquad\qquad\qquad\qquad\qquad\qquad\qquad\qquad\qquad] \tag{3.2}$$

$$V_5 = \frac{4V_{dc}}{\pi}[\cos(5\theta_1) + \cos(5\theta_2) + \cos(5\theta_3) + \cos(5\theta_4)]$$
$$V_7 = \frac{4V_{dc}}{\pi}[\cos(7\theta_1) + \cos(7\theta_2) + \cos(7\theta_3) + \cos(7\theta_4)]$$
$$V_{11} = \frac{4V_{dc}}{\pi}[\cos(11\theta_1) + \cos(11\theta_2) + \cos(11\theta_3) + \cos(11\theta_4)]$$

The first equation (at the fundamental frequency) is used to set the fundamental component. Equation (3.3) defines the modulation index, which will vary from 0 to 1 in order to obtain the required angles, where the fundamental component can be controlled by varying the value of the modulation index [75]

$$M = \frac{V_1}{4\left(\frac{\mathrm{n}V_{dc}}{\pi}\right)} \qquad (0 < M < 1) \tag{3.3}$$

Where n is number of cells per phase, 4 in this case, by substituting (3.3) in (3.2), and to eliminate the 5^{th}, 7^{th}, and 11^{th} order harmonics, the corresponding voltages are set to zero, this will give the set of equations to be solved using numerical methods or optimization methods.

$$\begin{aligned} 4M &= [\cos(\theta_1) + \cos(\theta_2) + \cos(\theta_3) + \cos(\theta_4)] \\ 0 &= [\cos(5\theta_1) + \cos(5\theta_2) + \cos(5\theta_3) + \cos(5\theta_4)] \\ 0 &= [\cos(7\theta_1) + \cos(7\theta_2) + \cos(7\theta_3) + \cos(7\theta_4)] \\ 0 &= [\cos(11\theta_1) + \cos(11\theta_2) + \cos(11\theta_3) + \cos(11\theta_4)] \end{aligned} \tag{3.4}$$

The modulation index M can be set in two regions:

(i) Linear region, where the set of equations can be solved, and can give multiple set of solutions

(ii) Infeasible region, known as over modulation, where there is no solution can be obtained for the equations. As a result, the set of equations will be solved with a small error to be tolerated for the high harmonics [71].

One easy way to solve the set of nonlinear transcendental equations in (3.4) would be an iterative method such as the Newton–Raphson method, but the other way, which is being used here, is the mathematical model of switching [70]. This approach here is based on solving polynomial equations using the theory of resultants, which returns all the possible solutions for (5). The first step requires transforming the transcendental equations in (3.5) into polynomial equations using the change of variables,

$$\begin{aligned} x_1 &= \cos(\theta_1) \\ x_2 &= \cos(\theta_2) \\ x_3 &= \cos(\theta_3) \\ x_4 &= \cos(\theta_4) \end{aligned} \tag{3.5}$$

The trigonometric identities are expanded as follows:

$$\begin{aligned} \cos(5\theta) &= 5\cos(\theta) - 20\cos^3(\theta) + 16\cos^5(\theta) \\ \cos(7\theta) &= -7\cos(\theta) + 56\cos^3(\theta) - 112\cos^5(\theta) + 64\cos^7(\theta) \\ \cos(11\theta) &= -11\cos(\theta) + 220\cos^3(\theta) - 1232\cos^5(\theta) + 2816\cos^7(\theta) \\ &\quad - 2816\cos^9(\theta) + 1024\cos^{11}(\theta) \end{aligned} \tag{3.6}$$

By substituting equation (3.5) in (3.6)

$$\begin{aligned} \cos(5\theta) &= 5x - 20\mathrm{x}^3 + 16\mathrm{x}^5 \\ \cos(7\theta) &= -7x + 56\mathrm{x}^3 - 112\mathrm{x}^5 + 64\mathrm{x}^7 \\ \cos(11\theta) &= -11x + 220\mathrm{x}^3 - 1232\mathrm{x}^5 + 2816\mathrm{x}^7 - 2816\mathrm{x}^9 + 1024\mathrm{x}^{11} \end{aligned} \tag{3.7}$$

Then by using the same technique with equation in (3.4), the resultant equations will be

$$\begin{aligned} 4M &= x_1 + x_2 + x_3 + x_4 \\ 0 &= \sum_{i=1}^{4} \left(5x_i - 20x_i^3 + 16x_i^5\right) \end{aligned} \tag{3.8}$$

$$0 = \sum_{i=1}^{4} \left(-7x_i + 56x_i^3 - 112x_i^5 + 64x_i^7\right)$$

$$0 = \sum_{i=1}^{4} \left(-11x_i + 220x_i^3 - 1232x_i^5 + 2816x_i^7 - 2816x_i^9 + 1024x_i^{11}\right)$$

Finally, by using any iterative method to obtain the answers of (3.8), it is easy to obtain the angles by using the inverse of (3.5) given in (3.9).

$$\begin{aligned} \theta_1 &= \cos^{-1}(x_1) \\ \theta_2 &= \cos^{-1}(x_2) \\ \theta_3 &= \cos^{-1}(x_3) \\ \theta_4 &= \cos^{-1}(x_4) \end{aligned} \tag{3.9}$$

The next chapter introduces three different SHE techniques for MLIs, namely, conventional SHE, Quasi SHE and Asymmetrical SHE.

CHAPTER 4: SHE TECHNIQUES FOR SSBC-MMCC

4.1 Conventional SHE (C-SHE) Technique For SSBC-MMCC

In order to obtain an output phase voltage with a low THD, the H-bridges in the SSBC-MMCC are controlled to eliminate the low order harmonics and yield the required fundamental component. This means that for an m-level SSBC-MMCC, (m-3)/2 harmonics can be eliminated for a single pulse operation of each H-bridge with a controllable modulation index. Generally, the Fourier series expansion of the output phase voltage, in the case of unequal DC voltages, can be expressed as follows:

$$v_o(\omega \mathrm{t}) = \sum_{h=1,3,5,\ldots}^{n} \frac{4}{h\pi} (V_{dc1}\, cos(h\alpha_1) + V_{dc2}\, cos(h\alpha_2) + \cdots V_{dcn}\, cos(h\alpha_n)) sin(h\omega t) \quad (4.1)$$

Then, following expresses the harmonic components:

$$V_h = \frac{4V_{dc}}{h\pi} (k_1\, cos(h\alpha_1) + k_2\, cos(h\alpha_2) + \cdots k_n\, cos(h\alpha_n)) \quad (4.2)$$

Where n denotes the number of cascaded H-bridges in each phase, V_{dc} is the nominal DC voltage source of all H-bridges and k_1,k_2,… k_n are the unbalance factor in DC voltage where $k_n = {}^{V_{dcn}}/_{V_{dc}}$, and (4.3) defines the modulation index (M):

$$M = \frac{V_1}{4\left(\frac{V_{dc1} + V_{dc2} + \cdots V_{dcn}}{\pi}\right)} \quad (0 < M < 1) \quad (4.3)$$

For equal voltages of the cascaded H-bridges and in order to eliminate the hth harmonic(s) ($V_h = 0\ where\ h \neq 1$), and to maintain the modulation index at M, the following set of equations should be fulfilled.

$$\begin{aligned} \mathrm{M}(k_1 + k_2 + .. + k_\mathrm{n}) &= [k_1 cos(\alpha_1) + k_2 cos(\alpha_2) + \cdots + k_\mathrm{n} cos(\alpha_n)] \\ V_h &= [k_1 cos(h\alpha_1) + k_2 cos(h\alpha_2) + \ldots + k_n cos(h\alpha_n)] = 0 \end{aligned} \quad (4.4)$$

Increasing the number of levels in the SSBC-MMCC increases the number of equations to be solved, which adds more complexity.

For instance, in the three-phase 17-level SSBC-MMCC (i.e. 8 cells), Conventional SHE (C-SHE) is based on cancelling the seven low order harmonics (5^{th}, 7^{th}, 11^{th}, 13^{th}, 17^{th}, 19^{th}, and 23^{rd}) and setting the required modulation index throughout 8 controlling and independent angles.

To eliminate the 5^{th}, 7^{th}, 11^{th}, 13^{th}, 17^{th}, 19^{th}, and 23^{rd} order harmonics,

$$V_5 = V_7 = V_{11} = V_{12} = V_{13} = V_{19} = V_{23} = 0 \tag{4.5}$$

The number of switching angles are representing the harmonics that require to be eliminated, where one angle will control the desire fundamental voltage and the rest are needed to eliminate harmonics [75]. For example, in the 17-level C-SHE operation of a 17-level converter (shown in Fig. 4.1), the required equations are formulated as follows (assuming equal dc voltage of the cells):

$$\begin{aligned}
0 &= [cos(\theta_1) + cos(\theta_2) + \cdots cos(\theta_8)] - 8M \\
0 &= [cos(5\theta_1) + cos(5\theta_2) + \cdots cos(5\theta_8)] \\
0 &= [cos(7\theta_1) + cos(7\theta_2) + \cdots cos(7\theta_8)] \\
0 &= [cos(11\theta_1) + cos(11\theta_2) + \cdots cos(11\theta_8)] \\
0 &= [cos(13\theta_1) + cos(13\theta_2) + \cdots cos(13\theta_8)] \\
0 &= [cos(17\theta_1) + cos(17\theta_2) + \cdots cos(17\theta_8)] \\
0 &= [cos(19\theta_1) + cos(19\theta_2) + \cdots cos(19\theta_8)] \\
0 &= [cos(23\theta_1) + cos(23\theta_2) + \cdots cos(23\theta_8)]
\end{aligned} \tag{4.6}$$

After obtaining the eight independent switching angles ($\theta_1 \; to \; \theta_8$) using (4.6) for every modulation index, these eight angles shown in Fig. 4.2 will control all the switches of the 8 cells. Finally, the obtained angles are saved in a lookup table, which

will be used later to train the Artificial Neural Network (ANN) which is clarified in Chapter 5.

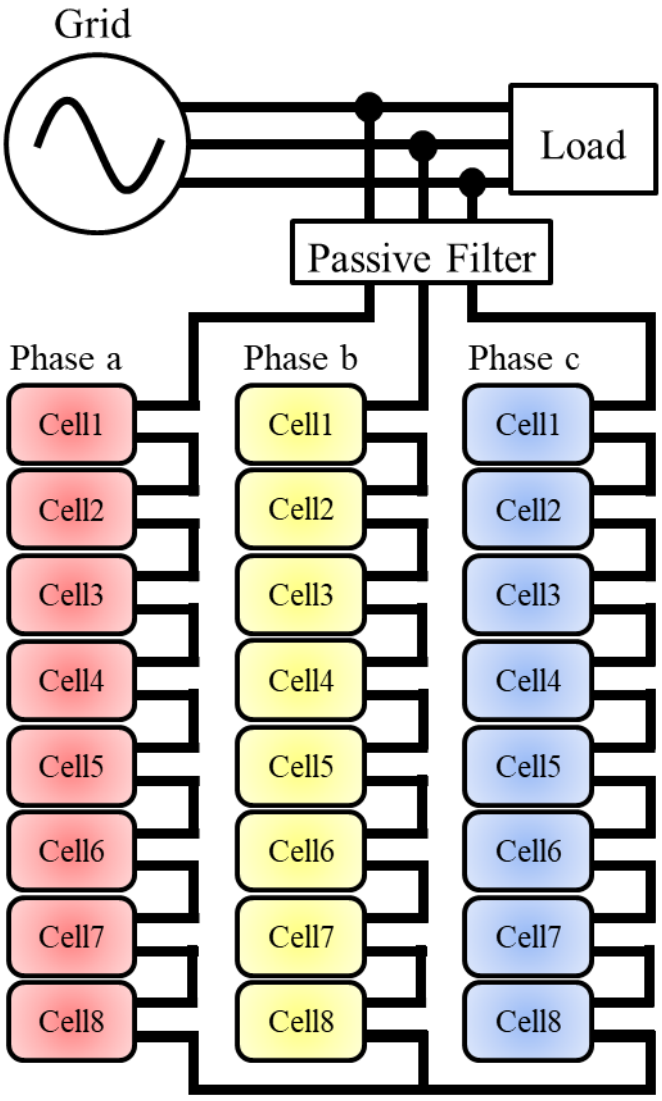

Fig. 4.1 17-level (8 H-bridges) 3-phase grid-connected SSBC-MMCC.

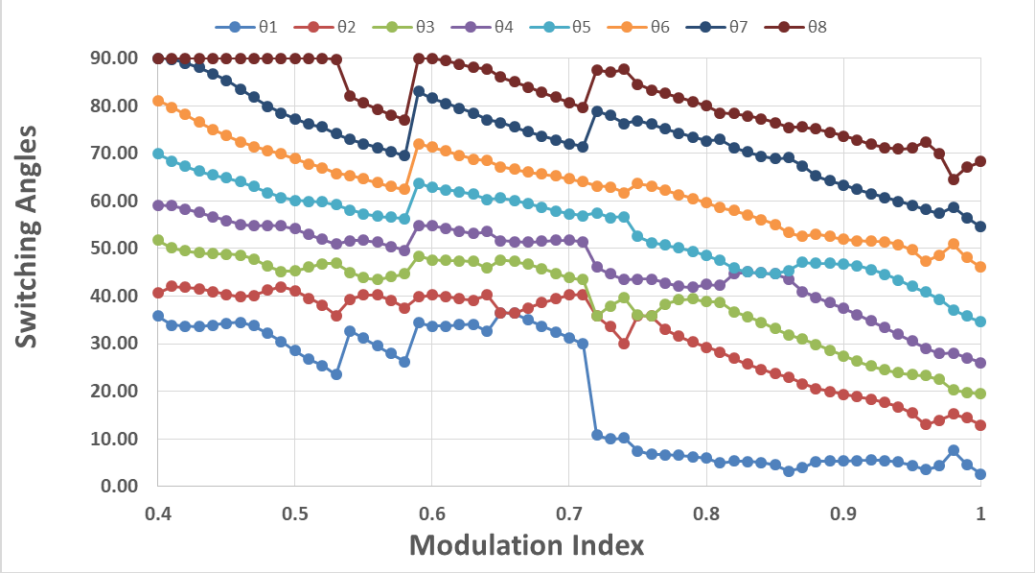

Fig. 4.2 The switching angles change with the modulation index in C-SHE of three-phase SSBC-MMCC.

Simulating the system with modulation index of 0.8, the output phase voltage is shown in Fig. 4.3 while it is shown that the 5^{th}, 7^{th}, 11^{th}, 13^{th}, 17^{th}, 19^{th}, and the 23^{rd} order harmonics are successfully eliminated in the Frequency spectrum in Fig. 4.4.

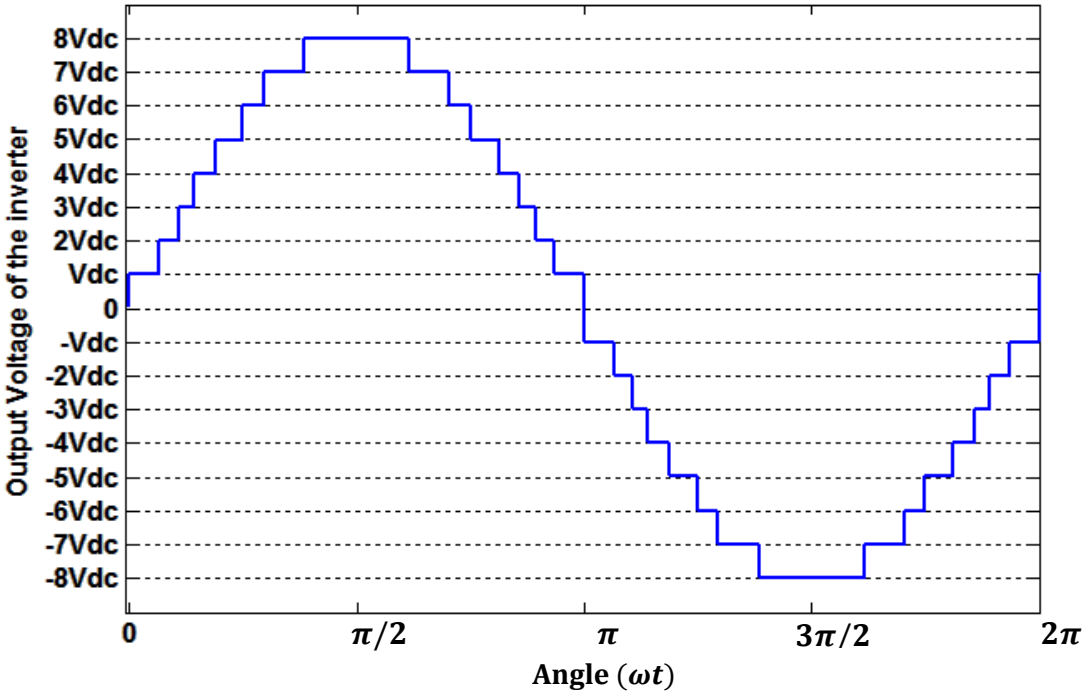

Fig. 4.3 Output phase voltage of 17-level converters using C-SHE @ M=0.8

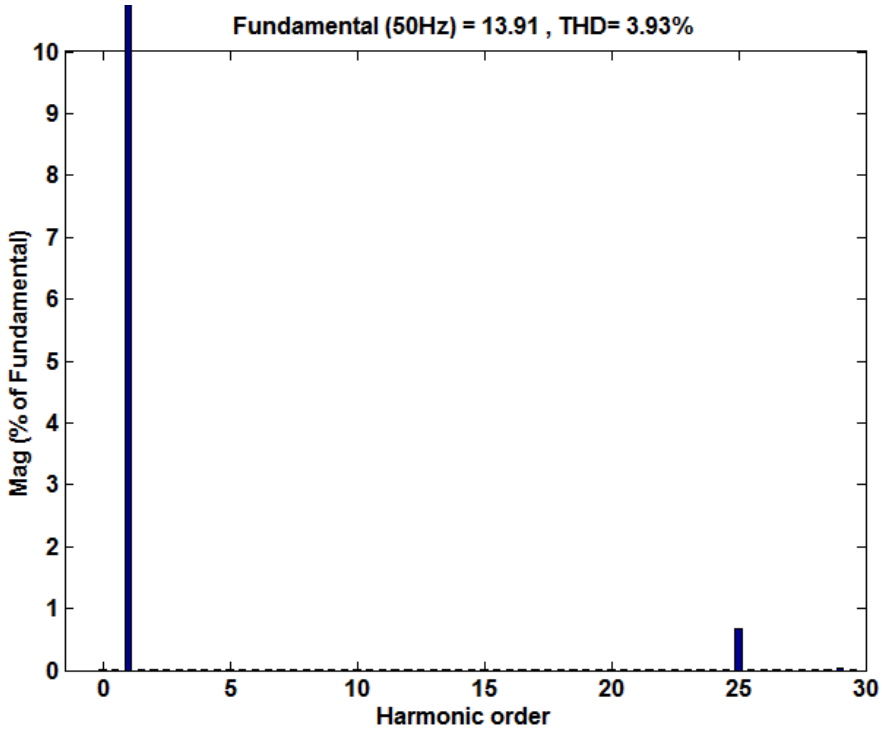

Fig. 4.4 Frequency spectrum of the 17-level output phase voltage using C-SHE

4.2 Quasi 7-Level SHE (Q-SHE)

It is clear that the C-SHE complexity for MLIs increases with the increase in the number of levels as the number of independent variables, correspondingly the nonlinear transcendental equations, increases. To overcome this complexity, the Quasi 7-Level SHE (Q-SHE) operation of MLIs is proposed. The presented technique is based on cancelling the 5^{th} and 7^{th} order harmonics irrelevant of the number of levels in three-phase MLIs, such that the solution for the angles required for the Q-SHE approach mimics that of the seven-level inverter operation. This simplifies the solution concept of the nonlinear equations, particularly with the increase in number of levels. The proposed approach can be extended for more of low order harmonic cancellation (quasi hc-level operation of an m-level converter). In the Q-SHE operation, the 5^{th} and 7^{th} order harmonics are eliminated while the dv/dt level is the same as the C-SHE operation. In general, n cells inverter can eliminate harmonics up to (n-1) harmonics. The number of the controlling angles is equal to hc+1, where hc is the number of harmonics to be eliminated (where hc < n-1). In the Q-SHE operation, for instance, 8 cells (17-level) inverter eliminating 2 low order harmonics requires 3 main controlling and independent angles. Where the first angle controls the first 6 cells and the other two controlling angles control the last two cells. Generally, the first controlling angle in the quasi hc-level operation controls all the cells from the first cell to the cell number (n-hc), as follows

$$\alpha_1 = \theta_1,\ \alpha_2 = 2\theta_1, \alpha_3 = 3\theta_1, \dots \alpha_{n-h_c} = (n - h_c)\theta_1 \tag{4.7}$$

Then the rest of the switching angles will be controlled with the rest of the controlling angles, which are $\theta_2, .., \theta_{h_c+1}$. The set of equations can be generally expressed as follows

$$V_h = \sum_{i=1}^{n-h_c} \cos(hi\theta_1) + \sum_{i=2}^{h_c+1} \cos(h\theta_i) \tag{4.8}$$

To eliminate the 5th and the 7th harmonics, their equations should be equal to zero, which means that:

$$V_5 = 0 \ \ and \ \ \ V_7 = 0 \tag{4.9}$$

For example, in the Q-SHE operation of a 17-level converter (shown in Fig. 4.1), the 5th and 7th harmonics will be eliminated and the required equations are formulated as follows:

$$\begin{aligned}
8M &= \cos(\theta_1) + \cos(2\theta_1) + \cos(3\theta_1) + \cos(4\theta_1) + \cos(5\theta_1) + \cos(6\theta_1) \\
&\quad + \cos(\theta_2) + \cos(\theta_3) \\
0 &= cos(5\theta_1) + cos(10\theta_1) + cos(15\theta_1) + cos(20\theta_1) + cos(25\theta_1) \\
&\quad + cos(30\theta_1) + cos(5\theta_2) + cos(5\theta_3) \\
0 &= cos(7\theta_1) + cos(14\theta_1) + cos(21\theta_1) + cos(28\theta_1) + cos(35\theta_1) \\
&\quad + cos(42\theta_1) + cos(7\theta_2) + cos(7\theta_3)
\end{aligned} \tag{4.10}$$

As seen from equations (4.10) all the angles are multiples of the first one except the last angles, which corresponds to eliminate the harmonics. After obtaining the three independent switching angles ($\theta_1, \theta_2, and\ \theta_3$) using (4.10) for every modulation index, these three angles will control all the switches of the 8 cells, whereas $\alpha_1 = \theta_1$, $\alpha_2 = 2\theta_1$, $\alpha_3 = 3\theta_1$, $\alpha_4 = 4\theta_1$, $\alpha_5 = 5\theta_1$, $\alpha_6 = 6\theta_1$, $\alpha_7 = \theta_2$, and $\alpha_8 = \theta_3$ are the switching angles for the 8 cells. The variation of the switching angles with the modulation index is shown in Fig. 4.5. All the 8 angles are saved in a lookup table.

Finally, after saving all the 8 angles for each modulation index from 0.1 to 1 in a lookup table, this lookup table is used to train the ANN. As seen from Fig. 4.6, all the

angles are multiple of the first angle except the last two angles. The last two angles used to eliminate the harmonics, one used to eliminate the 5th harmonic, and the other one used to eliminate the 7th order harmonic.

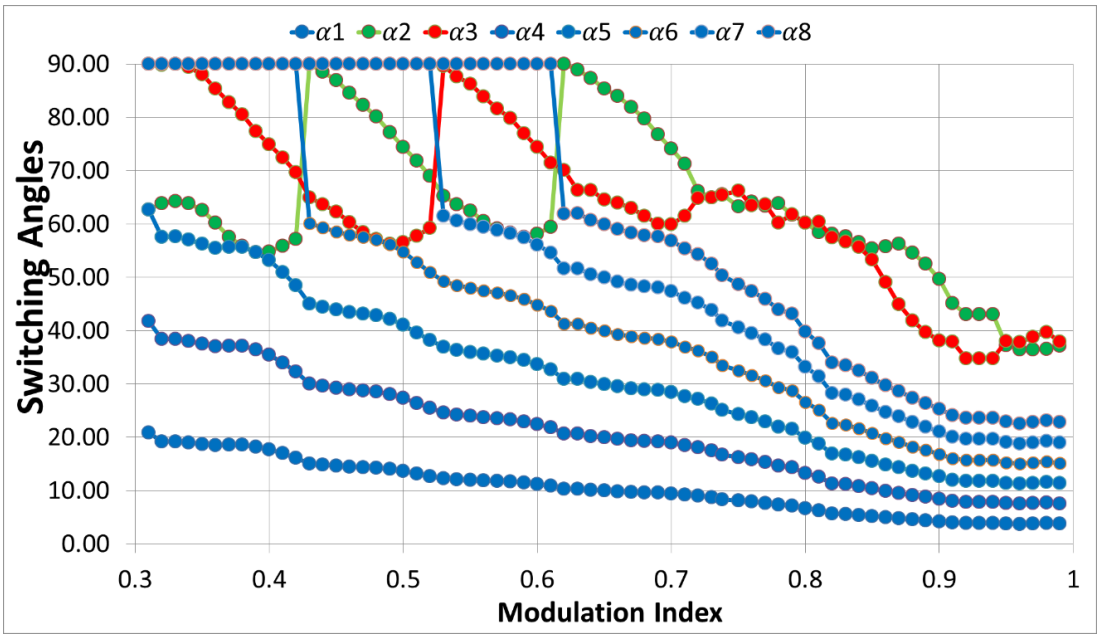

Fig. 4.5 Modulation index with its corresponding switching angles in Q-SHE of three-phase SSBC-MMCC.

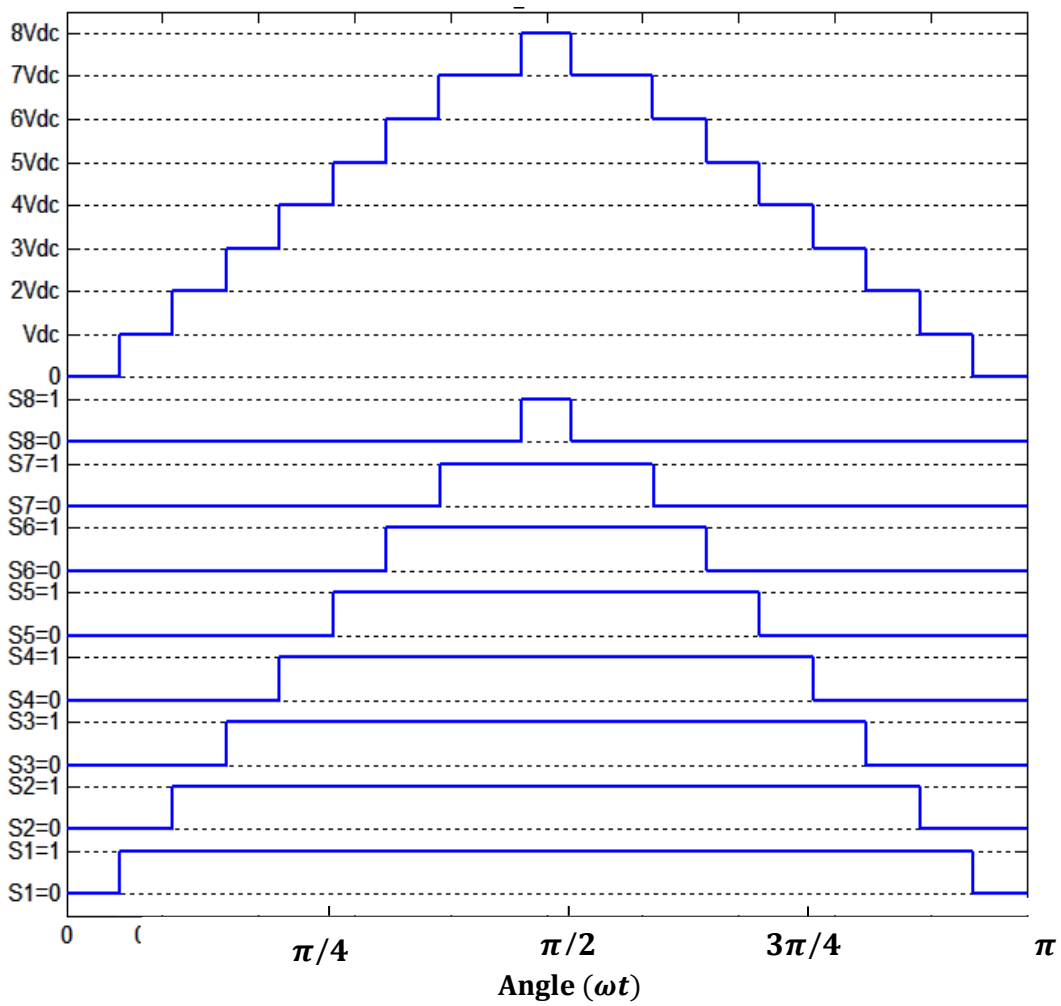

Fig. 4.6 17-level of the Q-SHE with 6 equal angles and 2 different angles

Running the system simulation for a modulation index of 0.8, the output phase voltage shown in Fig. 4.6 is obtained and the spectrum is shown in Fig. 4.7. It can be seen that the 5^{th} and 7^{th} order harmonics are successfully eliminated.

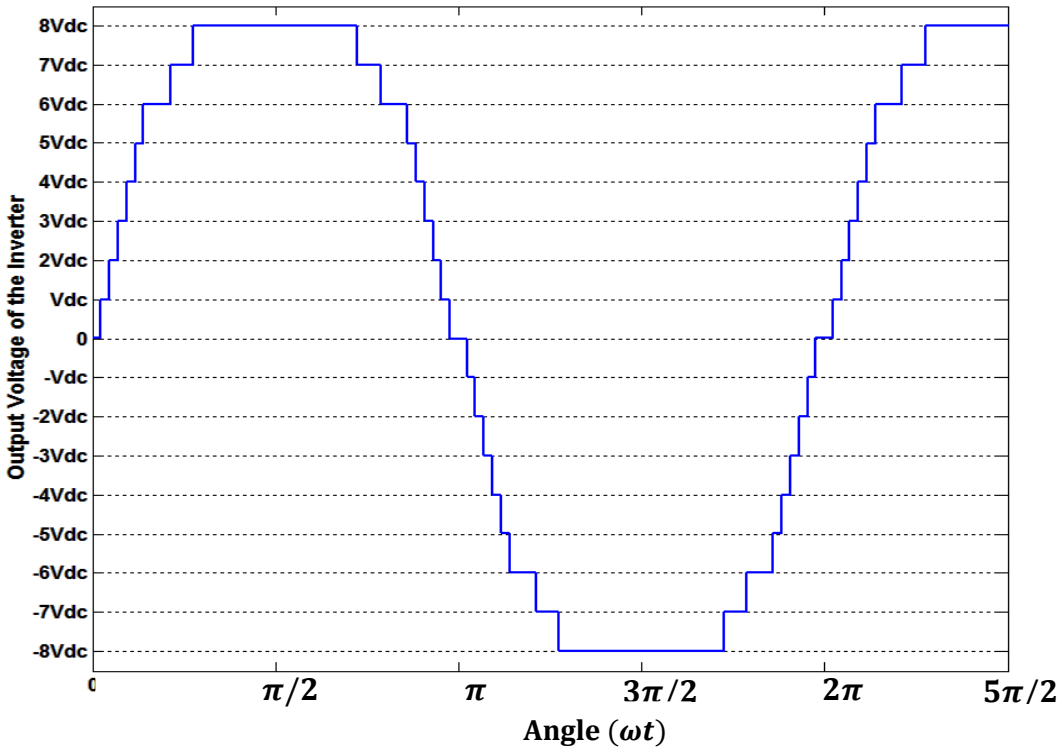

Fig. 4.7 Output phase voltage of 17-level converters using Q-SHE @ M=0.8

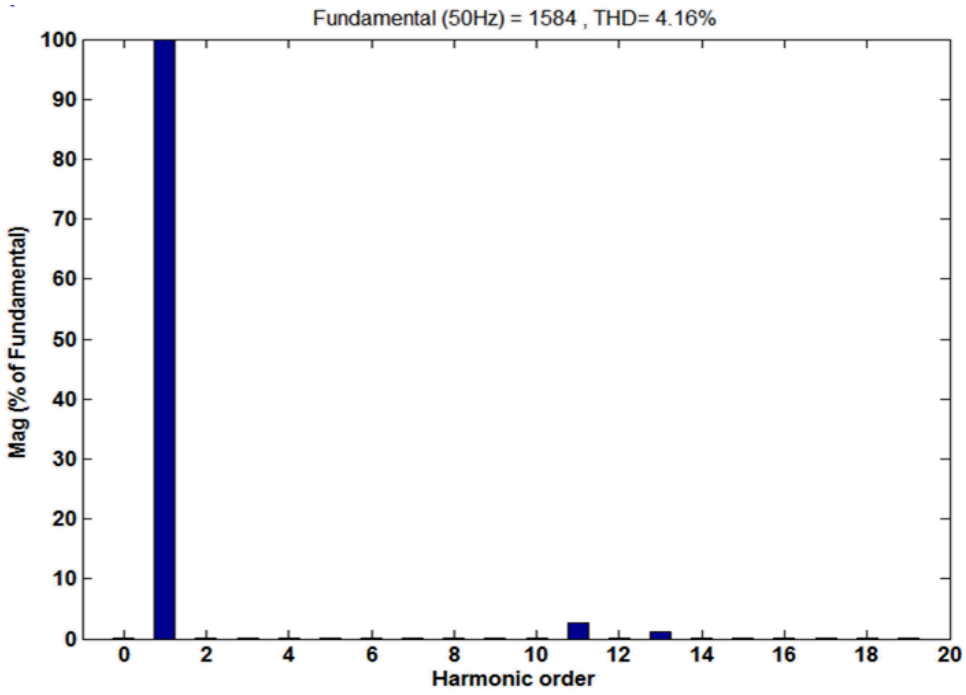

Fig. 4.8 Frequency spectrum of the 17-level output phase voltage using Q-SHE

4.3 Asymmetrical 7-Level SHE (A-SHE)

Similar to the Q-SHE, the A-SHE technique, as well, is based on eliminating the 5th and 7th harmonics irrelevant to the SSBC-MMCCs number of levels. In order to eliminate the 5th and 7th order harmonics, three angles are obtained and all the 8 angles will be controlled using the obtained 3 angles. This approach can be extended for more of low order harmonics elimination. The dv/dt level is higher than the Q-SHE operation.

In the A-SHE operation, for instance, 8 H-bridges (17-level) SSBC-MMCC, eliminating 2 low order harmonics requires 3 controlling and independent angles to control the 8 H-bridges. The first angle controls the first 2 H-bridges, the second angle controls the 3rd-5th H-bridges, and the third angle controls 6th to 8th H-bridges.

$$\alpha_1 = \alpha_2 = \theta_1, \alpha_3 = \alpha_4 = \alpha_5 = \theta_2$$
$$\alpha_6 = \alpha_7 = \alpha_8 = \theta_3 \quad (4.11)$$

In a similar fashion to Q-SHE, and to eliminate the 5th and 7th harmonics, the required equations are formulated from (4.11) as follows:

$$8M = 2\cos(\theta_1) + 3\cos(\theta_2) + 3\cos(\theta_3)$$
$$0 = 2\,cos(5\theta_1) + 3\,cos(5\theta_2) + 3\,cos(5\theta_3) \quad (4.12)$$
$$0 = 2\,cos(7\theta_1) + 3\,cos(7\theta_2) + 3\,cos(7\theta_3)$$

After obtaining the three independent switching angles ($\theta_1, \theta_2, and\ \theta_3$) using (4.12), these three angles will control the 8 H-bridges. Fig. 4.8 shows each modulation index with its corresponding switching angles.

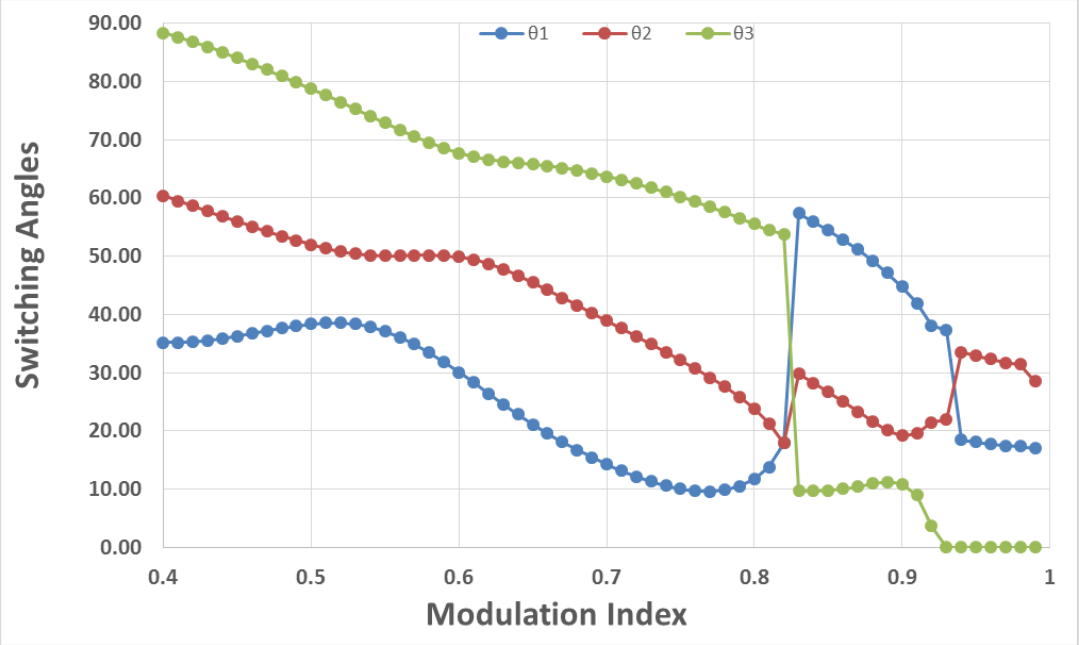

Fig. 4.9 Modulation index with its corresponding switching angles in A-SHE of three- phase SSBC-MMCC.

After obtaining, the independent switching angles which will control the 8 H-bridges. The obtained angles are saved in a lookup table which will be used later to train the Artificial Neural Network (ANN) which is clarified in Chapter 5.

Running the system simulation for a modulation index of 0.8, the output phase voltage shown in Fig. 4.9 is obtained and the spectrum is shown in Fig. 4.10. It can be seen that the 5^{th} and 7^{th} order harmonics are successfully eliminated.

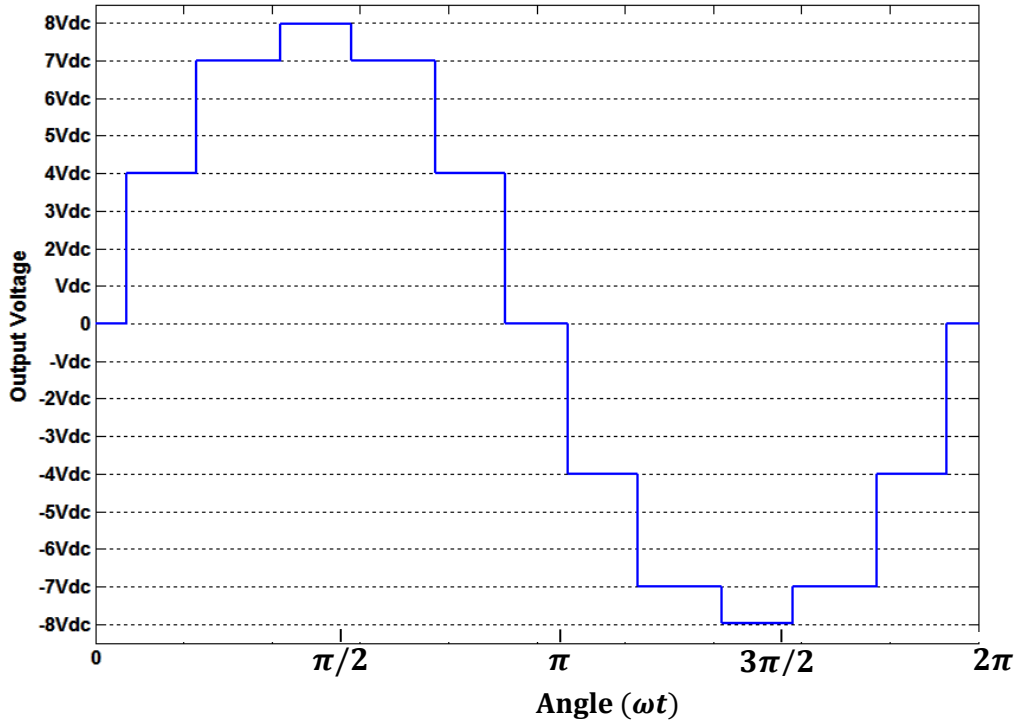

Fig. 4.10 Output phase voltage of 17-level converters using A-SHE @ M=0.8

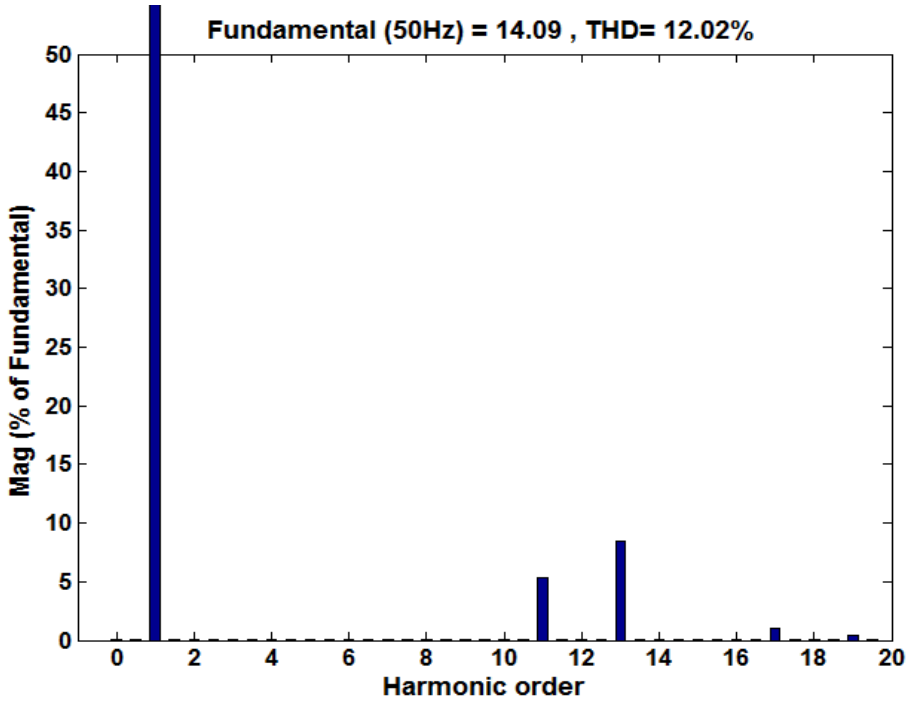

Fig. 4.11 Frequency spectrum of the 17-level output phase voltage using A-SHE

Running the system simulation for a modulation index of 0.8, the output phase voltage for the three techniques shown in Fig. 4.11. In Fig. 4.12, a comparison of THD vs modulation index is shown.

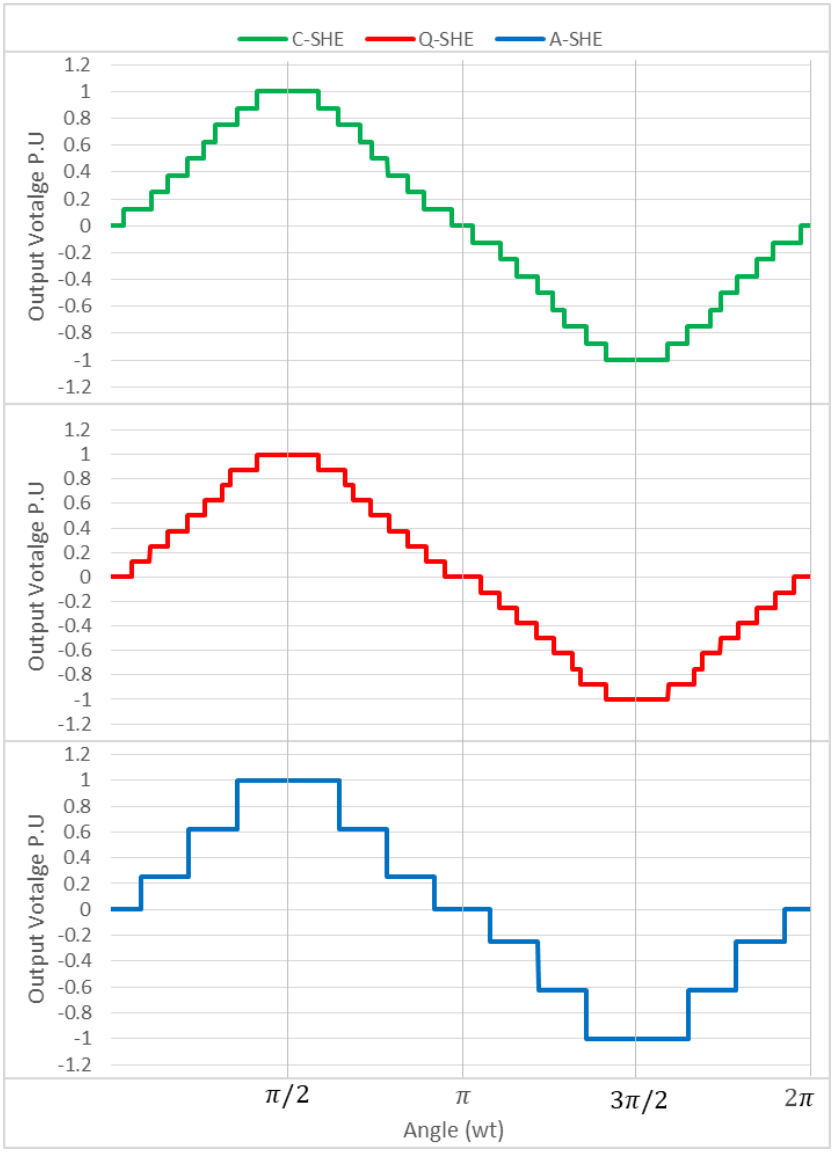

Fig. 4.12 Output phase-voltage using the three SHE approaches @ M=0.8

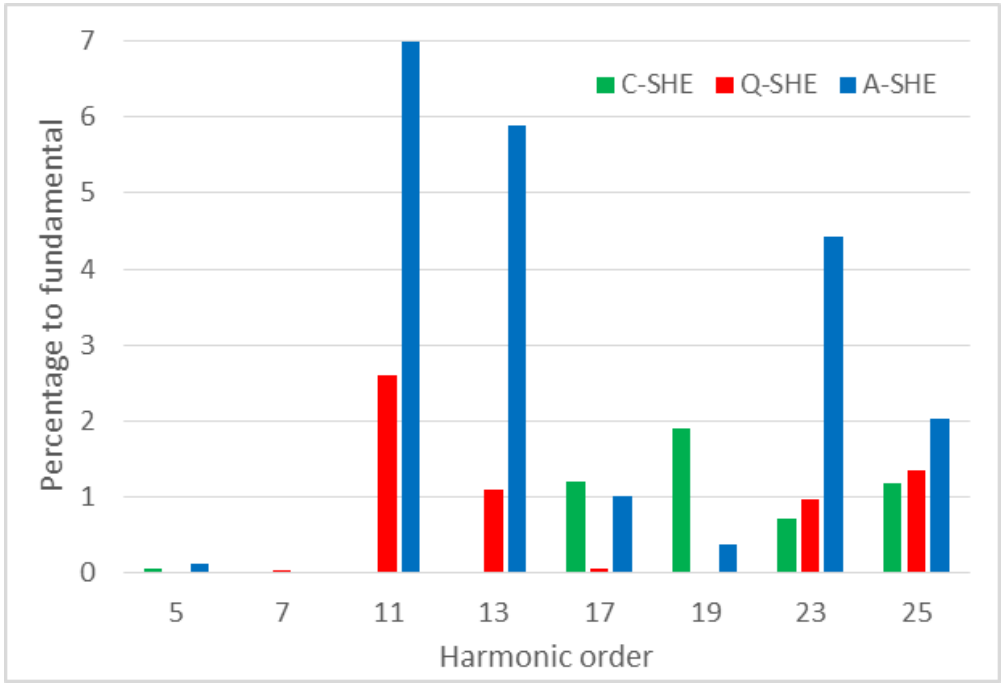

Fig. 4.13 Harmonic spectrum for the three SHE approaches @ M=0.8

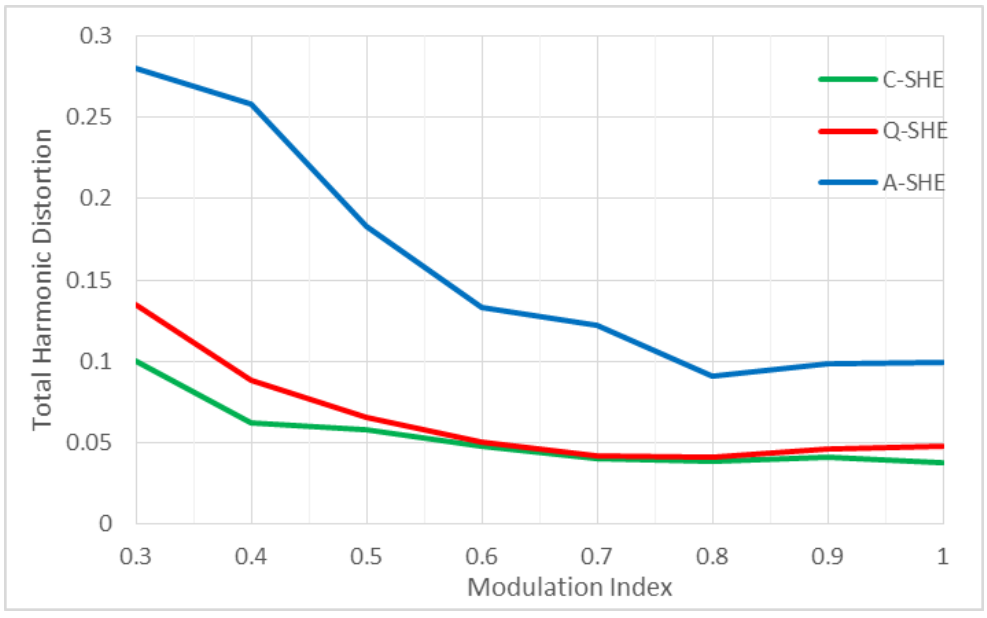

Fig. 4.14 THD % Vs. Modulation Index for the three SHE approaches conventional SHE, Quasi SHE and Asymmetrical SHE.

CHAPTER 5: GRID-CONNECTED THREE-PHASE SSBC-MMCC

In this chapter, the grid-connection mode of the three-phase SSBC-MMCC using the three SHE approaches is presented. A closed loop controller is used to control the grid-connected inverter, by supporting the inverter with both, the modulation index and the angle needed online, to maintain the inverter output power and to synchronize the inverter with the grid. Using PLL and dq synchronously rotating reference frame, the inverter output power is controlled. A 5MW medium voltage 17-level grid-connected SSBC-MMCC is considered to validate the proposed concept. Simulation results using the MATLAB/SIMULINK platform have been presented to elucidate the proposed concept.

5.1 Artificial Neural Network (ANN) For Online SHE

Artificial Neural Network (ANN) is used to produce a generalized function that takes the modulation index as an input and gives the corresponding switching angles as output for C-SHE, Q-SHE or A-SHE. The nonlinear equations at different modulation indices are solved offline, and the answers are stored in a lookup table. The lookup table is used to train the ANN yielding the corresponding switching angles as output at the required modulation index. First the ANN block is trained based on the results obtained from solving the equations of C-SHE, Q-SHE, and A-SHE, then the fitting functions are calculated according to the given data as seen in Fig. 4.2 for C-SHE, Fig. 4.5 for Q-SHE, and Fig. 4.8 for A-SHE. To use this controller online the ANN is used to give online the corresponding switching angles for the needed modulation index.

Using Matlab type “nnstart” and choose “fitting tool” for input-output and curve fitting to start training a neural network. The standard network that is used for function fitting is a two-layer feed forward network, with a sigmoid transfer function in the hidden layer and a linear transfer function in the output layer. The default number of hidden neurons is set to 10. This number might be increased later, if the network training performance is poor. In each training, the user should check and if the error is higher, the user should retrain the neural network more, until the user finds the smallest error possible. The ANN fitted function is shown in Fig. 5.1

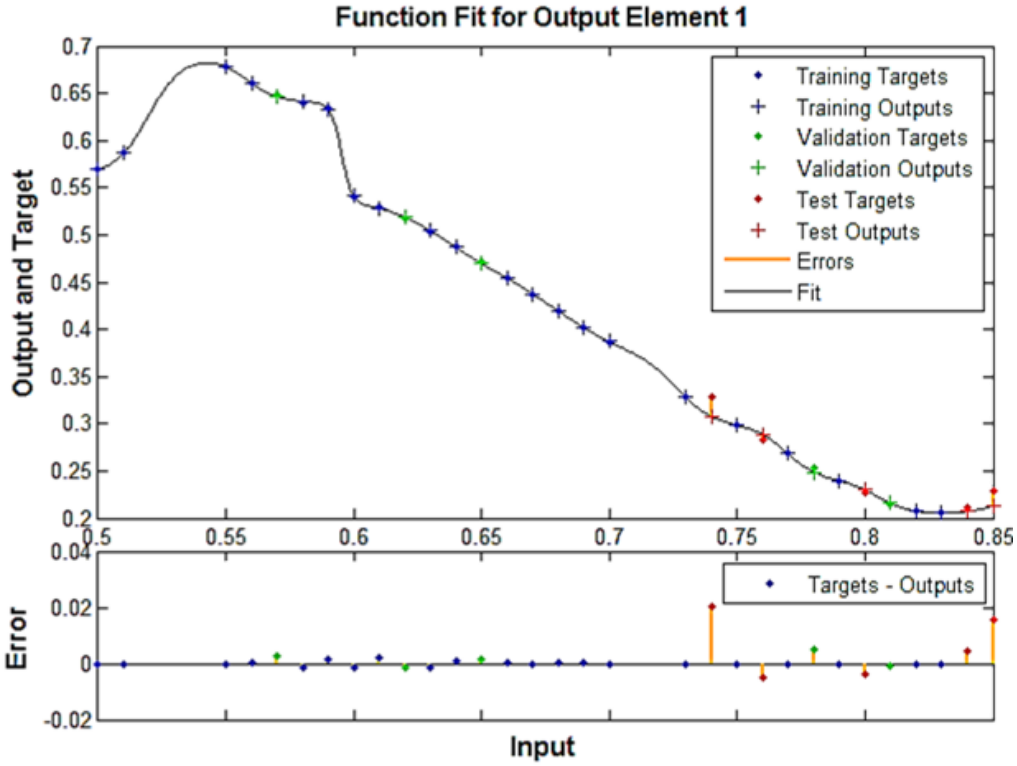

Fig 5.1 ANN Function fit output after training

Then after the user finds the best fit with the lowest error then to proceed to the next step for choosing the generated the neural network diagram type. The ANN generated diagram could be extracted as a Script, Neural Network Diagram, or Simulink Diagram block (which is the one used here).

5.2 Grid-Connected Three-Phase 17-Level SSBC-MMCC With C-SHE, Q-SHE, and A-SHE

The active and reactive power of the three-phase 17-level grid-connected SSBC-MMCC is controlled in the dq synchronously rotating reference frame. To control the dq current components Proportional-Integral (PI) controllers are used. The output of these controllers feeds the SSBC-MMCC with the modulation index and angle to maintain the required active and reactive output power. The measured 3-phase voltages and currents supply to the controller, by considering the active and reactive power references (P_{ref}, Q_{ref}) that control the modulation index and the angle to control the SSBC-MMCC as depicted in Fig. 4.2 for C-SHE, Fig. 4.5 for Q-SHE, and Fig. 4.9 for A-SHE HE. A PLL is employed to convert the variables in the abc stationary reference frame to that in dq synchronously rotating reference frame. The direct-axis and quadrature-axis currents (I_{dref} and I_{qref}) is obtained from P_{ref} and Q_{ref}. Then by comparing I_d with I_{dref} and I_q with I_{qref} to obtain the errors then PI controllers are used to control the I_d and I_q. Then, the output of the PI controller is converted from real-imaginary complex form to magnitude-angle complex form. The magnitude and angle variables are used to control the SSBC-MMCC, whereas the magnitude is the modulation index, but scaled up with the number of H-bridges, and the angle δ is the phase shift between the SSBC-MMCC output phase voltage and grid voltage. Finally,

the ANN considers the needed modulation index, in order to support the SSBC-MMCC with the 8 switching angles, and δ is used by the SSBC-MMCC to introduce the required phase shift with the grid.

5.2.1 The Simulation Results Of The Grid-Connected 17-Level Multilevel Inverter Using Q-SHE

In order to control the 17-level SSBC-MMCC using the Q-SHE approach with the ability to eliminate the 5th and the 7th order harmonic, first the three independent switching angles were obtained by solving the equations in (4.7). The block diagram of the simulated case study is presented in Fig. 5.2. Table 5.1 presents the system parameters. The parameters are set to the first power state (3MW and 2MVAr) and after 0.7 seconds they are changed to the second power state (4MW and 2MVAr), and then at 0.8 seconds they are changed to the third power state (4MW and 1MVAr). Fig. 5.3 illustrates P, P_{ref}, Q, and Q_{ref}. As illustrated in Fig. 5.3 the output reactive and active power track their references. The three-phase currents, and the direct-axis and quadrature-axis actual and reference currents are illustrated in Fig. 5.4 and Fig. 5.5, respectively.

Table 5.1: System parameters

Parameters		Value
3-phase Grid	Line voltage	11KV
	Frequency	50Hz
SSBC-MMCC	H-bridge dc voltage	2000 V
PI controller	P	10
	I	100
	ZOH	1080 Hz
First power state	Real (P)	3 MW
	Reactive (Q)	2 MVAr
Second power state	Real (P)	4 MW
	Reactive (Q)	2 MVAr
Third power state	Real (P)	4 MW
	Reactive (Q)	1 MVAr

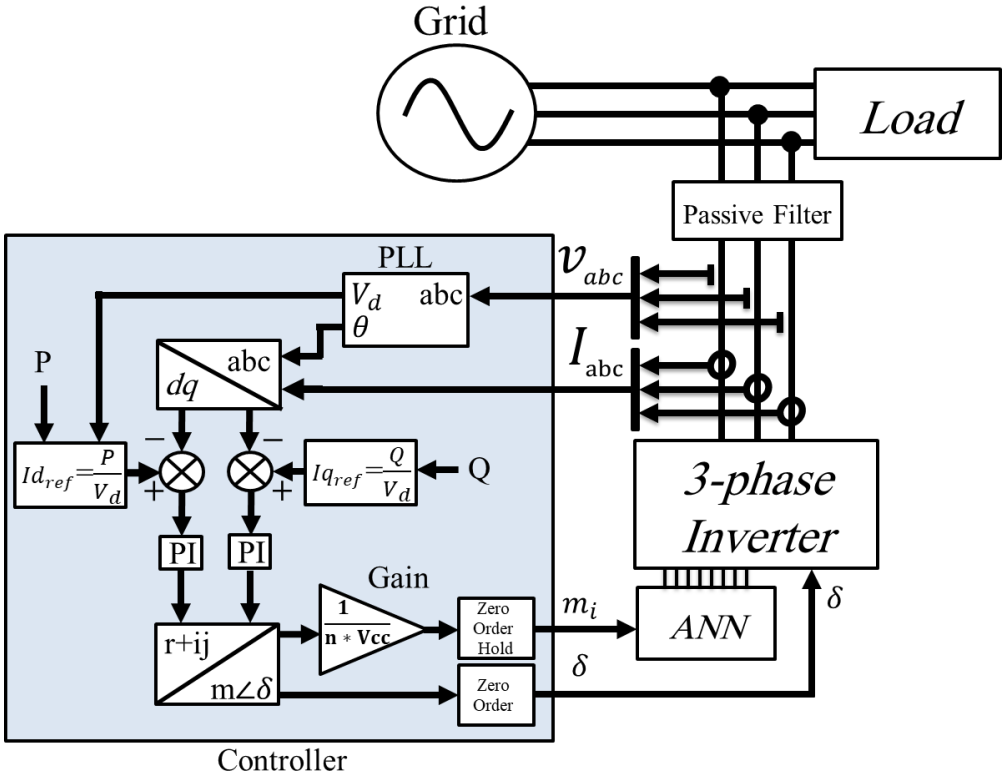

Fig 5.2 Block diagram of the grid-connected SSBC-MMCC with Q-SHE

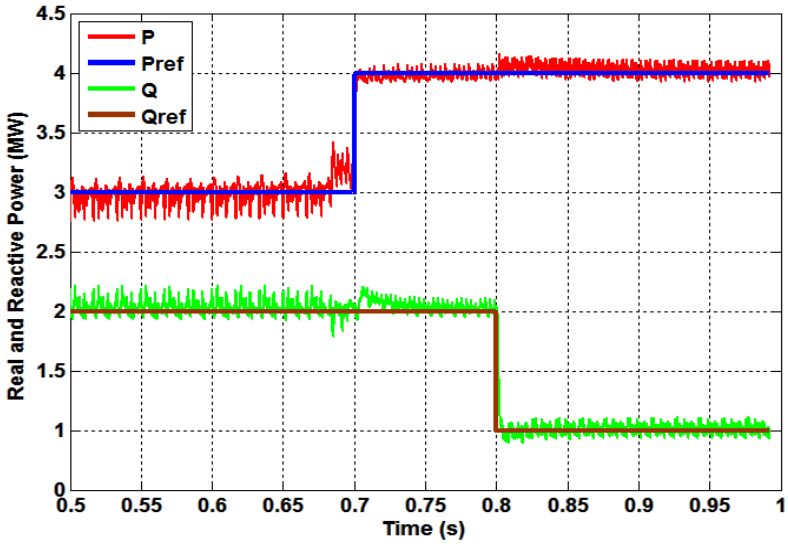

Fig 5.3 Active and Reactive power of the SSBC-MMCC using Q-SHE.

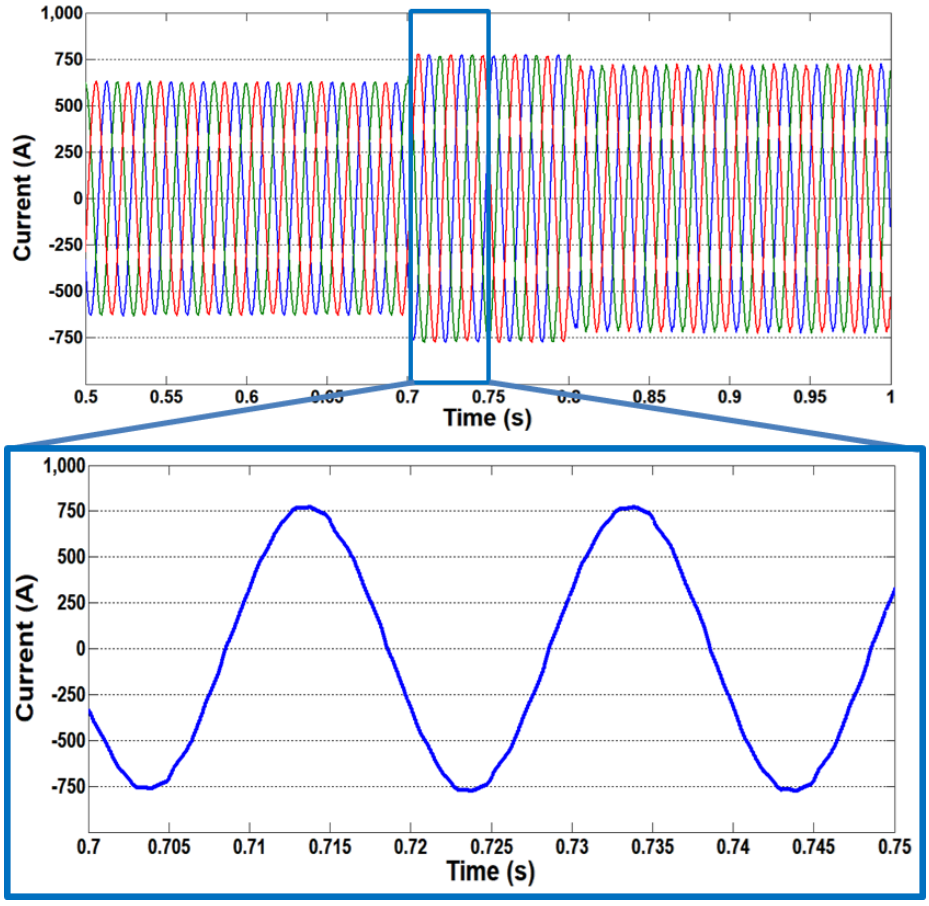

Fig 5.4 The SSBC-MMCC three-phase output currents using Q-SHE.

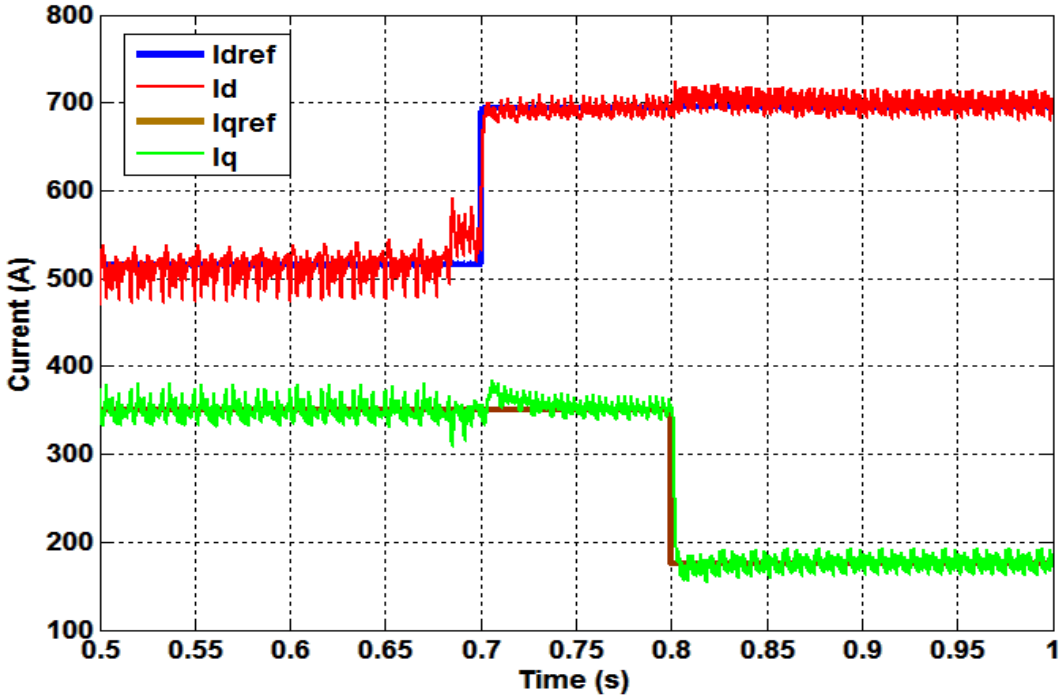

Fig 5.5 Direct-axis and quadrature-axis actual and reference currents using Q SHE

5.2.2 The Simulation Results Of The Grid-Connected 17-Level SSBC-MMCC Using A-SHE

Similar to the aforementioned subsection to simulation results of the grid-connected 17-level SSBC-MMCC uses Q-SHE, the A-SHE approach is presented in this subsection. The block diagram of the simulated case study is presented in Fig. 5.2. illustrates P, P_{ref}, Q, and Q_{ref} using A-SHE. As illustrated in Fig. 5.6 the output reactive and active power track their references. The three-phase currents, and the direct-axis and quadrature-axis actual and reference currents are illustrated in Fig. 5.7 and Fig. 5.8, respectively.

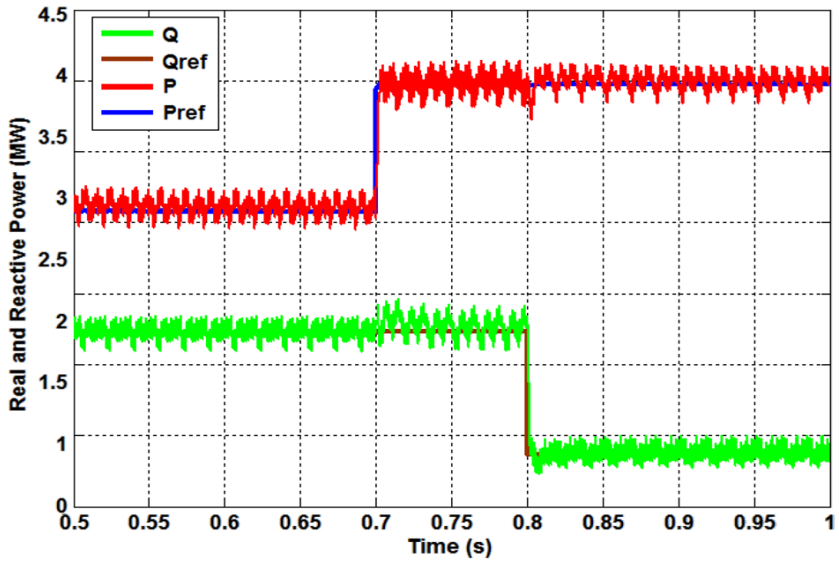

Fig 5.6 Active and Reactive power of the SSBC-MMCC using A-SHE.

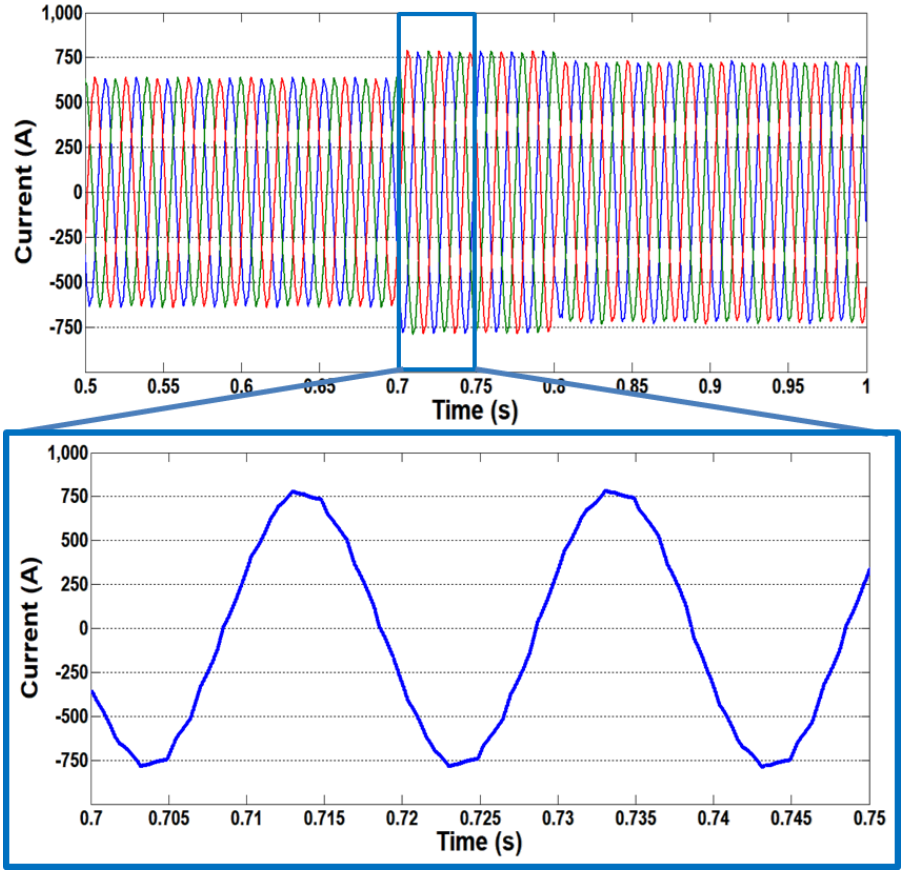

Fig 5.7 The SSBC-MMCC three-phase output currents using A-SHE.

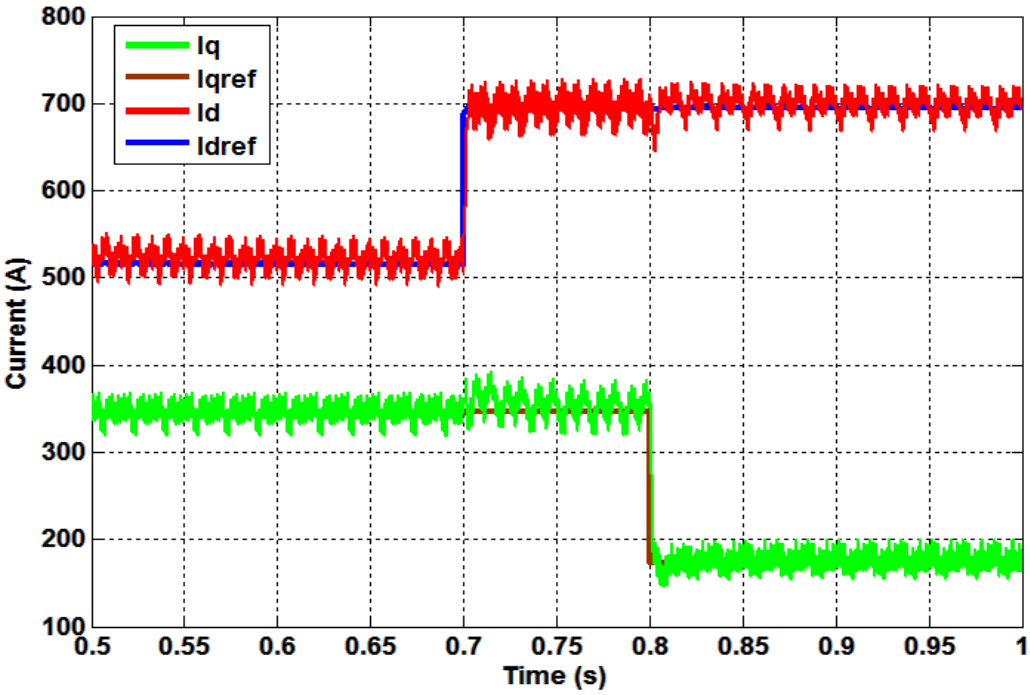

Fig 5.8 Direct-axis and quadrature-axis actual and reference currents using A-SHE.

5.2.3 The Simulation Results Of The Grid-Connected 17-Level SSBC-MMCC Using C-SHE

This subsection illustrated the simulation results of the grid connected SSBC-MMCC uses C-SHE. Fig. 5.2 illustrates P, P_{ref}, Q, and Q_{ref}. As illustrated in Fig. 5.9 the output reactive and real power track their references. The three-phase currents, and the direct-axis and quadrature-axis actual and reference currents are illustrated in Fig. 5.10 and Fig. 5.11, respectively.

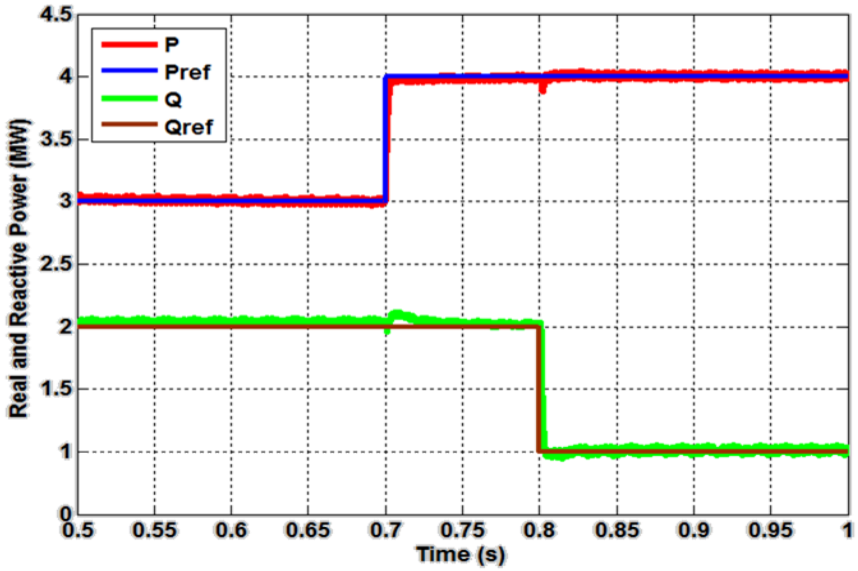

Fig 5.9 Active and Reactive power of the SSBC-MMCC using C-SHE.

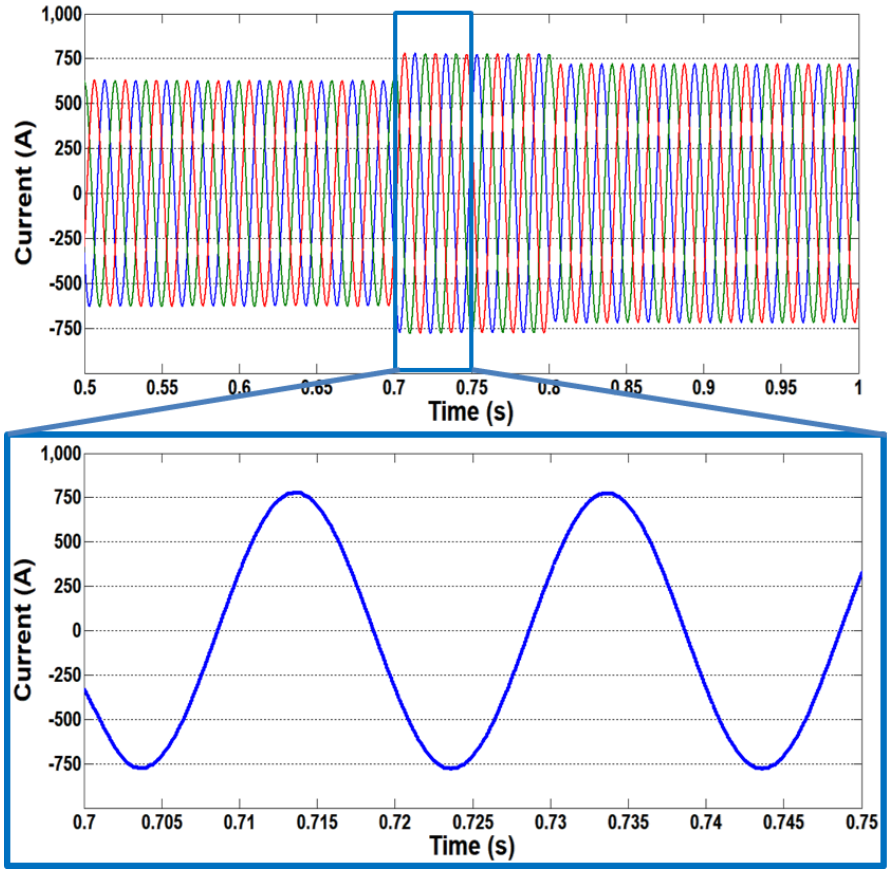

Fig 5.10 The SSBC-MMCC three-phase output currents using C-SHE.

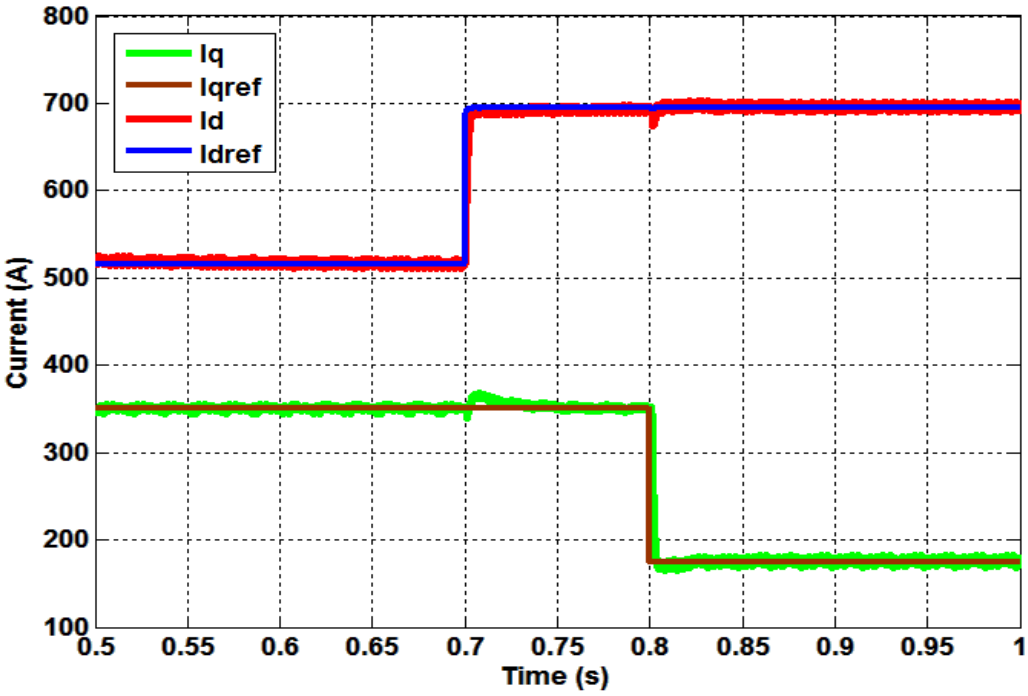

Fig 5.11 Direct-axis and quadrature-axis actual and reference currents using C-SHE.

5.3 Discussion On The Results

As seen in the above subsection the grid connected SSBC-MMCC was simulated using the three techniques (Q-SHE, A-SHE, and C-SHE), the three techniques performed well in tracking the reference active and reactive power. The C-SHE exhibits the best current quality (corresponding power) among the three presented approaches, since the output wave of the C-SHE is the closest to sine wave as seen in Fig 5.10. The Q-SHE output wave is also close to sine wave as seen in Fig 5.4. the A-SHE is also the same but with some deformations as seen in Fig.5.7

5.4 Fault Tolerant Of The SSBC- MMCC

With the cumulative dependence on electronic systems, now days it is highly required for the power systems to be reliable and efficient. One of the motivation that is considered in this thesis is fault tolerance of the SSBC-MMCC. The SSBC-MMCC secures power to the power system loads yet the overall reliability has to be considered. The fault tolerant technique can overcome any fault that occurs in cell(s) of the SSBC-MMCC, which enhances the system reliability. One of the main advantages of the SSBC-MMCC is the redundancy and fault ride through capability. When fault occurs in a cell of the SSBC- MMCC, the failed cell is bypassed. Therefore to maintain proper operation with balanced three phase voltage, two cells in the other two phases are controlled to produce zero-voltage (virtually bypassed). As a result, the inverter will lose two levels in each phase, which will cause m-level SSBC-MMCC to operate as (m-2)-level SSBC-MMCC.

For example, in 19-level SSBC-MMCC shown in figure 5.12, if cell number 5 of phase a fails, then it will be bypassed and another cell (e.g. cell 5) in the other two phases will produce zero voltage. Therefore the 19-level SSBC-MMCC will operate with 17-level only, with a derating factor of 89.5%.

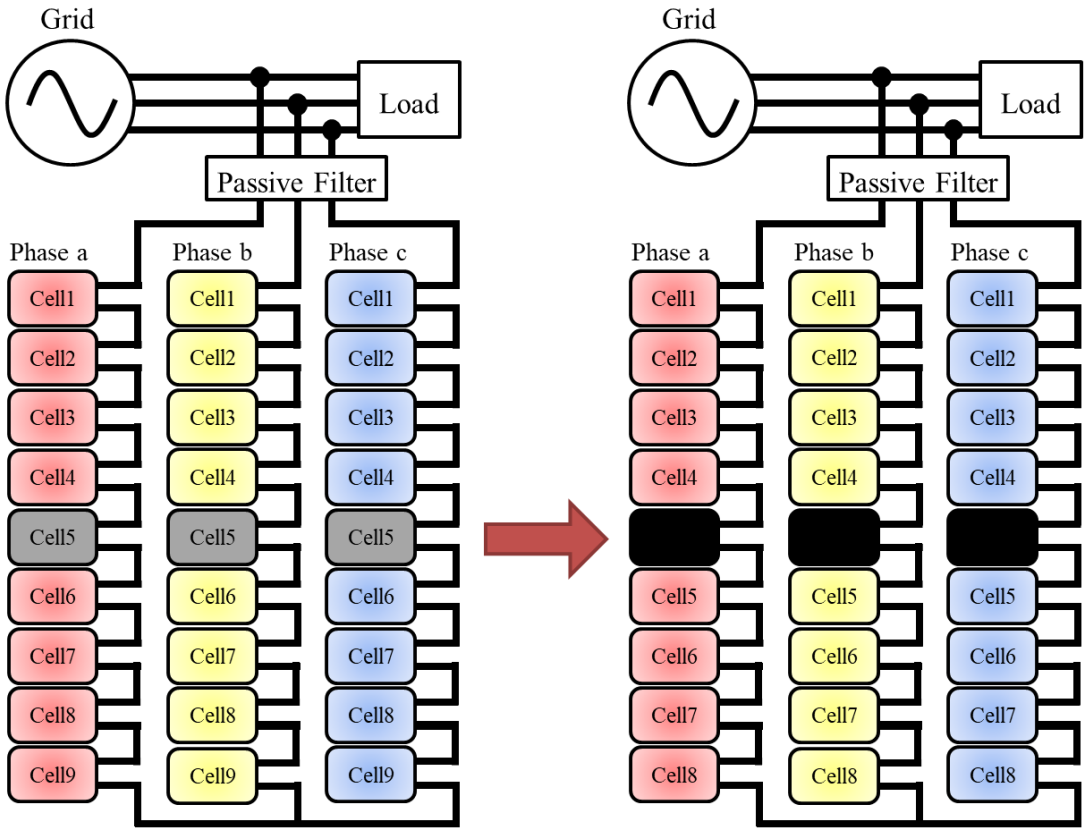

Fig 5.12 19-level Inverter with failed cell and the technique to bypass the fault and operate as 17-level Inverter

Generally, in (2n+1)-level SSCB-MMCC, after cell failure, the SSCB-MMCC operates as (2n-1)-level converter, with a derating factor of (2n-1)/(2n+1). With that faulty cell, if a fault occurs in another cell, the same aforementioned steps will be repeated, and the SSCB-MMCC will end up working with (2n-3) levels, with a derating factor of (2n-3)/(2n+1).

The presented SHE approaches can be implemented after adopting them to (2n-1)-level or (2n-3)-level in case of a single faulty cell or two faulty cells, respectively. For instance in 19-level SSCB-MMCC and with a faulty cell, the number of harmonics

to be eliminated is reduced from 8 to 7, which will affect the harmonic performance. In Q-SHE, the number of harmonics to be eliminated will be the same but the problem will be solved for quasi 7-level operation of 17-level SSCB-MMC instead of quasi 7-level operation of 19-level SSCB, maintaining the same harmonic performance. The same will be valid with the A-SHE.

CHAPTER 6: GRID-CONNECTED SSBC-MMCC IN A MODIFIED IEEE TEST SYSTEM: CASE STUDY

In this chapter, the SSBC-MMCC is tested and simulated in grid-connected mode to a modified IEEE test system to validate the presented concept.

6.1 IEEE Test System

The IEEE Test System contains 13 Buses, is representative of a medium-voltage distribution network [76]. The system is fed from grid supply at 69 kV and the distributed system operates at 13.8 kV. Starting from the point of common coupling, overhead and underground lines, shunt capacitors, transformers, and 5 loads. This IEEE Test system is used as a benchmark system for studies, and is commonly used to test common features of distribution analysis in simulations since it is small, simple and relatively highly loaded [76, 77]. Fig 6.1 shows the IEEE Test system Single Line Diagram.

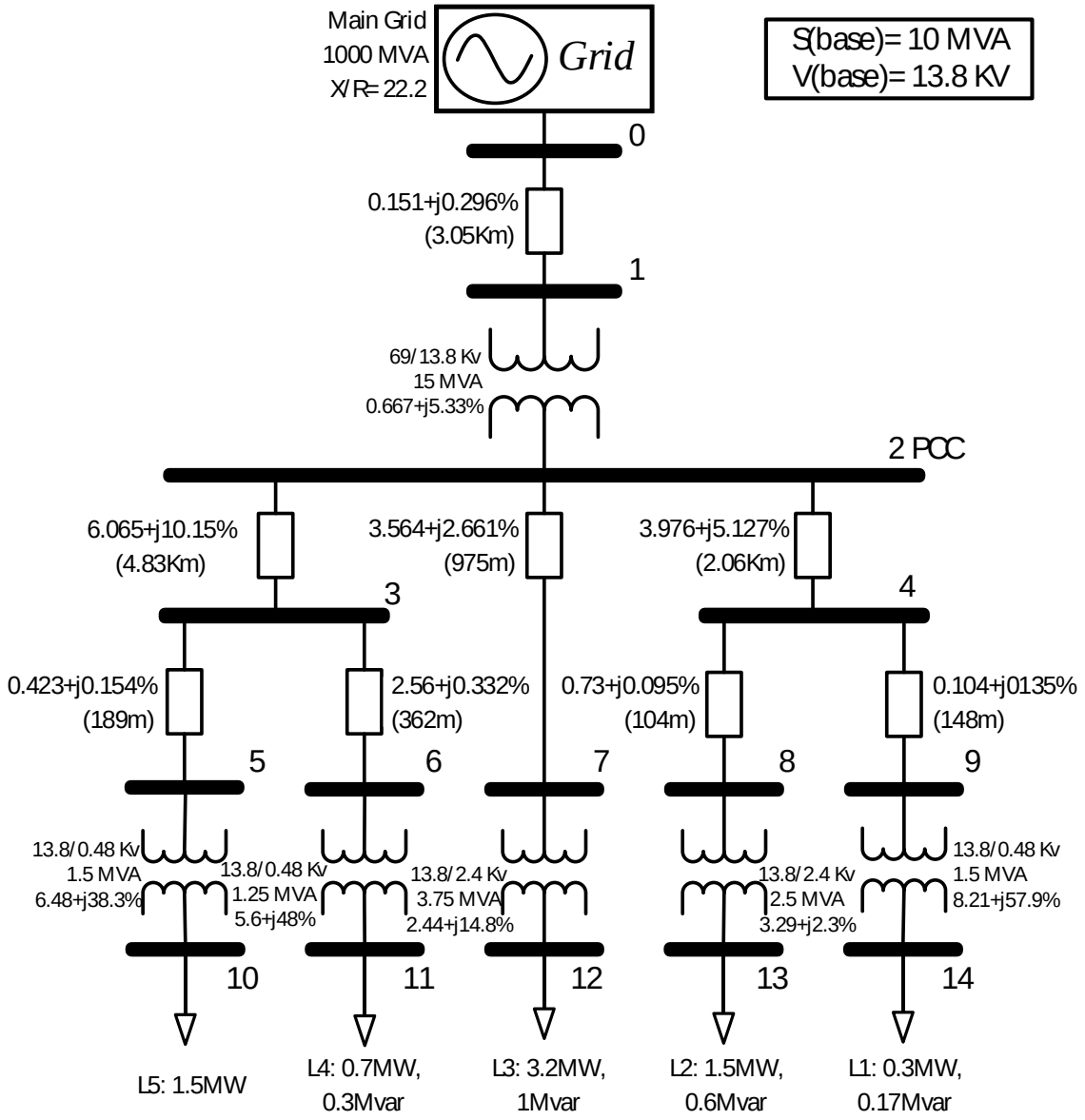

Fig. 6. 1 IEEE Test system Single Line Diagram

6.2 Renewable Energy Source Added To IEEE Test Network

First, the IEEE Test system is simulated (without integrating any renewable energy source to the system); and the values of voltages, currents, real and reactive powers for each bus are shown in Figure 6.1.

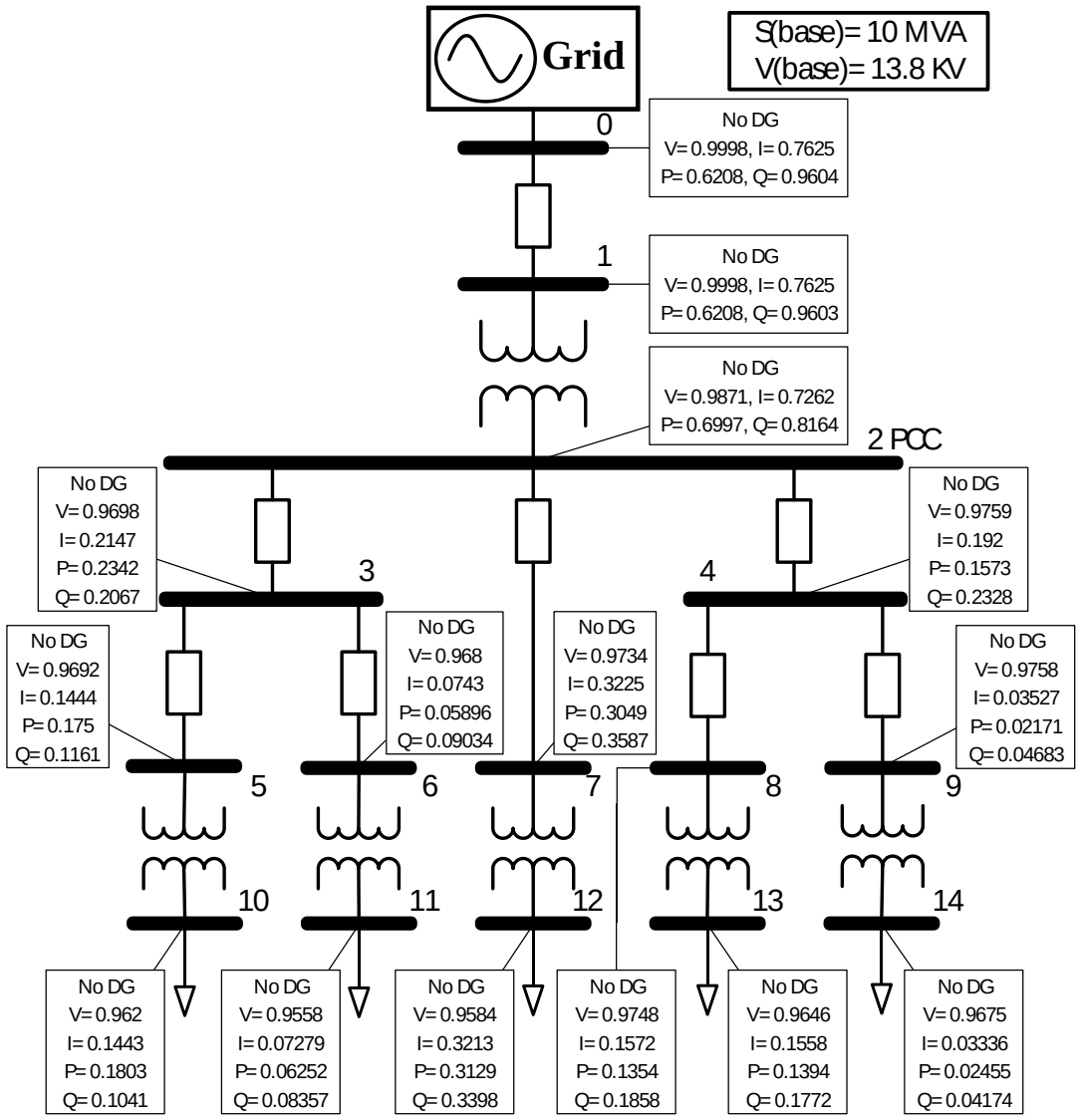

Fig. 6.2 IEEE Test system simulation showing voltage, current, real and reactive power in each bus

Next, a 15 MVA PV generator is added to the IEEE system PCC bus (69 kV bus) to reduce the power sourced by the Grid. The PV system in integrated to the IEEE test bus through the presented 17-level SSBC-MMCC operated by the three techniques mentioned in the previous chapters (i.e. Q-SHE, A-SHE, and C-SHE). The three techniques are simulated where the SSBC-MMCC controls the required active and reactive powers. The SSBC-MMCC is set to control the supplied real power from the PV and the reactive power to regulate the voltage. The SSBC-MMCC DG system is controlled to supply active and reactive power for two cases,

1- Minimal contribution of grid in active power and 1 p.u Voltage at PCC bus
2- Full Active power utilization of distribution generation

These values of P and Q (active and reactive power) can be set by the Distribution Network Operator (DNO)

6.2.1 Minimal Contribution Of Grid In Active Power And 1 P.U Voltage At PCC Bus

To minimize the contribution of the grid active power, the real power DG output is set to 0.6997 p.u. To control the voltage at the PCC bus to 1p.u Voltage, the reactive power DG output is set to 0.8164 p.u. The set point is assigned to the SSBC-MMCC to control the supplied real power and reactive power to reduce the real power supplied by the grid and control the voltage, respectively.

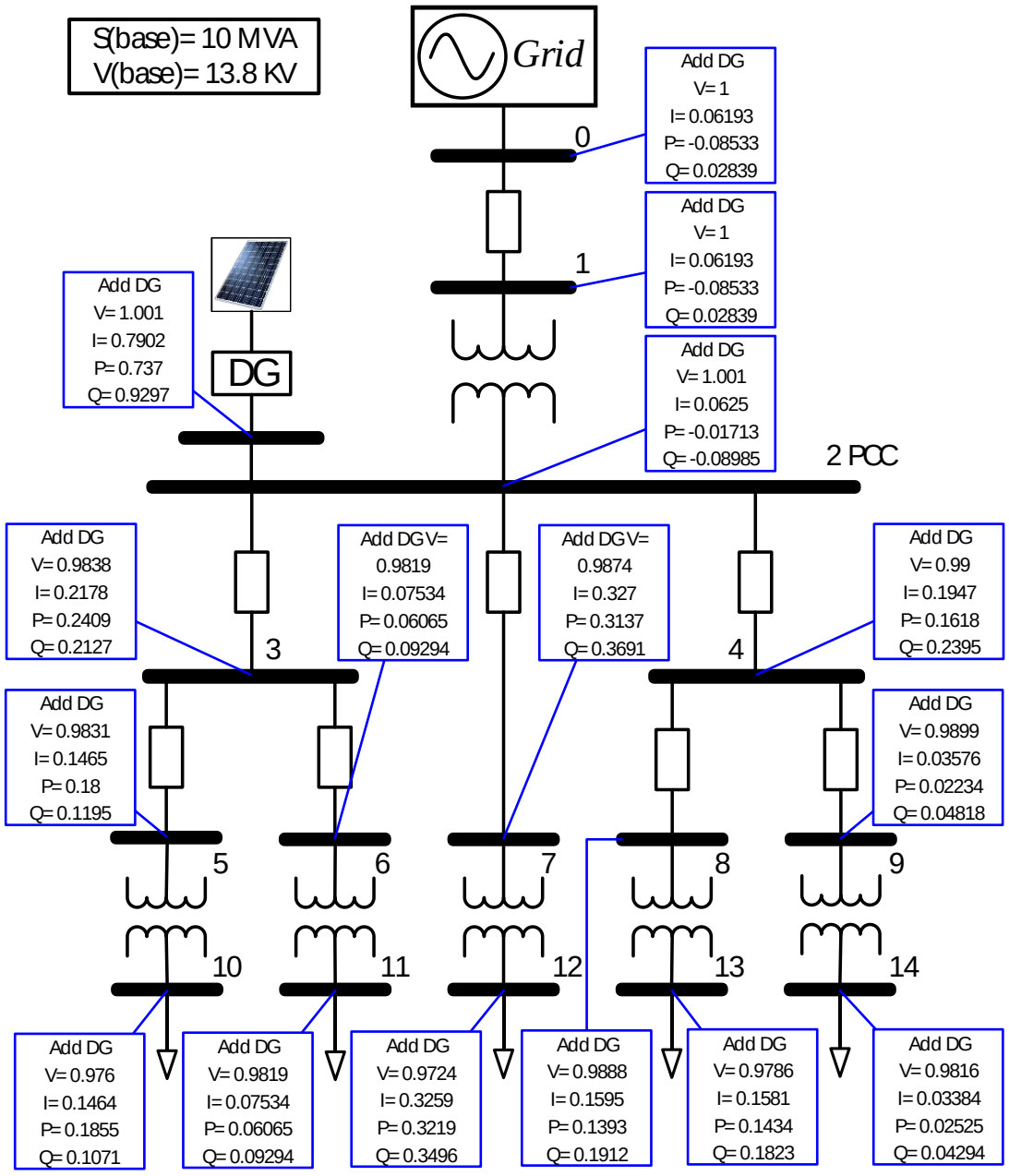

Fig. 6.3 Voltage, current, real and reactive power in each bus with distributed generation

The PCC bus Real power was reduced from 0.6997 p.u to -0.01713 p.u. The Bus voltage can be enhanced by controlling the Reactive power, the grid bus Reactive power was reduced from 0.8164 p.u to 0.08985 p.u, which enhances the bus voltage from 0.9871 p.u to 1.001 p.u. where the output real and reactive power of the SSBC-MMCC is controlled to the above-mentioned real and reactive power. The PCC Bus voltages of the three techniques are the same shown in figure 6.4.

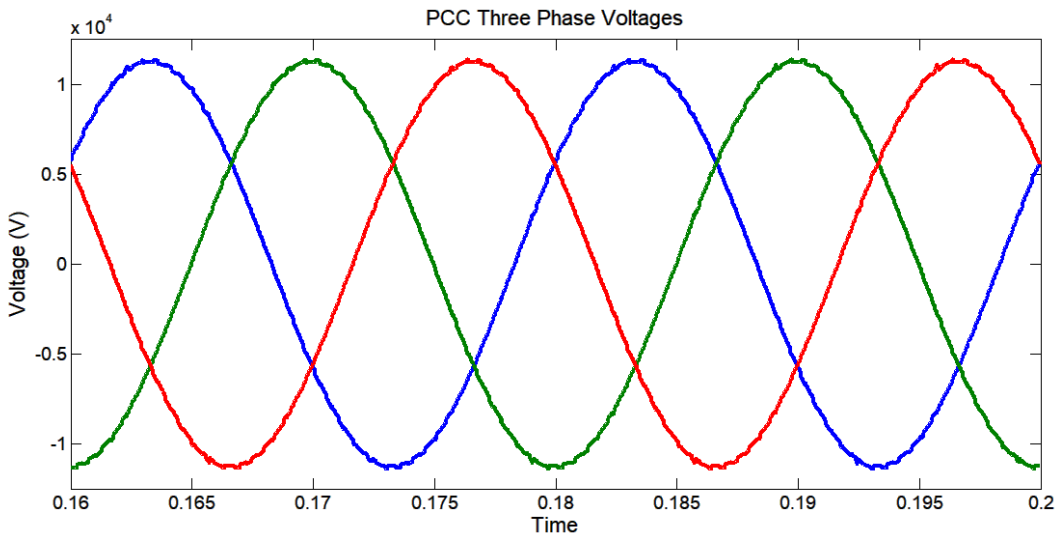

Fig. 6.4 PCC Bus 3 phase Voltages typical for the three Techniques

Figure 6.5 shows the current injected from the DG to the PCC Bus for the three SHE techniques. As can be noticed, the C-SHE technique shows the best performance among the three techniques, then the Q-SHE technique shows less harmonic, finally the A-SHE technique shows the highest harmonic.

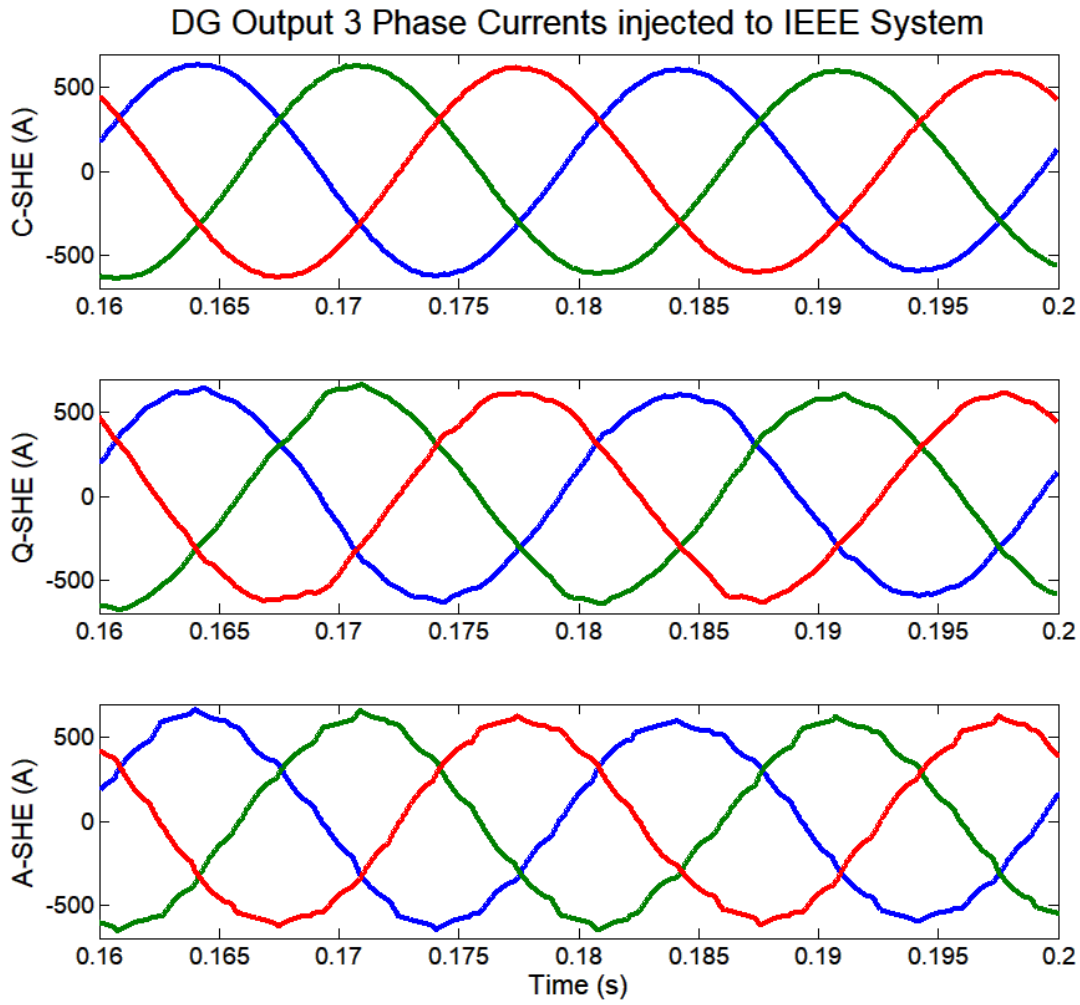

Fig. 6.5 Distributed Generation 3 phase output Currents for the three Techniques

Figure 6.6 shows the current injected from the Grid to the PCC Bus for the three SHE techniques. As can be noticed, the current flow between the Grid and the PCC bus is low for the three techniques.

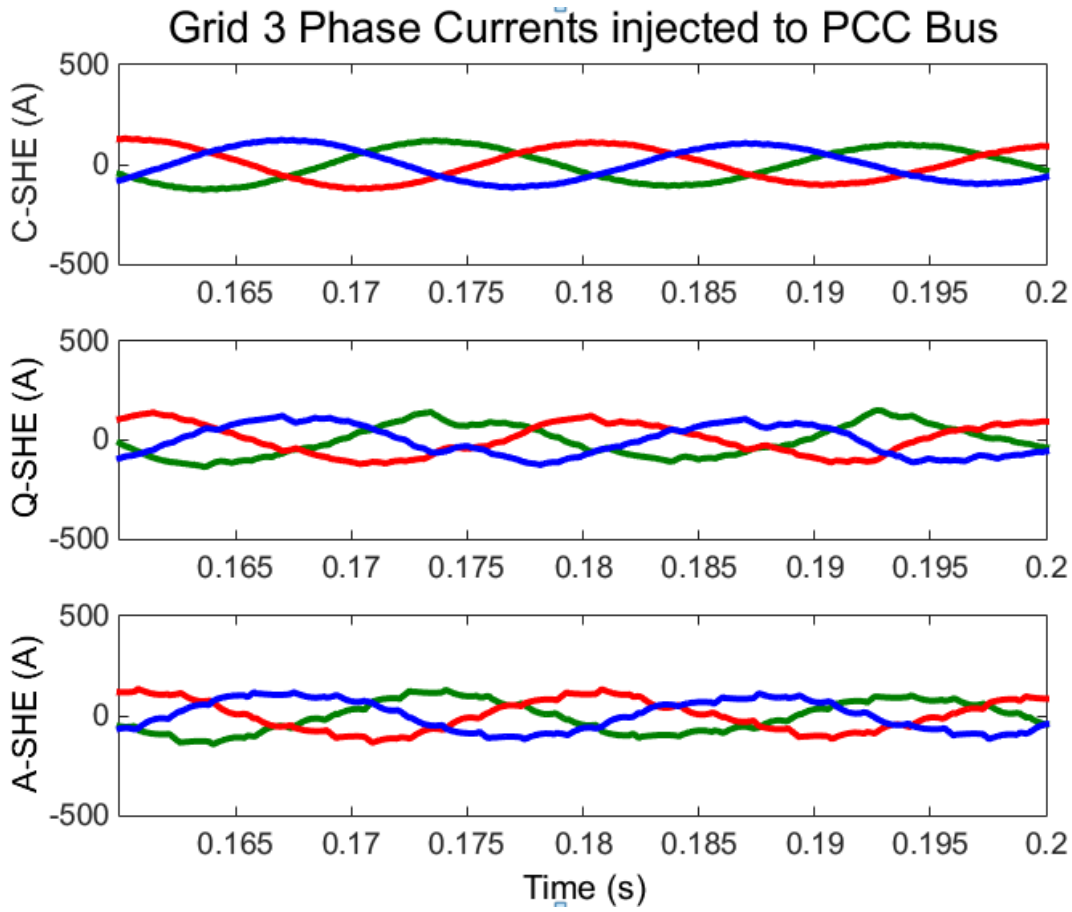

Fig. 6.6 Grid 3 phase Currents injected to the PCC Bus for the three Techniques

Table 6.1 shows the THD for each bus when using the three techniques, where the layout of the IEEE system is shown in Fig 6.3

Table 6. 1 THD Percentage for each bus in the IEEE system using the three techniques

Buss Number	Conventional SHE THD	Quasi SHE THD	Asymmetrical SHE THD
0	0.0114	0.0114	0.0114
1	0.01275	0.01275	0.01275
2	0.6267	0.6267	0.6267
3	0.4852	0.4852	0.4852
4	0.6186	0.6186	0.6186
5	0.4834	0.4834	0.4834
6	0.4858	0.4858	0.4858
7	0.619	0.619	0.619
8	0.619	0.619	0.619
9	0.6185	0.6185	0.6185
10	0.2603	0.2603	0.2603
11	0.4653	0.4653	0.4653
12	0.5692	0.5692	0.5692
13	0.5975	0.5975	0.5975
14	0.6098	0.6098	0.6098
15 (DG output)	0.6267	0.6267	0.6267

As seen in Table 6.1, measuring the THD when using the three techniques, it can be noticed that the difference in THD between the three systems is insignificant. This difference may be clear when applied in a weak grid.

6.2.2 Full Active Power Utilization Of Distribution Generation

To utilize the full active power of the Distributed, the real power DG output is set to 1.5 p.u. and the reactive power DG output is set to 0 p.u. The set point is assigned to the SSBC-MMCC to control the supplied real power and reactive power.

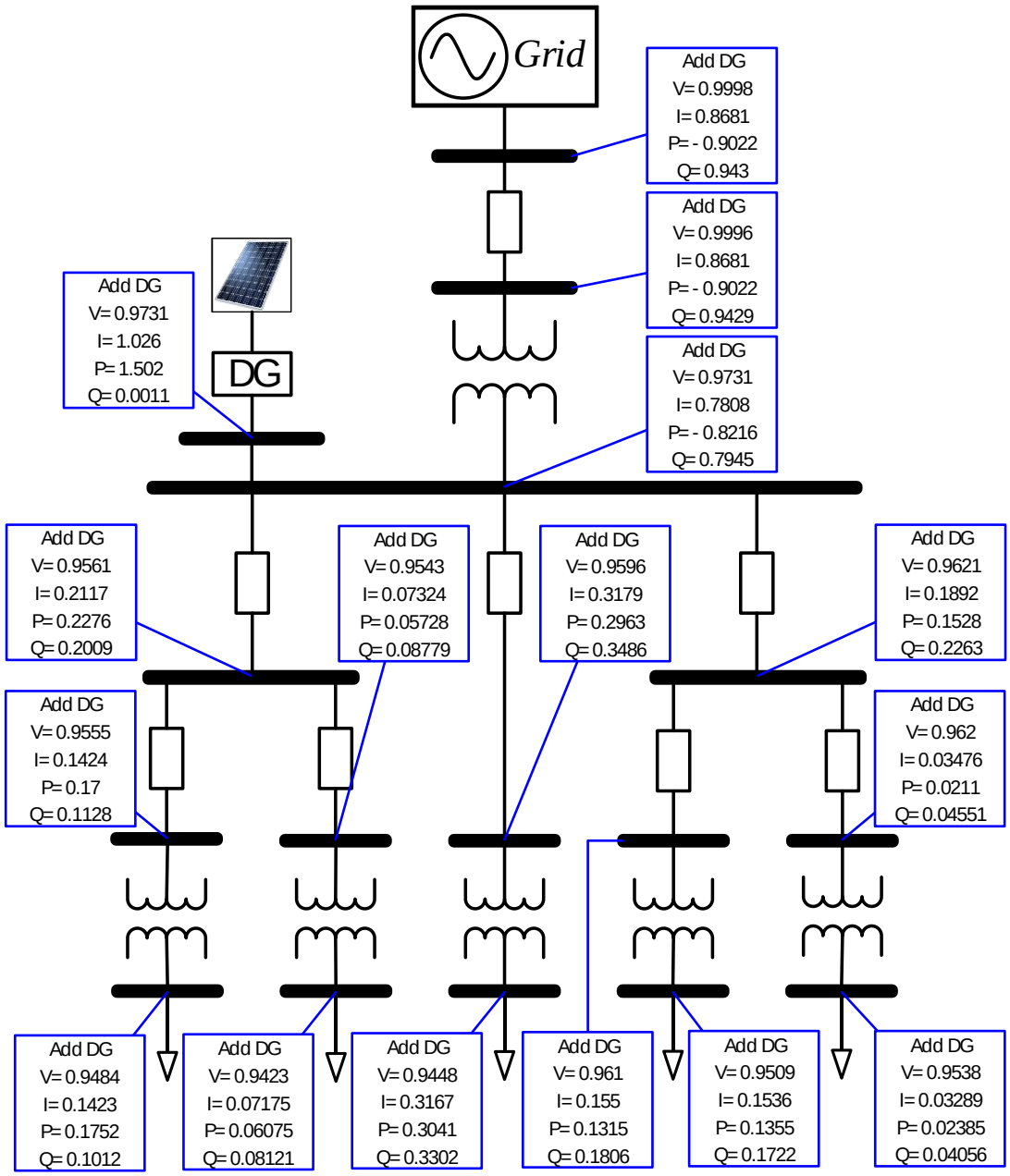

Fig. 6.7 Voltage, current, real and reactive power in each bus with distributed generation

The DG supplied the modified system with the required power and the extra active power is returned to the grid. The grid bus Reactive power didn't change since

the DG output power was controlled to be at zero p.u. where the output real and reactive power of the SSBC- MMCC is controlled to the above-mentioned real and reactive power. The PCC Bus voltages of the three techniques are the same shown in figure 6.8.

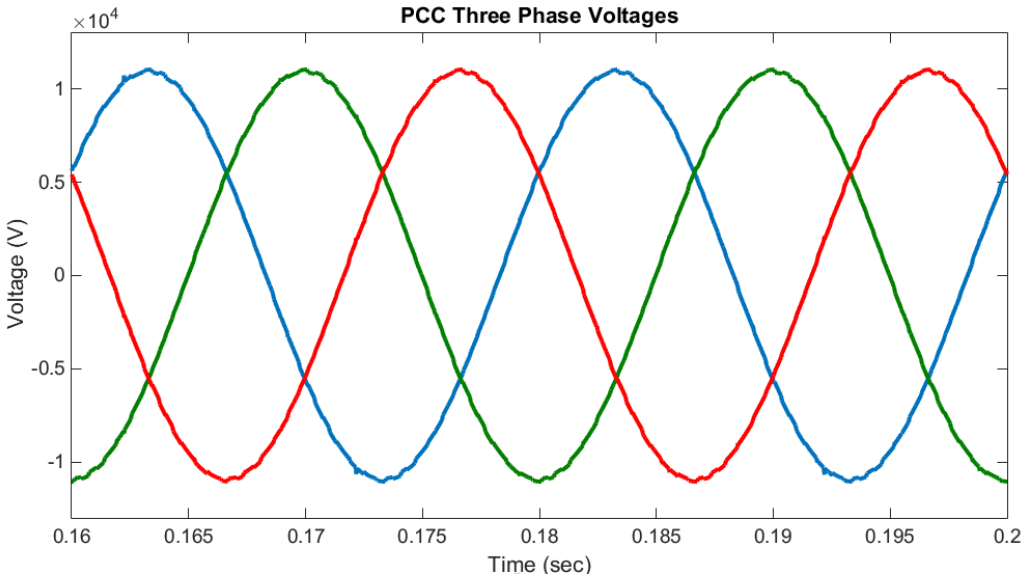

Fig. 6.8 PCC Bus 3 phase Voltages typical for the three Techniques

The Below figure shows the current injected from the DG to the PCC Bus for the three techniques. As can be noticed, the C-SHE technique shows the best harmonic performance among the three SHE approaches, then the Q-SHE technique shows less harmonic, finally the A-SHE technique shows the highest harmonic.

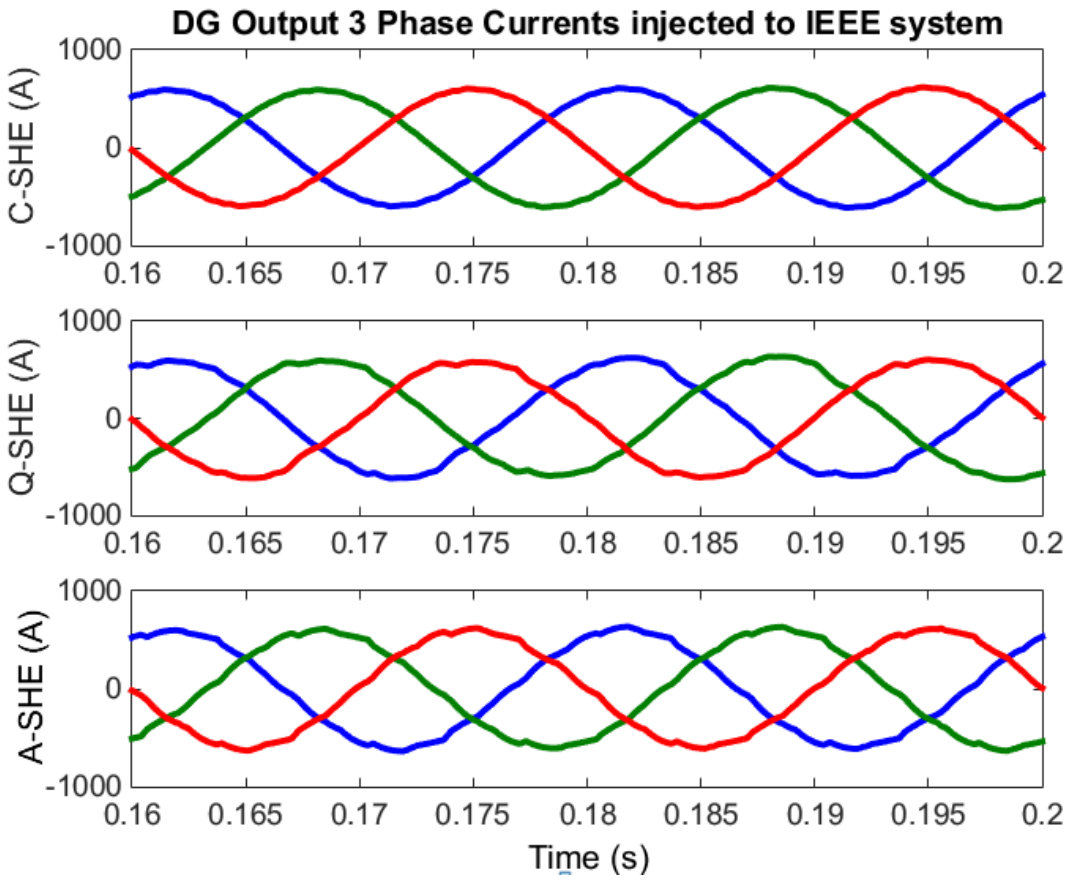

Fig. 6.9 Distributed Generation 3 phase output Currents for the three Techniques

The Below figure shows the current injected from the Grid to the PCC Bus for the three techniques. As can be noticed, the current flow between the Grid and the PCC bus is low for the three techniques.

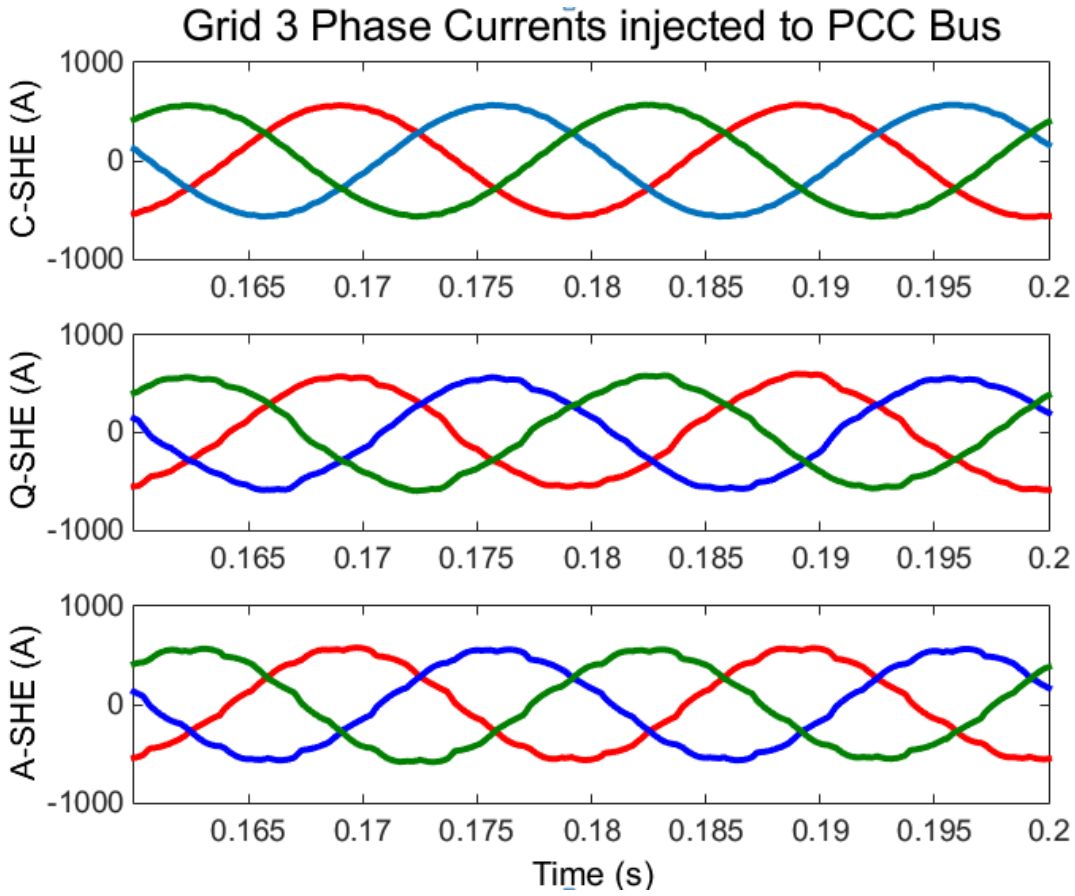

Fig. 6.10 Grid 3 phase Currents injected to the PCC Bus for the three Techniques

CONCLUSIONS

There are several techniques to control the SSBC-MMCC. This thesis focused on comparing between three different SHE techniques, appropriate for limited switching frequency, where the output voltage quality of the inverter is enhanced by eliminating the low order harmonics, using the unified approach presented in [70] for solving the SHE equations in SSBC-MMCCs. In order to alleviate the complexity of employing SHE at high-level order, Quasi 7-level SHE (Q-SHE) approach and Asymmetrical seven-level SHE (A-SHE) were studied and compared with Conventional SHE (C-SHE). Q-SHE and A-SHE were based on eliminating the 5^{th} and 7^{th} order harmonics.

Next simplified non-linear equations are solved first offline for the required range of modulation index. Then all the angles are stored in a lookup table or a trained Artificial Neural Network (ANN). Using ANN, the online SHE technique can be applied. By using a proportional-integral (PI) control, the control can perform a real-time calculation for multilevel inverter's (MLI) switching angles over a wide range of modulation indexes.

Finally, the performance of a high power 17-level grid-connected SSBC-MMCC operating with the three different SHE techniques (C-SHE, Q-SHE, and A-SHE) is assessed. The C-SHE, A-SHE, and Q-SHE approaches are considered, simulated, and compared. The THD is reduced by eliminating low order harmonics, where the 5^{th} and 7^{th} harmonics are eliminated using Q-SHE and A-SHE. The C-SHE is controlled to eliminate all harmonic orders between 5^{th} and 23^{rd} harmonic. Compared with the C-SHE approach, the Q-SHE and A-SHE methods require less computational

burden in solving the required equation groups. The following table concludes the comparison between the three different techniques.

Table 7. 1: Conclusion of each controlling technique

Controlling technique	**Advantages**	**Disadvantages**
C-SHE	Lowest THD	Most complicated
Q-SHE	Low THD & Less complicated	Higher THD compared with C-SHE
A-SHE	Least complicated	Highest THD

A 5MW grid-connected three-phase SSBC-MMCC (17-level) is controlled in the synchronous rotating reference frame to reveal the proposed concept. Next, 15 MVA PV panels were added to the IEEE Modified Test systems' PCC buss to support the grid in supplying active power, and to control the voltage through supplying reactive power component. The 17-level SSBC- MMCC is operated by the three SHE techniques (Q-SHE, A-SHE, and C-SHE). The three techniques were simulated for the SSBC-MMCC in the IEEE test system controlling the active and reactive power. All the validation of the present assessment has been done through simulation using Matlab/Simulink platform.

REFERENCES

[1] Renewable Energy Policy Network for the 21st Century, "Renewables Global Status Report 2016", Renewable Energy Policy Network for the 21st Century, Paris, France, 2017. ISBN 978-3-9818107-0-7 http://www.ren21.net/wp-content/uploads/2016/05/GSR_2016_Full_Report_lowres.pdf

[2] United States, Department of Energy, "The Future Arrives for Five Clean Energy Technologies – 2016 Update", United States, Department of Energy, United States, 2016. https://www.energy.gov/sites/prod/files/2016/09/f33/Revolutiona%CC%82%E2%82%ACNow%202016%20Report_2.pdf

[3] World Energy Council, "World Energy Perspectives Renewables Integration - 2016", World Energy Council, London, United Kingdom, 2016.

[4] Aaron VanderMeulen and John Maurin, " Current source inverter vs. Voltage source inverter topology" in Eaton, June 2014

[5] Ningxia in Tengger Desert built the country's largest desert PV integrated area - China daily In-text: (Escn.com.cn, 2017) Your Bibliography: Escn.com.cn. (2017). [online] Available at: http://www.escn.com.cn/news/show-310093.html [Accessed 8 Jun. 2017]

[6] AZURE POWER STARTS CONSTRUCTING 100MW SOLAR PROJECT IN ANDHRA PRADESH In-text: (PV Tech, 2017) Your Bibliography: PV Tech. (2017). [online] Available at: https://www.pv-tech.org/news/azure-power-starts-constructing-100mw-solar-project-in-andhra-pradesh [Accessed 8 Jun. 2017].

[7] T. C. Lim, B. W. Williams, S. J. Finney and P. R. Palmer, "Series-Connected IGBTs Using Active Voltage Control Technique," in IEEE Transactions on Power

Electronics, vol. 28, no. 8, pp. 4083-4103, Aug. 2013.

[8] H. Ben Abdelghani, A. Bennani Ben Abdelghani, F. Richardeau, J. M. Blaquière, F. Mosser and I. Slama-Belkhodja, "Fault tolerant-topology and controls for a three-level hybrid neutral point clamped-flying capacitor converter," in IET Power Electronics, vol. 9, no. 12, pp. 2350-2359, 10 5 2016.

[9] A. Khoshkbar-Sadigh, V. Dargahi and K. Corzine, "New Flying-Capacitor-Based Multilevel Converter With Optimized Number of Switches and Capacitors for Renewable Energy Integration," in IEEE Transactions on Energy Conversion, vol. 31, no. 3, pp. 846-859, Sept. 2016.

[10] F. Salinas, M. A. González and M. F. Escalante, "Finite Control Set-Model Predictive Control of a Flying Capacitor Multilevel Chopper Using Petri Nets," in IEEE Transactions on Industrial Electronics, vol. 63, no. 9, pp. 5891-5899, Sept. 2016.

[11] B. Sharma and J. Nakka, "Cascaded flying capacitor half bridge inverter for power rating enhancement in PV based inverter system," 2016 IEEE 7th Power India International Conference (PIICON), Bikaner, Rajasthan, India, 2016, pp. 1-6.

[12] A. Ashraf Gandomi, S. Saeidabadi and S. H. Hosseini, "A high step up flying capacitor inverter with the voltage balancing control method," 2017 8th Power Electronics, Drive Systems & Technologies Conference (PEDSTC), Mashhad, 2017, pp. 55-60.

[13] P. R. Kumar, R. S. Kaarthik, K. Gopakumar, J. I. Leon and L. G. Franquelo, "Seventeen-Level Inverter Formed by Cascading Flying Capacitor and Floating Capacitor H-Bridges," in IEEE Transactions on Power Electronics, vol. 30, no. 7, pp. 3471-3478, July 2015.

[14] G. P. Adam, S. J. Finney, A. M. Massoud and B. W. Williams, "Capacitor Balance Issues of the Diode-Clamped Multilevel Inverter Operated in a Quasi Two-State Mode," in IEEE Transactions on Industrial Electronics, vol. 55, no. 8, pp. 3088-3099, Aug. 2008.

[15] A. A. Ashaibi, S. J. Finney, B. W. Williams and A. M. Massoud, "Switched mode power supplies for charge-up, discharge and balancing dc-link capacitors of diode-clamped five-level inverter," in IET Power Electronics, vol. 3, no. 4, pp. 612-628, July 2010.

[16] H. Zhang, S. Jon Finney, A. Massoud and B. Wayne Williams, "An SVM Algorithm to Balance the Capacitor Voltages of the Three-Level NPC Active Power Filter," in IEEE Transactions on Power Electronics, vol. 23, no. 6, pp. 2694-2702, Nov. 2008.

[17] M. Dave and M. Bhagdev, "A comparative study of photovoltaic (PV) based diode clamped multilevel inverter (DCMLI)," 2016 7th India International Conference on Power Electronics (IICPE), Patiala, India, 2016, pp. 1-5.

[18] A. Saha, A. Elrayyah and Y. Sozer, "A novel three-phase multilevel diode-clamped inverter topology with reduced device count," 2016 IEEE Energy Conversion Congress and Exposition (ECCE), Milwaukee, WI, 2016, pp. 1-6.

[19] Z. Boussada, O. Elbeji and M. Benhamed, "Modeling of diode clamped inverter using SPWM technique," 2017 International Conference on Green Energy Conversion Systems (GECS), Hammamet, 2017, pp. 1-5.

[20] A. Abdelhakim and P. Mattavelli, "Analysis of the three-level diode-clamped split-source inverter," IECON 2016 - 42nd Annual Conference of the IEEE Industrial Electronics Society, Florence, 2016, pp. 3259-3264.

[21] M. E. Tamasas, M. Saleh, M. Shaker and A. Hammoda, "Comparison of different third harmonic injected PWM strategies for 5-level diode clamped inverter," 2017 IEEE Power and Energy Conference at Illinois (PECI), Champaign, IL, 2017, pp. 1-6.

[22] W. Jiang, L. Huang, L. Zhang, H. Zhao, L. Wang and W. Chen, "Control of Active Power Exchange With Auxiliary Power Loop in a Single-Phase Cascaded Multilevel Converter-Based Energy Storage System," in IEEE Transactions on Power Electronics, vol. 32, no. 2, pp. 1518-1532, Feb. 2017.

[23] A. M. Massoud, S. Ahmed, P. N. Enjeti and B. W. Williams, "Evaluation of a Multilevel Cascaded-Type Dynamic Voltage Restorer Employing Discontinuous Space Vector Modulation," in IEEE Transactions on Industrial Electronics, vol. 57, no. 7, pp. 2398-2410, July 2010.

[24] A. M. Massoud, S. J. Finney, A. J. Cruden and B. W. Williams, "Three-Phase, Three-Wire, Five-Level Cascaded Shunt Active Filter for Power Conditioning, Using Two Different Space Vector Modulation Techniques," in IEEE Transactions on Power Delivery, vol. 22, no. 4, pp. 2349-2361, Oct. 2007.

[25] I. A. Gowaid, G. P. Adam, A. M. Massoud, S. Ahmed, D. Holliday and B. W. Williams, "Quasi Two-Level Operation of Modular Multilevel Converter for Use in a High-Power DC Transformer With DC Fault Isolation Capability," in IEEE Transactions on Power Electronics, vol. 30, no. 1, pp. 108-123, Jan. 2015.

[26] A. A. Elserougi, A. M. Massoud and S. Ahmed, "Modular Multilevel Converter-Based Bipolar High-Voltage Pulse Generator With Sensorless Capacitor Voltage Balancing Technique," in IEEE Transactions on Plasma Science, vol. 44, no. 7, pp. 1187-1194, July 2016.

[27] Yang and M. Saeedifard, "A Capacitor Voltage Balancing Strategy With Minimized AC Circulating Current for the DC–DC Modular Multilevel Converter," in IEEE Transactions on Industrial Electronics, vol. 64, no. 2, pp. 956-965, Feb. 2017.

[28] F. A. d. C. Bahia, C. B. Jacobina, I. R. F. M. P. da Silva, N. Rocha, B. E. d. O. B. Luna and P. L. S. Rodrigues, "Hybrid nine-level single-phase inverter based on modular multilevel cascade converter," 2016 IEEE Energy Conversion Congress and Exposition (ECCE), Milwaukee, WI, 2016, pp. 1-7.

[29] I. Da Silva, A. Oliveira, C. Jacobina, "Hybrid single-phase AC-AC double-star chopper-cells (DSCC) converters with modulation and dc-link voltage ripple improvement", Energy Conversion Congress and Exposition (ECCE) 2015 IEEE, pp. 5938-5945, Sept 2015.

[30] X. She, A. Huang, "Circulating current control of double-star chopper-cell modular multilevel converter for hvdc system", IECON 2012–38th Annual Conference on IEEE Industrial Electronics Society, pp. 1234-1239, Oct 2012.

[31] A. A. Elserougi, A. M. Massoud and S. Ahmed, "A Switched-Capacitor Submodule for Modular Multilevel HVDC Converters With DC-Fault Blocking Capability and a Reduced Number of Sensors," in IEEE Transactions on Power Delivery, vol. 31, no. 1, pp. 313-322, Feb. 2016.

[32] N. Thitichaiworakorn, M. Hagiwara and H. Akagi, "A single-phase to three-phase direct AC/AC modular multilevel cascade converter based on double-star bridge-cells (MMCC-DSBC)," 2013 1st International Future Energy Electronics Conference (IFEEC), Tainan, 2013, pp. 476-481.

[33] S. i. Hamasaki, K. Okamura and M. Tsuji, "Power flow control of Modular

Multilevel Converter based on double-star bridge cells applying to grid connection," 2012 15th International Conference on Electrical Machines and Systems (ICEMS), Sapporo, 2012, pp. 1-6.

[34] J. I. Y. Ota, T. Sato and H. Akagi, "Enhancement of Performance, Availability, and Flexibility of a Battery Energy Storage System Based on a Modular Multilevel Cascaded Converter (MMCC-SSBC)," in IEEE Transactions on Power Electronics, vol. 31, no. 4, pp. 2791-2799, April 2016.

[35] R. A. Mastromauro, S. Pugliese, D. Ricchiuto, S. Stasi and M. Liserre, "DC Multibus based on a Single-Star Bridge Cells Modular Multilevel Cascade Converter for DC smart grids," 2015 International Conference on Clean Electrical Power (ICCEP), Taormina, 2015, pp. 55-60.

[36] P. Sochor and H. Akagi, "Theoretical Comparison in Energy-Balancing Capability Between Star- and Delta-Configured Modular Multilevel Cascade Inverters for Utility-Scale Photovoltaic Systems," in IEEE Transactions on Power Electronics, vol. 31, no. 3, pp. 1980-1992, March 2016.

[37] P. H. Wu, Y. T. Chen and P. T. Cheng, "The Delta-Connected Cascaded H-Bridge Converter Application in Distributed Energy Resources and Fault Ride Through Capability Analysis," in IEEE Transactions on Industry Applications, vol. 53, no. 5, pp. 4665-4672, Sept.-Oct. 2017.

[38] P. H. Wu, H. C. Chen, Y. T. Chang and P. T. Cheng, "Delta-Connected Cascaded H-Bridge Converter Application in Unbalanced Load Compensation," in IEEE Transactions on Industry Applications, vol. 53, no. 2, pp. 1254-1262, March-April 2017.

[39] M. Hagiwara, R. Maeda and H. Akagi, "Negative-Sequence Reactive-Power

Control by a PWM STATCOM Based on a Modular Multilevel Cascade Converter (MMCC-SDBC)," in IEEE Transactions on Industry Applications, vol. 48, no. 2, pp. 720-729, March-April 2012.

[40] K. M. Kotb, A. E. W. Hassan and E. M. Rashad, "Simplified sinusoidal pulse width modulation for cascaded half-bridge multilevel inverter," 2016 Eighteenth International Middle East Power Systems Conference (MEPCON), Cairo, 2016, pp. 907-913.

[41] M. S. Aspalli and A. Wamanrao, "Sinusoidal pulse width modulation (SPWM) with variable carrier synchronization for multilevel inverter controllers," 2009 International Conference on Control, Automation, Communication and Energy Conservation, Perundurai, Tamilnadu, 2009, pp. 1-6.

[42] K. V. V. S. R. Chowdary and T. N. Sekhar, "Performance analysis of transformer operated by Sinusoidal pulse width modulation Inverter," 2014 International Conference on Advances in Electrical Engineering (ICAEE), Vellore, 2014, pp. 1-3.

[43] V. Manimala, N. Geetha and P. Renuga, "Design and simulation of five level cascaded inverter using multilevel sinusoidal pulse width modulation strategies," 2011 3rd International Conference on Electronics Computer Technology, Kanyakumari, 2011, pp. 280-283.

[44] M. Y. M. Ghias, J. Pou, V. G. Agelidis and M. Ciobotaru, "Voltage Balancing Method for a Flying Capacitor Multilevel Converter Using Phase Disposition PWM," in IEEE Transactions on Industrial Electronics, vol. 61, no. 12, pp. 6538-6546, Dec. 2014.

[45] F. Rojas, R. Kennel, R. Cardenas, R. Repenning, J. C. Clare and M. Diaz, "A New

Space-Vector-Modulation Algorithm for a Three-Level Four-Leg NPC Inverter," in IEEE Transactions on Energy Conversion, vol. 32, no. 1, pp. 23-35, March 2017.

[46] A. M. Massoud, S. J. Finney and B. W. Williams, "Mapped hybrid spaced vector modulation for multilevel cascaded-type voltage source inverters," in IET Power Electronics, vol. 1, no. 3, pp. 318-335, September 2008.

[47] A. M. Massoud, S. J. Finney and B. W. Williams, "Systematic analytical-based generalised algorithm for multilevel space vector modulation with a fixed execution time," in IET Power Electronics, vol. 1, no. 2, pp. 175-193, June 2008.

[48] A. M. Massoud, S. J. Finney, A. Cruden and B. W. Williams, "Mapped phase-shifted space vector modulation for multi-level voltage-source inverters," in IET Electric Power Applications, vol. 1, no. 4, pp. 622-636, July 2007.

[49] J. Wang, Y. Gao and W. Jiang, "A Carrier-Based Implementation of Virtual Space Vector Modulation for Neutral-Point-Clamped Three-Level Inverter," in IEEE Transactions on Industrial Electronics, vol. 64, no. 12, pp. 9580-9586, Dec. 2017.

[50] S. Mohammadalizadeh and M. Ghayeni, "A new strategy in selective harmonic elimination for a photovoltaic multilevel inverter," 2016 Iranian Conference on Renewable Energy & Distributed Generation (ICREDG), Mashhad, 2016, pp. 50-55.

[51] Y. H. Wang, R. Tian, J. J. Liu and L. Song, "The Simplification and Solution of Transcendental Equations in Selective Harmonic Elimination Inverter," 2012 Asia-Pacific Power and Energy Engineering Conference, Shanghai, 2012, pp. 1-3.

[52] Konstantinou, G.; Ciobotaru, M.; Agelidis, V., "Selective harmonic elimination

pulse-width modulation of modular multilevel converters," Power Electronics, IET , vol.6, no.1, pp.96,107, Jan. 2013

[53] W. Zhang, W. Chen, Q. Zhang and L. Zhang, "Analyzing of voltage-source selective harmonic elimination inverter," 2011 IEEE International Conference on Mechatronics and Automation, Beijing, 2011, pp. 1888-1892.

[54] S. Bhadra, D. Gregory and H. Patangia, "An analytical solution of switching angles for Selective Harmonic Elimination (SHE) in a cascaded seven level inverter," 2016 IEEE 2nd Annual Southern Power Electronics Conference (SPEC), Auckland, 2016, pp. 1-5.

[55] E. H. E. Aboadla, S. Khan, M. H. Habaebi, T. Gunawan, B. A. Hamidah and M. Tohtayong, "Selective Harmonics Elimination technique in single phase unipolar H-bridge inverter," 2016 IEEE Student Conference on Research and Development (SCOReD), Kuala Lumpur, 2016, pp. 1-4.

[56] Pulikanti, S.R.; Konstantinou, G.; Agelidis, V.G., "DC-Link Voltage Ripple Compensation for Multilevel Active-Neutral-Point-Clamped Converters Operated With SHE-PWM," Power Delivery, IEEE Transactions on , vol.27, no.4, pp.2176,2184, Oct. 2012

[57] Kavousi, A.; Vahidi, B.; Salehi, R.; Bakhshizadeh, M.; Farokhnia, N.; Fathi, S.S., "Application of the Bee Algorithm for Selective Harmonic Elimination Strategy in Multilevel Inverters," Power Electronics, IEEE Transactions on , vol.27, no.4, pp.1689,1696, April 2012

[58] Konstantinou, G.S.; Dahidah, M.S.A.; Agelidis, V.G., "Solution trajectories for selective harmonic elimination pulse-width modulation for seven-level waveforms: analysis and implementation," Power Electronics, IET, vol.5, no.1,

pp.22,30, January 2012

[59] Wanmin Fei; Xinbo Ruan; Bin Wu, "A Generalized Formulation of Quarter-Wave Symmetry SHE-PWM Problems for Multilevel Inverters," Power Electronics, IEEE Transactions on , vol.24, no.7, pp.1758,1766, July 2009

[60] Cowell, D.M.J.; Smith, P.R.; Freear, S., "Phase-inversion-based selective harmonic elimination (PI-SHE) in multi-level switched-mode tone- and frequency- modulated excitation," Ultrasonics, Ferroelectrics and Frequency Control, IEEE Transactions on , vol.60, no.6, pp.1084,1097, June 2013

[61] M. S. A. Dahidah, G. Konstantinou and V. G. Agelidis, "A Review of Multilevel Selective Harmonic Elimination PWM: Formulations, Solving Algorithms, Implementation and Applications," in IEEE Transactions on Power Electronics, vol. 30, no. 8, pp. 4091-4106, Aug. 2015.

[62] S. A. Azmi, G. P. Adam, K. H. Ahmed, S. J. Finney and B. W. Williams, "Grid Interfacing of Multimegawatt Photovoltaic Inverters," in IEEE Transactions on Power Electronics, vol. 28, no. 6, pp. 2770-2784, June 2013.

[63] M. Zabaleta, E. Burguete, D. Madariaga, I. Zubimendi, M. Zubiaga and I. Larrazabal, "LCL Grid Filter Design of a Multimegawatt Medium-Voltage Converter for Offshore Wind Turbine Using SHEPWM Modulation," in IEEE Transactions on Power Electronics, vol. 31, no. 3, pp. 1993-2001, March 2016.

[64] D. Ahmadi, K. Zou, C. Li, Y. Huang and J. Wang, "A Universal Selective Harmonic Elimination Method for High-Power Inverters," in IEEE Transactions on Power Electronics, vol. 26, no. 10, pp. 2743-2752, Oct. 2011.

[65] L. G. Franquelo, J. Napoles, R. C. P. Guisado, J. I. Leon and M. A. Aguirre, "A Flexible Selective Harmonic Mitigation Technique to Meet Grid Codes in Three-

Level PWM Converters," in IEEE Transactions on Industrial Electronics, vol. 54, no. 6, pp. 3022-3029, Dec. 2007.

[66] D. Yazdani, A. Bakhshai, G. Joos and M. Mojiri, "A Real-Time Three-Phase Selective-Harmonic-Extraction Approach for Grid-Connected Converters," in IEEE Transactions on Industrial Electronics, vol. 56, no. 10, pp. 4097-4106, Oct. 2009.

[67] H. Zhou, Y. W. Li, N. R. Zargari, Z. Cheng, R. Ni and Y. Zhang, "Selective Harmonic Compensation (SHC) PWM for Grid-Interfacing High-Power Converters," in IEEE Transactions on Power Electronics, vol. 29, no. 3, pp. 1118-1127, March 2014.

[68] M. S. A. Dahidah and V. G. Agelidis, "Selective Harmonic Elimination PWM Control for Cascaded Multilevel Voltage Source Converters: A Generalized Formula," in IEEE Transactions on Power Electronics, vol. 23, no. 4, pp. 1620-1630, July 2008.

[69] Y. H. Wang, R. Tian, J. J. Liu and L. Song, "The Simplification and Solution of Transcendental Equations in Selective Harmonic Elimination Inverter," 2012 Asia-Pacific Power and Energy Engineering Conference, Shanghai, 2012, pp. 1-3.

[70] J. N. Chiasson, L. M. Tolbert, K. J. McKenzie and Zhong Du, "A unified approach to solving the harmonic elimination equations in multilevel converters," in IEEE Transactions on Power Electronics, vol. 19, no. 2, pp. 478-490, March 2004.

[71] M. S. A. Dahidah, G. Konstantinou and V. G. Agelidis, "A Review of Multilevel Selective Harmonic Elimination PWM: Formulations, Solving Algorithms, Implementation and Applications," in IEEE Transactions on Power Electronics,

vol. 30, no. 8, pp. 4091-4106, Aug. 2015. doi: 10.1109/TPEL.2014.2355226

[72] P. Farhadi, M. Navidi, M. Gheydi, M. Pazhoohesh and H. Bevrani, "Online selective harmonic minimization for cascaded Half-bridge multilevel inverter using artificial neural network," 2015 Intl Aegean Conference on Electrical Machines & Power Electronics (ACEMP), 2015 Intl Conference on Optimization of Electrical & Electronic Equipment (OPTIM) & 2015 Intl Symposium on Advanced Electromechanical Motion Systems (ELECTROMOTION), Side, 2015, pp. 331-335.

[73] N. V. Kumar, V. K. Chinnaiyan, M. Pradish and M. S. Divekar, "Selective harmonic elimination: An comparative analysis for seven level inverter," 2016 IEEE Students' Technology Symposium (TechSym), Kharagpur, 2016, pp. 157-162.

[74] N. Farokhnia, S. H. Fathi, R. Salehi, G. B. Gharehpetian and M. Ehsani, "Improved selective harmonic elimination pulse-width modulation strategy in multilevel inverters," in IET Power Electronics, vol. 5, no. 9, pp. 1904-1911, November 2012.

[75] H. H. Goh, C. W. Ling, Q. S. Chua, K. C. Goh and S. S. Lee, "Multilevel inverter for standalone application with selective harmonic elimination," 2016 International Symposium on Industrial Electronics (INDEL), Banja Luka, 2016, pp. 1-6.

[76] Shammya Saha, Nathan Johnson, " Modeling and Simulation in XENDEE IEEE 13 Node Test Feeder ", XENDEE, IRA A. Fulton School of Engineering, Arizona State University, 2016. https://www.xendee.com/IEEE/Xendee_ASU_IEEE_13_BUS.pdf

[77] S. H. Hosseini, A. Nazarloo and E. Babaei, "Super-Capacitor based D-STATCOM applied in IEEE 13-bus industrial distribution system," The 8th Electrical Engineering/ Electronics, Computer, Telecommunications and Information Technology (ECTI) Association of Thailand - Conference 2011, Khon Kaen, 2011, pp. 715-718.

APPENDIX

Appendix A.1 Published Research Conference Papers (Total: 5 Papers)

[1] M. G. Fakhry, A. Massoud and S. Ahmed, " Performance Assessment of Three Selective Harmonic Elimination Techniques for Gird-Connected Three-Phase Cascaded H-Bridge Multilevel Converters," 9th IEEE GCC Conference & Exhibition (IEEE GCC 2017), Manama, Bahrain, 2017.

[2] Fakhry, M.G.; Massoud, A.; Ahmed, S.: 'Grid-Connected Cascaded 17-Level H-Bridge Converter with Selective Harmonic Elimination', The 8th IET International Conference on Power Electronics, Machines and Drives (PEMD 2016) Glasgow, United Kingdom, IET Conference Proceedings, 2016, p. 5-5.

[3] M. G. Fakhry, A. Massoud and S. Ahmed, "A grid-connected cascaded H-bridge multilevel converter with quasi seven-level Selective Harmonic Elimination," Electric Power and Energy Conversion Systems (EPECS), 2015 4th International Conference on, Sharjah, 2015, pp. 1-6.

[4] M. G. Fakhry, A. Massoud and S. Ahmed, "Selective harmonic elimination for quasi seven-level operation of cascaded-type multilevel converters with unequal DC sources," Smart Grid and Renewable Energy (SGRE), 2015 First Workshop on, Doha, 2015, pp. 1-5.

[5] M. G. Fakhry, A. Massoud and S. Ahmed, "Quasi seven-level operation of multilevel converters with selective harmonic elimination," 2014 26th International Conference on Microelectronics (ICM), Doha, 2014, pp. 216-219.

Appendix A.2 SSBC-MMCC 8 Angles Lookup Table for all modulation indexes

Lookup Table for C-SHE 8 Angles

Mi	A1	A2	A3	A4	A5	A6	A7	A8
0.27	35.7970	48.0821	60.8362	76.2561	90.0000	90.0000	90.0000	90.0000
0.28	35.6605	47.8247	60.2426	75.3941	89.5636	90.0000	90.0000	90.0000
0.29	35.4103	47.2416	59.0492	73.4802	88.4288	90.0000	90.0000	90.0000
0.3	35.3174	46.5650	58.0801	71.5606	87.0496	90.0000	90.0000	90.0000
0.31	35.4599	45.7258	57.3570	69.6621	85.3869	90.0000	90.0000	90.0000
0.32	35.7528	44.8006	56.7722	67.8920	83.4213	90.0000	90.0000	90.0000
0.33	35.7822	44.1605	56.0260	66.4623	81.1879	90.0000	90.0000	90.0000
0.34	34.9120	44.3482	54.7308	65.5602	78.7447	90.0000	90.0000	90.0000
0.35	34.9447	43.7796	54.1288	64.2939	77.1300	89.0931	90.0000	90.0000
0.36	34.9026	43.3050	53.4803	63.1735	75.4446	88.0254	90.0000	90.0000
0.37	34.3847	43.2890	52.5214	62.4091	73.6263	86.9442	90.0000	90.0000
0.38	33.3778	43.7382	51.1868	62.0252	71.6765	85.8605	90.0000	90.0000
0.39	32.4650	44.2063	49.7712	61.8186	69.7224	84.5618	90.0000	90.0000
0.4	35.8476	40.6821	51.7345	59.0854	69.9235	81.0981	90.0000	90.0000
0.41	33.8498	42.0748	50.1237	59.0243	68.3819	79.6474	89.8111	90.0000
0.42	33.6762	41.8582	49.5591	58.3248	67.2590	78.1366	89.0200	90.0000
0.43	33.6318	41.5400	49.1216	57.5771	66.2858	76.6062	88.0255	90.0000
0.44	33.8481	41.0017	48.8995	56.7156	65.4873	75.0775	86.7778	90.0000
0.45	34.2533	40.3221	48.8381	55.8376	64.8345	73.7093	85.3574	90.0000
0.46	34.4663	39.7951	48.5947	55.0429	64.0210	72.3931	83.5502	90.0000
0.47	33.7673	40.1396	47.7759	54.7895	62.9983	71.4419	81.7597	90.0000
0.48	32.1333	41.2147	46.2995	54.9007	61.6967	70.6166	79.9140	90.0000
0.49	30.4224	41.9234	45.1566	54.8170	60.7266	69.8683	78.5140	90.0000
0.5	28.5012	41.1950	45.2689	54.1253	60.1456	68.8891	77.2350	90.0000
0.51	26.7105	39.5459	46.1464	52.9711	59.9547	67.8213	76.2084	90.0000
0.52	25.3826	38.1353	46.7683	51.9837	59.8630	66.9683	75.5041	90.0000
0.53	23.4583	35.9232	46.8550	50.9792	59.2563	65.7815	74.1072	89.7626
0.54	32.7258	39.3071	45.0131	51.6949	58.0911	65.3242	72.9728	81.9927
0.55	31.1454	40.2350	43.8418	51.7267	57.2956	64.6614	72.0180	80.6141
0.56	29.5272	40.2631	43.4449	51.3067	56.8363	63.8706	71.1916	79.2941
0.57	27.8868	39.1220	44.0553	50.4660	56.6316	63.0401	70.3990	78.0967
0.58	26.2435	37.5708	44.7291	49.5916	56.3121	62.3894	69.5045	77.0830
0.59	34.3575	39.8013	48.4103	54.9044	63.7290	72.0634	82.9878	90.0000
0.6	33.6450	40.2206	47.6582	54.7910	62.8820	71.3603	81.5820	90.0000
0.61	33.7361	39.9100	47.4782	54.2582	62.3571	70.4632	80.5388	89.4622
0.62	33.9609	39.4848	47.3931	53.6793	61.8862	69.5932	79.5076	88.7907
0.63	34.1284	39.1202	47.2606	53.1653	61.3885	68.8078	78.4465	88.0532
0.64	32.6131	40.2850	45.9345	53.5711	60.2939	68.4904	77.0757	87.7732
0.65	36.4658	36.4658	47.6315	51.6933	60.6488	67.2262	76.5075	86.0299
0.66	36.3713	36.3715	47.3209	51.3986	60.0807	66.6367	75.5133	85.0012

0.67	34.9636	37.5682	46.7284	51.3442	59.4415	66.1133	74.5667	83.9214
0.68	33.6910	38.5906	45.8001	51.5477	58.6794	65.6810	73.6425	82.8517
0.69	32.4660	39.4880	44.8010	51.7255	57.9403	65.2254	72.8033	81.7647
0.7	31.2245	40.2032	43.8882	51.7367	57.3261	64.6993	72.0611	80.6829
0.71	29.9591	40.3937	43.4249	51.4669	56.9235	64.0899	71.4024	79.6346
0.72	10.7558	35.8012	35.8044	46.0904	57.4987	63.1138	78.9160	87.6049
0.73	9.9832	33.5814	37.8861	44.7271	56.5162	62.9497	77.9330	87.0645
0.74	10.1376	30.0667	39.6317	43.4554	56.6578	61.6840	76.2702	87.7085
0.75	7.4464	35.8639	36.0044	43.5500	52.5828	63.6565	76.8446	84.5304
0.76	6.7819	35.7976	35.7979	43.5635	51.2090	63.1616	76.1752	83.3329
0.77	6.6906	32.9661	38.3242	42.7369	50.7598	62.1974	75.1480	82.5823
0.78	6.5118	31.5790	39.2417	42.0425	50.1702	61.3159	74.2200	81.7573
0.79	6.2583	30.3664	39.4239	41.8749	49.4279	60.4831	73.3912	80.8885
0.8	5.9587	29.2017	38.8060	42.4153	48.5392	59.6625	72.6328	80.0229
0.81	4.9698	28.2309	38.7777	42.2397	47.5492	58.5844	72.9390	78.4630
0.82	5.2904	26.9399	36.7167	44.6526	45.8880	57.9579	71.2376	78.3961
0.83	5.2165	25.7223	35.6645	45.1181	45.1224	57.0577	70.2647	77.8497
0.84	5.0301	24.6143	34.4978	44.9146	44.9147	56.1291	69.4278	77.2474
0.85	4.5197	23.6699	33.2235	44.6701	44.6558	55.0255	68.9298	76.4989
0.86	3.2345	22.9531	31.8611	43.5338	45.4072	53.3568	69.0862	75.4389
0.87	3.9175	21.5907	30.9894	40.9253	47.0913	52.5678	67.3770	75.5253
0.88	5.2291	20.5999	29.8524	39.7017	46.9443	53.0850	65.2376	75.1900
0.89	5.3061	19.9606	28.6055	38.6272	46.8886	52.5199	64.2718	74.4316
0.9	5.3303	19.3964	27.4135	37.4250	46.7496	51.9624	63.3861	73.6275
0.91	5.4121	18.8770	26.2972	36.1404	46.3586	51.6345	62.4767	72.7806
0.92	5.5041	18.3208	25.3059	34.7925	45.6294	51.5206	61.5578	71.9508
0.93	5.4858	17.6286	24.4907	33.4036	44.5967	51.3943	60.6756	71.2571
0.94	5.1679	16.6948	23.8848	31.9954	43.3582	50.8865	59.8807	70.8993
0.95	4.4490	15.3899	23.4911	30.5699	42.0418	49.7108	59.1258	71.0779
0.96	3.5552	13.0046	23.3401	29.0357	40.8658	47.2668	58.2426	72.3782
0.97	4.3309	13.8828	22.4972	27.9840	39.3431	48.6217	57.4125	69.8969
0.98	7.5842	15.2123	20.2346	28.0325	37.1612	50.8942	58.7238	64.5092
0.99	4.6247	14.3883	19.7476	27.0344	35.8474	48.1314	56.4413	67.1013

Lookup Table for Q-SHE 8 Angles

mi	del1	2*del1	3*del1	4*del1	5*del1	6*del1	del2	del3
0.31	20.9077	41.8154	62.7231	90.0000	90.0000	90.0000	62.7056	90.0000
0.32	19.1915	38.3831	57.5746	90.0000	90.0000	90.0000	63.8706	89.7694
0.33	19.2087	38.4174	57.6261	90.0000	90.0000	90.0000	64.2861	90.0000
0.34	19.0096	38.0192	57.0289	90.0000	90.0000	90.0000	63.8544	89.4267
0.35	18.7501	37.5003	56.2504	90.0000	90.0000	90.0000	62.6305	88.0253
0.36	18.5081	37.0162	55.5243	90.0000	90.0000	90.0000	60.2264	85.3966
0.37	18.5758	37.1516	55.7274	90.0000	90.0000	90.0000	57.5959	82.7690
0.38	18.5605	37.1211	55.6816	90.0000	90.0000	90.0000	55.8450	80.5442
0.39	18.2202	36.4403	54.6605	90.0000	90.0000	90.0000	54.7079	77.3851
0.4	17.7428	35.4855	53.2283	90.0000	90.0000	90.0000	54.8037	74.9615
0.41	16.9948	33.9896	50.9844	90.0000	90.0000	90.0000	55.8465	72.4049
0.42	16.1555	32.3111	48.4666	90.0000	90.0000	90.0000	57.1767	69.6919
0.43	15.0213	30.0425	45.0638	60.0850	90.0000	90.0000	90.0000	64.9668
0.44	14.8280	29.6559	44.4839	59.3118	90.0000	90.0000	88.5322	63.6471
0.45	14.6409	29.2819	43.9228	58.5638	90.0000	90.0000	86.9086	62.3379
0.46	14.4933	28.9865	43.4798	57.9730	90.0000	90.0000	84.6119	60.2912
0.47	14.3780	28.7561	43.1341	57.5121	90.0000	90.0000	82.2984	58.4590
0.48	14.2783	28.5566	42.8349	57.1132	90.0000	90.0000	80.1347	57.1317
0.49	14.0499	28.0998	42.1497	56.1996	90.0000	90.0000	77.1424	56.2505
0.5	13.7105	27.4210	41.1315	54.8420	90.0000	90.0000	74.4151	56.5356
0.51	13.2080	26.4159	39.6239	52.8318	90.0000	90.0000	71.8215	57.7872
0.52	12.7364	25.4729	38.2093	50.9458	90.0000	90.0000	69.0063	59.2360
0.53	12.3091	24.6183	36.9274	49.2365	61.5457	90.0000	65.2678	89.5912
0.54	12.1162	24.2323	36.3485	48.4647	60.5808	90.0000	63.6562	87.6068
0.55	11.9919	23.9838	35.9756	47.9675	59.9594	90.0000	62.5031	86.2544
0.56	11.8835	23.7670	35.6505	47.5340	59.4175	90.0000	60.5668	83.8783
0.57	11.7708	23.5416	35.3124	47.0832	58.8541	90.0000	59.1038	81.6401
0.58	11.6589	23.3178	34.9767	46.6356	58.2945	90.0000	58.3073	79.8810
0.59	11.4895	22.9790	34.4685	45.9580	57.4475	90.0000	57.5616	76.9723
0.6	11.2183	22.4366	33.6549	44.8732	56.0915	90.0000	58.1512	74.4179
0.61	10.9174	21.8347	32.7521	43.6695	54.5868	90.0000	59.4358	71.4902
0.62	10.3228	20.6455	30.9683	41.2910	51.6138	61.9365	90.0000	70.0598
0.63	10.3256	20.6512	30.9769	41.3025	51.6281	61.9537	88.9189	66.3029
0.64	10.1149	20.2299	30.3448	40.4598	50.5747	60.6896	87.3325	66.3318
0.65	9.9958	19.9917	29.9875	39.9834	49.9792	59.9751	85.4109	64.5817
0.66	9.8409	19.6819	29.5228	39.3637	49.2046	59.0456	84.0126	63.9982
0.67	9.7215	19.4430	29.1645	38.8860	48.6075	58.3290	81.9583	62.9916
0.68	9.6483	19.2965	28.9448	38.5930	48.2413	57.8896	79.7140	61.5034
0.69	9.6101	19.2203	28.8304	38.4406	48.0507	57.6609	76.7919	60.0093
0.7	9.4773	18.9546	28.4319	37.9092	47.3865	56.8639	74.0843	59.9121
0.71	9.2338	18.4676	27.7014	36.9352	46.1690	55.4028	71.2954	61.4771
0.72	9.0530	18.1059	27.1589	36.2118	45.2648	54.3177	66.1689	64.8565

0.73	8.7610	17.5220	26.2830	35.0440	43.8050	52.5660	64.9569	64.9672
0.74	8.3858	16.7715	25.1573	33.5430	41.9288	50.3146	65.5223	65.4087
0.75	8.1207	16.2414	24.3621	32.4828	40.6035	48.7243	63.2485	66.2888
0.76	7.9049	15.8097	23.7146	31.6194	39.5243	47.4292	64.1598	63.5225
0.77	7.6565	15.3129	22.9694	30.6258	38.2823	45.9387	63.3332	63.6462
0.78	7.3327	14.6653	21.9980	29.3307	36.6633	43.9960	63.9147	60.1911
0.79	7.1921	14.3841	21.5762	28.7682	35.9603	43.1523	61.7242	61.7756
0.8	6.6416	13.2832	19.9249	26.5665	33.2081	39.8497	60.1863	60.1809
0.81	6.2775	12.5550	18.8324	25.1099	31.3874	37.6649	58.4869	60.4109
0.82	5.6582	11.3164	16.9746	22.6328	28.2909	33.9491	58.1295	57.4474
0.83	5.5898	11.1796	16.7694	22.3592	27.9490	33.5388	57.6955	56.6763
0.84	5.4255	10.8510	16.2765	21.7019	27.1274	32.5529	56.6159	55.6663
0.85	5.1855	10.3711	15.5566	20.7421	25.9276	31.1132	55.3665	53.2828
0.86	4.9505	9.9010	14.8515	19.8020	24.7525	29.7029	55.7397	49.0604
0.87	4.7791	9.5582	14.3374	19.1165	23.8956	28.6747	56.2563	44.9753
0.88	4.5629	9.1258	13.6886	18.2515	22.8144	27.3773	54.5965	41.8889
0.89	4.4007	8.8013	13.2020	17.6027	22.0034	26.4040	52.5798	39.7086
0.9	4.2182	8.4363	12.6545	16.8726	21.0908	25.3089	49.6322	38.1075
0.91	4.0148	8.0297	12.0445	16.0593	20.0742	24.0890	45.1172	37.9689
0.92	3.9361	7.8721	11.8082	15.7443	19.6804	23.6164	43.0429	34.8208
0.93	3.9361	7.8721	11.8082	15.7443	19.6804	23.6164	43.0429	34.8208
0.94	3.9361	7.8721	11.8082	15.7443	19.6804	23.6164	43.0429	34.8208
0.95	3.8183	7.6366	11.4550	15.2733	19.0916	22.9099	37.2304	38.0533
0.96	3.7616	7.5233	11.2849	15.0465	18.8081	22.5698	36.4556	37.8525
0.97	3.8082	7.6164	11.4246	15.2327	19.0409	22.8491	36.4917	38.8113
0.98	3.8618	7.7237	11.5855	15.4474	19.3092	23.1711	36.5353	39.7584
0.99	3.8006	7.6012	11.4017	15.2023	19.0029	22.8035	37.0975	37.9502

Lookup Table for A-SHE 8 Angles

mi	del1	del1	del2	del2	del2	del3	del3	del3
0.4	35.1750	35.1750	60.3764	60.3764	60.3764	88.4278	88.4278	88.4278
0.41	35.1659	35.1659	59.5033	59.5033	59.5033	87.6587	87.6587	87.6587
0.42	35.2819	35.2819	58.6264	58.6264	58.6264	86.8373	86.8373	86.8373
0.43	35.5131	35.5131	57.7473	57.7473	57.7473	85.9655	85.9655	85.9655
0.44	35.8408	35.8408	56.8684	56.8684	56.8684	85.0470	85.0470	85.0470
0.45	36.2410	36.2410	55.9935	55.9935	55.9935	84.0868	84.0868	84.0868
0.46	36.6877	36.6877	55.1282	55.1282	55.1282	83.0893	83.0893	83.0893
0.47	37.1534	37.1534	54.2800	54.2800	54.2800	82.0586	82.0586	82.0586
0.48	37.6087	37.6087	53.4595	53.4595	53.4595	80.9975	80.9975	80.9975
0.49	38.0204	38.0204	52.6812	52.6812	52.6812	79.9083	79.9083	79.9083
0.5	38.3491	38.3491	51.9647	51.9647	51.9647	78.7928	78.7928	78.7928
0.51	38.5484	38.5484	51.3343	51.3343	51.3343	77.6527	77.6527	77.6527
0.52	38.5666	38.5666	50.8172	50.8172	50.8172	76.4901	76.4901	76.4901
0.53	38.3544	38.3544	50.4368	50.4368	50.4368	75.3086	75.3086	75.3086
0.54	37.8770	37.8770	50.2035	50.2035	50.2035	74.1144	74.1144	74.1144
0.55	37.1243	37.1243	50.1058	50.1058	50.1058	72.9179	72.9179	72.9179
0.56	36.1103	36.1103	50.1086	50.1086	50.1086	71.7351	71.7351	71.7351
0.57	34.8649	34.8649	50.1579	50.1579	50.1579	70.5901	70.5901	70.5901
0.58	33.4235	33.4235	50.1863	50.1863	50.1863	69.5152	69.5152	69.5152
0.59	31.8220	31.8220	50.1198	50.1198	50.1198	68.5500	68.5500	68.5500
0.6	30.0972	30.0972	49.8861	49.8861	49.8861	67.7341	67.7341	67.7341
0.61	28.2886	28.2886	49.4290	49.4290	49.4290	67.0935	67.0935	67.0935
0.62	26.4408	26.4408	48.7261	48.7261	48.7261	66.6252	66.6252	66.6252
0.63	24.6013	24.6013	47.7963	47.7963	47.7963	66.2917	66.2917	66.2917
0.64	22.8148	22.8148	46.6904	46.6904	46.6904	66.0326	66.0326	66.0326
0.65	21.1152	21.1152	45.4695	45.4695	45.4695	65.7864	65.7864	65.7864
0.66	19.5212	19.5212	44.1864	44.1864	44.1864	65.5072	65.5072	65.5072
0.67	18.0384	18.0384	42.8766	42.8766	42.8766	65.1688	65.1688	65.1688
0.68	16.6633	16.6633	41.5594	41.5594	41.5594	64.7611	64.7611	64.7611
0.69	15.3899	15.3899	40.2424	40.2424	40.2424	64.2834	64.2834	64.2834
0.7	14.2131	14.2131	38.9259	38.9259	38.9259	63.7398	63.7398	63.7398
0.71	13.1322	13.1322	37.6063	37.6063	37.6063	63.1357	63.1357	63.1357
0.72	12.1523	12.1523	36.2776	36.2776	36.2776	62.4765	62.4765	62.4765
0.73	11.2865	11.2865	34.9325	34.9325	34.9325	61.7666	61.7666	61.7666
0.74	10.5573	10.5573	33.5620	33.5620	33.5620	61.0096	61.0096	61.0096
0.75	9.9980	9.9980	32.1557	32.1557	32.1557	60.2080	60.2080	60.2080
0.76	9.6529	9.6529	30.7003	30.7003	30.7003	59.3635	59.3635	59.3635
0.77	9.5754	9.5754	29.1779	29.1779	29.1779	58.4767	58.4767	58.4767
0.78	9.8257	9.8257	27.5617	27.5617	27.5617	57.5476	57.5476	57.5476
0.79	10.4765	10.4765	25.8065	25.8065	25.8065	56.5751	56.5751	56.5751
0.8	11.6511	11.6511	23.8190	23.8190	23.8190	55.5576	55.5576	55.5576
0.81	13.7412	13.7412	21.3129	21.3129	21.3129	54.4928	54.4928	54.4928

0.82	17.8736	17.8736	17.8736	17.8736	17.8736	53.7893	53.7893	53.7893
0.83	57.3509	57.3509	29.7855	29.7855	29.7855	9.6738	9.6738	9.6738
0.84	55.9511	55.9511	28.2594	28.2594	28.2594	9.6261	9.6261	9.6261
0.85	54.4602	54.4602	26.6747	26.6747	26.6747	9.7402	9.7402	9.7402
0.86	52.8632	52.8632	25.0284	25.0284	25.0284	10.0172	10.0172	10.0172
0.87	51.1383	51.1383	23.3292	23.3292	23.3292	10.4352	10.4352	10.4352
0.88	49.2531	49.2531	21.6227	21.6227	21.6227	10.9207	10.9207	10.9207
0.89	47.1568	47.1568	20.0733	20.0733	20.0733	11.2603	11.2603	11.2603
0.9	44.7627	44.7627	19.1498	19.1498	19.1498	10.8925	10.8925	10.8925
0.91	41.8996	41.8996	19.5180	19.5180	19.5180	8.9150	8.9150	8.9150
0.92	38.1215	38.1215	21.4266	21.4266	21.4266	3.6439	3.6439	3.6439
0.93	37.2874	37.2874	21.9454	21.9454	21.9454	0.0000	0.0000	0.0000
0.94	18.4105	18.4105	33.4910	33.4910	33.4910	0.0000	0.0000	0.0000
0.95	18.0498	18.0498	32.9060	32.9060	32.9060	0.0000	0.0000	0.0000
0.96	17.7367	17.7367	32.3118	32.3118	32.3118	0.0000	0.0000	0.0000
0.97	17.4727	17.4727	31.7078	31.7078	31.7078	0.0000	0.0000	0.0000
0.98	17.3598	17.3598	31.4017	31.4017	31.4017	0.0000	0.0000	0.0000
0.99	16.9944	16.9944	28.4701	28.4701	28.4701	0.0000	0.0000	0.0000

Appendix A.3 Simulation Matlab Appendix

17 Level SSBC-MMCC with Artificial Neural Network

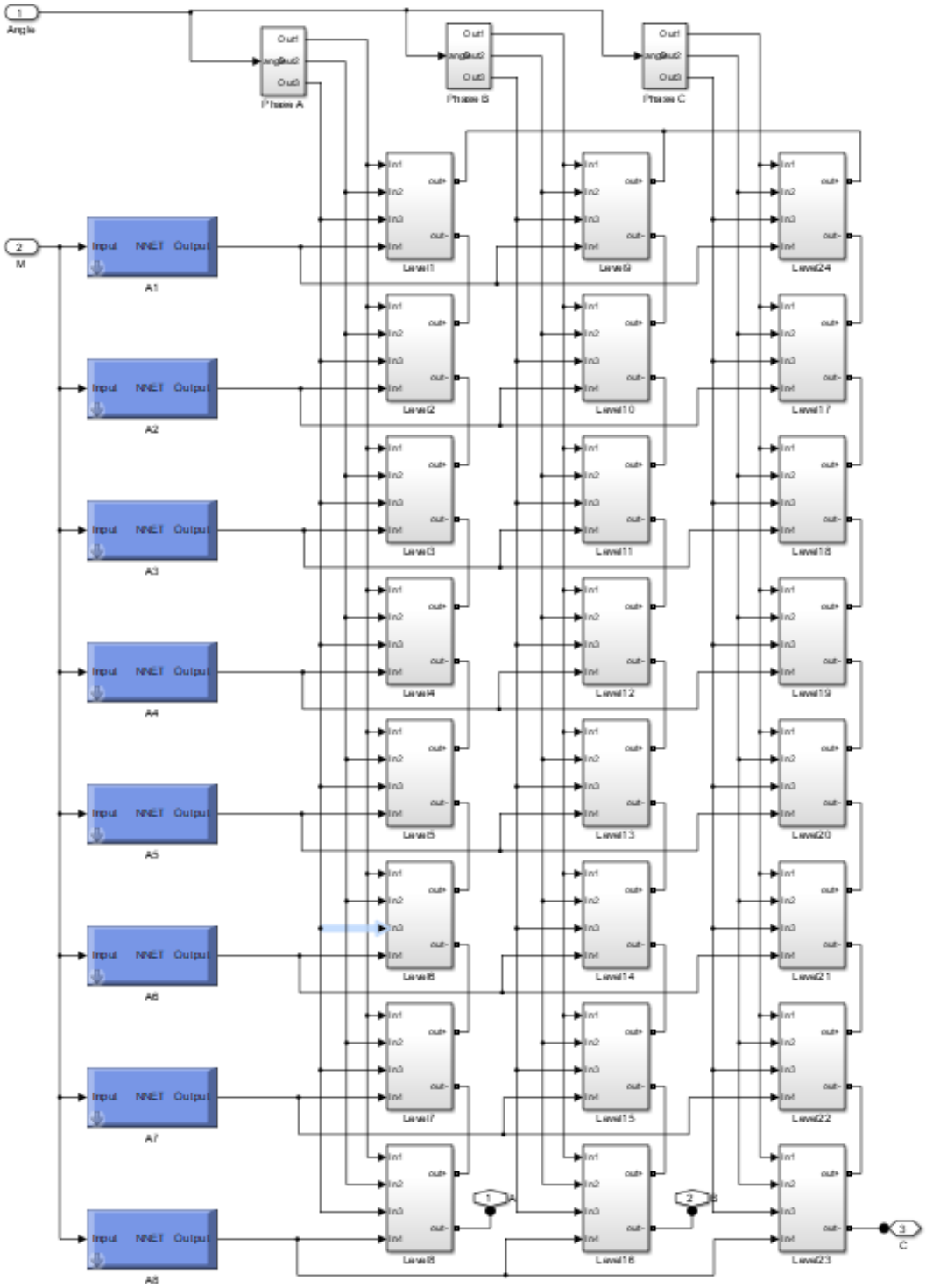

SSBC-MMCC Full wave H-Bridge Cell

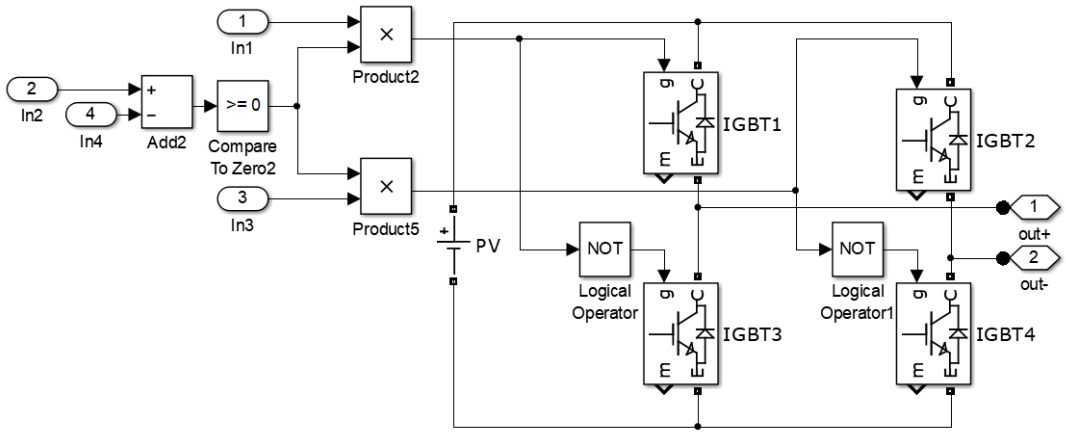

17 Level SSBC-MMCC Closed loop control

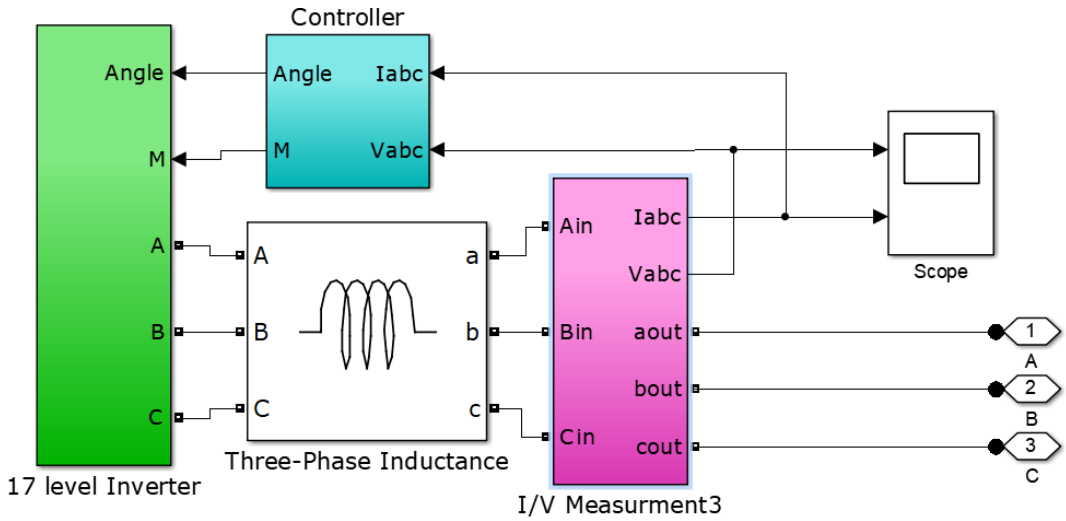

SSBC-MMCC Closed loop controller

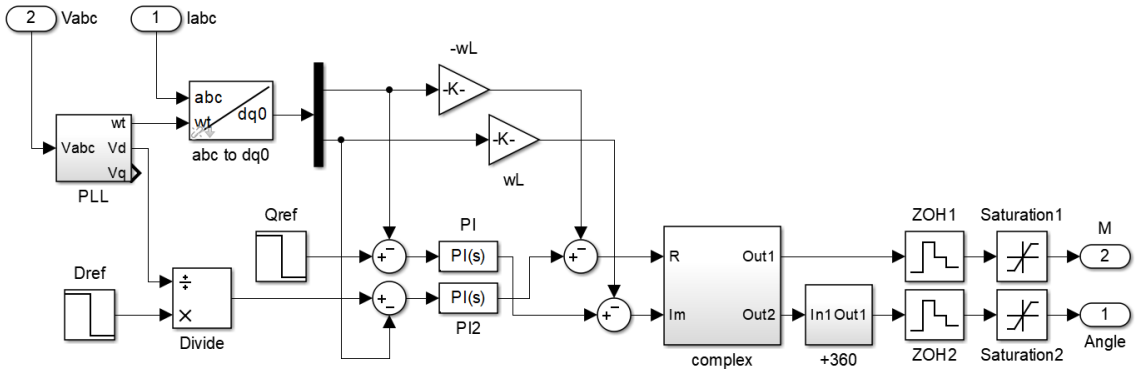

SSBC-MMCC connected to IEEE modified test System